



**HAL**  
open science

## Lower–Middle Jurassic facies patterns in the NW Afghan–Tajik Basin of southern Uzbekistan and their geodynamic context

Franz T. Fürsich, Marie-Françoise Brunet, Jean-Luc Auxière, Hermann Munsch

### ► To cite this version:

Franz T. Fürsich, Marie-Françoise Brunet, Jean-Luc Auxière, Hermann Munsch. Lower–Middle Jurassic facies patterns in the NW Afghan–Tajik Basin of southern Uzbekistan and their geodynamic context. Geological Society Special Publication, 2017, In: Brunet, M.-F., McCann, T. & Sobel, E. R. (eds) Geological Evolution of Central Asian Basins and the Western Tien Shan Range, 427, pp.SP427.9. 10.1144/SP427.9 . hal-01206129

**HAL Id: hal-01206129**

**<https://hal.science/hal-01206129>**

Submitted on 29 Sep 2015

**HAL** is a multi-disciplinary open access archive for the deposit and dissemination of scientific research documents, whether they are published or not. The documents may come from teaching and research institutions in France or abroad, or from public or private research centers.

L'archive ouverte pluridisciplinaire **HAL**, est destinée au dépôt et à la diffusion de documents scientifiques de niveau recherche, publiés ou non, émanant des établissements d'enseignement et de recherche français ou étrangers, des laboratoires publics ou privés.

1 **Lower to Middle Jurassic facies patterns in the northwestern Afghan-Tajik Basin of**  
2 **southern Uzbekistan and their geodynamic context**

3  
4  
5 FRANZ T. FÜRSICH<sup>1\*</sup>, MARIE-FRANCOISE BRUNET<sup>2,3</sup>, JEAN-LUC AUXIÈTRE<sup>4</sup> &  
6 HERMANN MUNSCH<sup>4</sup>

7  
8 <sup>1</sup>*Fachgruppe Paläoumwelt, GeoZentrum Nordbayern der Universität Erlangen-Nürnberg,*  
9 *Loewenichstrasse 28, D-91054 Erlangen Germany*

10 <sup>2</sup>*Sorbonne Universités, UPMC Univ. Paris 06, UMR 7193, Institut des Sciences de la Terre*  
11 *Paris (iSTeP), F-75005 Paris, France*

12 <sup>3</sup>*CNRS, UMR 7193, Institut des Sciences de la Terre Paris (iSTeP), F-75005 Paris, France*

13 <sup>4</sup>*TOTAL S.A., Tour Coupole, 2 Place Jean Millier - La Défense 6, 92078 Paris La Défense*  
14 *Cedex – France*

15 *\*Corresponding author (e-mail: franz.fuersich@fau.de)*

16  
17 abbreviated title: Jurassic facies patterns Afghan-Tajik Basin

18  
19  
20 text: 12,491 words

21 references: 1715 words

22 number of tables: 2

23 number of figures: 21

24

25

26 **Abstract:** Based on eleven sections, the palaeoenvironments and depositional history of the  
27 northwestern Afghan-Tajik Basin in southern Uzbekistan have been reconstructed for the time  
28 interval Early Jurassic to Early Callovian. The earliest sediments, resting on Palaeozoic  
29 basement rocks, date from the Early Jurassic Period. Up to the end of the Early Bajocian time  
30 up to more than 500 m of non-marine sediments accumulated due to extensional tectonics  
31 inducing active subsidence. In the Late Bajocian time interval, transgression led to the  
32 establishment of siliciclastic ramps that were influenced by storm processes. After a  
33 condensed unit in the Middle Bathonian, sedimentation resumed in an outer carbonate ramp □  
34 basinal setting as the subsidence rate outpaced the diminished siliciclastic sediment supply.  
35 The change from siliciclastic to carbonate sedimentation in the Middle Jurassic Period is  
36 thought to be multifactorial, reflecting levelling of relief in the hinterland, the subsidence  
37 moving to a thermally more quiet stage, and a change from humid to arid climatic conditions.  
38 These features are also observed in the area of present-day Iran. Similarly, the timing of the  
39 transgression coincides with that in eastern and northern Iran stressing the regional  
40 significance of this event.

41

42

43 After the collisions of the Cimmerian terranes with Eurasia in the Late Triassic (e.g., Stampfli  
44 & Borel 2002; Barrier & Vrielynck 2008; Wilmsen *et al.* 2009a; Zanchi *et al.* 2009, 2012) a  
45 number of new or re-activated sedimentary basins formed north of the collision zone in  
46 central Asia. Two of these basins are the Amu Darya Basin stretching across Turkmenistan  
47 and Uzbekistan and the Afghan-Tajik Basin extending across Uzbekistan, Tajikistan, and  
48 Afghanistan (e.g., Brookfield & Hashmat 2001; Ulmishek 2004; Klett *et al.* 2006) (Fig. 1).  
49 These two basins had a very close evolution from the Late Palaeozoic onwards. During the  
50 Jurassic, the Amu Darya Basin was connected with the Afghan-Tajik Basin in the east (e.g.,  
51 Ulmishek 2004). The important difference stems from Cenozoic shortening and indentation in  
52 the east due to the collision of India: The Pamirs evolution induced folding/thrusting of the  
53 sedimentary cover in the Afghan-Tajik Basin (Nikolaev 2002; Klett *et al.* 2006).

54 In the west, the Amu Darya Basin is bordered by the Kara Bogaz-Karakum High, in  
55 the south by the Kopet Dagh Foldbelt, and in the north by the Kyzyl Kum High (Ulmishek  
56 2004). The Afghan-Tajik Basin is bordered to the north by the western part of the Tien Shan  
57 (the West Gissar), in the east by the Pamirs and in the south by the North Afghanistan High  
58 and Bande Turkestan Mountains (Klett *et al.* 2006; Montenat 2009; Siehl 201X). The  
59 southwestern Gissar range stretches southwesterly between the northern parts of the Amu

60 Darya and Afghan-Tajik basins. Western and southwestern Gissar are the main areas where  
61 Jurassic sediments crop out and may be studied in the field. On the northern and southern  
62 margins of the Amu Darya and Afghan-Tajik basins they have been reached by wells.  
63 Sedimentation started in Permian-Triassic rift basins that formed in the folded and  
64 metamorphosed Palaeozoic basement. During the Jurassic Period the Amu Darya and Afghan-  
65 Tajik basins subsided very rapidly and became filled with a thick succession of siliciclastic  
66 (Lower and early Middle Jurassic), mixed carbonate-siliciclastic (Bathonian to Lower  
67 Callovian), carbonate (Middle Callovian-Kimmeridgian), and finally evaporitic  
68 (Kimmeridgian?-Tithonian) sediments. Due to their importance as hydrocarbon source and  
69 reservoir rocks (for summaries see Ulmishek 2004; Klett *et al.* 2006), the strata have been  
70 extensively studied since the Middle of the last century (e.g., Egamberdiev & Ishniyazov  
71 1990; Mitta 2001; D.P. Ishniyazov, pers. comm. 2011; V. Kharin, pers. comm. 2011; Tevelev  
72 & Georgievskii 2012), but mainly from a stratigraphic point of view and often published in  
73 Russian journals or reports not easily available internationally. No detailed  
74 palaeoenvironmental analysis of these rocks exists, but in several review papers the evolution  
75 of these sedimentary basins has been briefly outlined, usually in context with their petroleum  
76 potential (e.g., Brookfield & Hashmat 2001; Ulmishek 2004; Klett *et al.* 2006).

77 The aim of the present study is to provide a palaeoenvironmental reconstruction of the  
78 Lower and Middle Jurassic part of the basin fill in southern Uzbekistan, to relate the results to  
79 the palaeoclimatic and palaeotectonic setting, and to discuss the geodynamic framework  
80 governing the evolution of the basin. We do this with an integrated approach using, apart  
81 from sedimentological data, also biostratigraphic, ichnological, and taphonomic information.

82

83

#### 84 **Material and methods**

85

86 Altogether, eleven sections in five areas were measured (Fig. 1, Table 1): two sections  
87 (Vandob, Shalkan) in the Kugitang Mountains of southern Uzbekistan close to the  
88 Turkmenistan border, one section at Panjab (northern Kugitang Mountains), two sections in  
89 the southeastern part of Uzbekistan close to the border to Tajikistan (Sangardak, Shargun),  
90 two sections in the southernmost part of the Gissar Mountains (Iron Gate, Dalut Mine), and  
91 four sections at Vuariz in the west-central part of the Gissar Mountains, ESE of Shahrissabsz  
92 (Fig. 1). Of these sections the Vandob, Shalkan, Shargun, and Sangardak sections span the  
93 complete succession from the basement to the base of the upper Middle Jurassic carbonate

94 platform, with a thickness between 335 and 920 m. In the remaining sections either the base  
95 or the transition to the Upper Jurassic carbonates is missing. Strictly speaking the study area  
96 forms the western margin of the Afghan-Tajik Basin, but during the Jurassic the Amu Darya  
97 and Afghan-Tajik basins formed a single unit.

98 Field data were collected in the course of five field trips to the area in the years 2010,  
99 2011, 2013, and 2014. Sections were logged in detail, bed by bed wherever possible, but in  
100 some sections part of the fine-grained succession, consisting of argillaceous silt or silty marl,  
101 was overgrown or deeply weathered and could be measured only cursorily. Data retrieval  
102 involved recording of lithology, sedimentary structures, trace fossils, body fossils, and  
103 taphonomic features. Laboratory work involved analysis of thin-sections and preparation and  
104 identification of body fossils.

105

106

## 107 **Litho-, bio- and chronostratigraphy**

108

### 109 *Lithostratigraphy*

110

111 Several lithostratigraphic frameworks exist for the Jurassic succession in southern  
112 Uzbekistan, which is best developed in the Kugitang Mountains. Here, we follow the  
113 classification in Krymholts *et al.* (1988), who subdivided the Jurassic succession into seven  
114 formations (Fig. 2). The succession starts with the Hettangian □ Pliensbachian (possibly also  
115 lowermost Toarcian) Sandzhar Formation (also called Sanjar Formation; continental  
116 conglomerates, breccias, red mudstones and siltstones; Resolutions 1977), which is only  
117 locally present and apparently constitutes the fill of rifts and small basins developed at the top  
118 of the underlying basement. It was not encountered in the investigated area. The overlying  
119 Gurud Formation, again a non-marine siliciclastic unit, represents fluvial to lacustrine  
120 environments with local development of coal deposits. It comprises the time span Toarcian to  
121 early Bajocian. The Gurud Formation, 290 to 450 m thick in the Kugitang Mountains, is  
122 overlain by the marginal- to shallow-marine siliciclastic to mixed carbonate-siliciclastic,  
123 Upper Bajocian □ Lower Bathonian Degibadam Formation (~200 m), characterized by  
124 argillaceous silt, silt, and sandstones with occasional marine fossils (ammonites, bivalves).  
125 The overlying Lower Bathonian Tangidival Formation (~30-80 m) is difficult to differentiate  
126 from the Degibadam Formation, the major difference being a greater carbonate content in  
127 form of silty marl and calcareous and/or bioclastic sandstones. The carbonate and fossil

128 content increases gradually so that the boundary between the two formations is somewhat  
129 arbitrary. This is particularly true of the sections at Sangardak and Shargun. Carbonate  
130 sediments (lime mudstones, marl, and subordinate bioclastic and oncolitic floatstones)  
131 characterize the following Baysun Formation (50-225 m). According to the literature (e.g.,  
132 Krymholts *et al.* 1988), the formation starts in the Late Bathonian, but based on ammonite  
133 finds the base is here regarded still Middle Bathonian, the top extending to the Lower  
134 Callovian. The succession continues with thick-bedded carbonates of the Middle Callovian –  
135 Kimmeridgian Kugitang Formation, followed by anhydrites, dolostones, limestones, and salt  
136 deposits of the Kimmeridgian – Tithonian Gaurdak Formation (approximately 1000 m), and  
137 by continental red beds of the Karabil Formation, the latter spanning the Jurassic-Cretaceous  
138 boundary.

139 For the Middle Callovian □ Tithonian part of the succession in the northern part of the  
140 Afghan-Tajik Basin and the Uzbekistan northern margin of the neighbouring Amu Darya  
141 Basin a new, more elaborate classification scheme has been proposed, taking into account  
142 lateral facies variations within the carbonate complex and a Tithonian age for the Gaurdak  
143 evaporites (Abdullaev & Mirkamalov 1998). As this part of the succession is not the subject  
144 of the paper, we continue to use the term Kugitang Formation for the sake of simplicity.

145

146

#### 147 *Bio- and chronostratigraphy*

148

149 The biostratigraphic zonation of the marine part of the sedimentary succession is based on  
150 ammonites, which have been investigated in great detail (e.g., Krymholts & Zakharov 1971;  
151 Mitta 2001; Mitta & Besnosov 2007). They allow a relatively detailed subdivision of the  
152 strata and can be used to define the ages of the lithostratigraphic units. Unfortunately,  
153 ammonites were found only sporadically in the field, thus only a rough correlation of sections,  
154 based largely on lithological features, could be achieved. Finds of the ammonite *Parkinsonia*  
155 *parkinsoni* near the base of the marine succession (Degibadam Formation) in the Iron Gate  
156 section confirmed the Late Bajocian age of the transgression in the area (see also Krymholts  
157 *et al.* 1988), and ammonites such as *Procerites* provided a Middle Bathonian age for the  
158 condensed base of the Baysun Formation. As no age-diagnostic ammonites were recorded  
159 from sections at Vuariz, Shargun, and Sangardak it cannot be evaluated whether, and if to  
160 what extent, the marine transgression and the boundaries of the lithostratigraphic units are  
161 diachronous.

162 The lower, non-marine parts of the sections were more difficult to date. Russian  
163 workers subdivided this part into stages based on macroscopic plant remains and pollen and  
164 spore assemblages (e.g., Gomolitzky & Lobanova 1969; Renzhina & Fokina 1978; for a  
165 summary see Vakhrameev *et al.* 1988). However, during our field work no well preserved  
166 plant remains were found that could have been used for dating the succession. The age  
167 assignments of the non-marine formations are therefore taken from Krymholts *et al.* (1988).

168 Several regional stages have been proposed for the Jurassic succession defined either  
169 on the basis of land plant associations and freshwater molluscs (Sandzhar and Gurud regional  
170 stages) or on ammonites (in ascending order Sarydiirmen, Baysun, Kugitang, and Gaurdak  
171 regional stages) (Krymholts *et al.* 1988).

172

173

#### 174 **The sections**

175

176 In the following, the eleven sections are briefly described (for their precise position see Table  
177 1). In the Kugitang Mountains two sections have been measured, one at Vandob, the other at  
178 Shalkan. In both cases the Jurassic rocks rest with angular unconformity on Palaeozoic  
179 metamorphic basement.

180

181 (1) *Shalkan section (923 m; Figs. 3, 5a)*. – At Shalkan, these metamorphic rocks are overlain  
182 by up to 2 m of brown soil; clay with scattered gravel-sized rounded quartz grains and of  
183 poorly exposed silty clay. Four thick cross-bedded, conglomeratic to gravelly, coarse-grained  
184 sandstone units fining to medium-grained sandstones occur from 30-56 m and are followed by  
185 argillaceous silt with several carbonaceous levels and some fine-grained sandstone  
186 intercalations. The overlying, predominantly argillaceous-silty sediments with occasional thin  
187 sandstone interbeds are poorly exposed and contain some coal layers. From 375 to 394 m  
188 another conglomeratic to gravelly sandstone package is present. Up to 453 m it is overlain by  
189 finer-grained coarsening-upward hemi-cycles. Apart from plant and wood fragments and  
190 occasional rootlets no fossils are present. All these sediments belong to the non-marine Gurud  
191 Formation. From 453 m onwards marine trace fossils and shell fragments occur and rare  
192 ammonites indicate a Late Bajocian age of the rocks, which consist of silt alternating with  
193 hummocky cross-stratified sandstones, arranged in thickening- and coarsening-upward cycles.  
194 From 554 m onwards, the thickness of the sandstones increases and hummock cross-  
195 stratification (HCS) is replaced by large-scale trough cross-stratification. Fine-grained units

196 are commonly black and rarely carbonaceous. These rocks belong to the Degibadam  
197 Formation. Its boundary with the overlying Tangidival Formation has been drawn where  
198 shell fragments, bivalves, and carbonate cement increase in abundance. A richly fossiliferous  
199 unit (729-733 m) with abundant ammonites and bivalves forms the base of the next  
200 stratigraphic unit, the Baysun Formation. The ammonites indicate a Middle Bathonian age of  
201 this condensed unit. The Baysun Formation is composed of silty marl, which is deeply  
202 weathered. It appears unfossiliferous, but fresh samples display numerous small infaunal  
203 bivalves preserved as internal moulds. Intercalated between the silty marl are nodular  
204 oncoidal float- to micritic rudstones. The boundary to the overlying carbonates of the  
205 Kugitang Formation is gradual.

206

207 (2) *Vandob section (799 m; Fig. 6)*. – The Vandob section, situated 18 km SSW of Shalkan, is  
208 very similar to the Shalkan section except that the coarse-grained conglomeratic sandstones  
209 rest directly on the deeply weathered metamorphic basement. Much of the argillaceous-silty  
210 part of the Gurud Formation is overgrown. The upper part of the Degibadam Formation and  
211 the Tangidival Formation are organized in well developed coarsening-upward cycles. The  
212 condensed base of the Baysun Formation contains, as in the Shalkan section, numerous  
213 ammonites. The silty marl of the lower half of the formation gives way in the upper half to  
214 nodular floatstones and marlstones. The find of the ammonite *Macrocephalites* two-thirds up  
215 indicates an Early Callovian age.

216

217 (3) *Panjab section (330 m; Fig. 7)*. – Situated 27 km northeast of Shalkan, the well exposed  
218 Panjab section starts in the middle of the Degibadam Formation. Except for differences in  
219 thickness the section mirrors those at Vandob and Shalkan. The upper part of the Baysun  
220 Formation displays hemi-cycles characterized by increasing carbonate content (marl to  
221 marlstone or wackestone). The Lower Callovian ammonite *Macrocephalites* occurs 130 m  
222 above the base of the formation.

223

224 (4) *Dalut Mine section near the village of Toda (572 m; Fig. 8)*. – The incomplete section,  
225 situated 83 km SW of the Shargun section and 35 km NE of Panjab, has been measured on the  
226 northwestern limb of a large NE-SW trending anticline. At two levels the rocks are heavily  
227 folded and faulted and the recorded thickness probably contains some error. The base of the  
228 Jurassic succession is not exposed, but the 24-m-thick basal sandstone package (Fig. 9a) most  
229 likely corresponds to the coarse siliciclastic unit overlying the basement wherever the contact

230 has been observed. The thickness of the Gurud Formation is comparable to that of the  
231 Kugitang sections. The formation is composed of an alternation of argillaceous silt,  
232 sandstones, and thin coal layers. Root horizons are widespread and plant fragments are  
233 ubiquitous. Only the lower 37 m of the marine Degibadam Formation could be measured. It is  
234 characterised by alternations of argillaceous silt and fine-grained sandstone, the latter  
235 displaying HCS or parallel-lamination followed by ripple lamination. The following part of  
236 the section is too steep for measuring. Moreover it is disrupted by a major fault. The total  
237 thickness of the Jurassic succession up to the Kugitang Formation is in the order of 900-950  
238 m, taking into account information provided by the neighbouring Derbent section.

239

240 *(5) Derbent (Iron Gate) section (411 m; Fig. 10).* – The section north of Derbent at the so-  
241 called Iron Gate, situated 9 km WNW of the Dalut mine section, exposes the upper part of the  
242 Jurassic succession. The section has been measured on the western flank of a deeply cut  
243 valley which dissects a NE-SW trending anticline. The section starts close to the base of the  
244 Degibadam Formation, which consists of fine-grained siliciclastics with thin sandstone  
245 intercalations and a 45-m-thick sandstone package in the middle. The base of the Tangiduval  
246 Formation has been placed at the first limestone bed. The formation is largely organised as  
247 asymmetric coarsening-upward cycles. The top beds contain bivalves and ammonites. The  
248 boundary to the overlying Baysun Formation is sharp. The Baysun Formation is similar to  
249 that in the Kugitang Mountains, i.e. dominated by silty marl and marl with some  
250 intercalations of oncoidal floatstones and micritic rudstones. The transition to the Kugitang  
251 Formation is gradual (Fig. 5h). The Iron Gate section and the close-by Dalut Mine section  
252 together represent a complete section through the investigated succession with a thickness of  
253 approximately 935 m (Figs. 8, 10).

254

255 *(6)-(7) Shargun sections (358 m; Fig. 11).* – The coal mine north of the town Shargun lies 115  
256 km NE of Panjab. The metamorphic basement rocks are overlain by a thin conglomeratic  
257 gravelstone followed by lenticular coarse-grained sandstone with tree trunks, wood remains,  
258 abundant plant fragments, rootlet horizons, and a 2-m-thick coal bed. From 40 m to 290 m the  
259 succession is dominated by stacked, several-m-thick sandstone packages with erosional base,  
260 large-scale trough cross-bedding, and abundant wood pieces and wood logs (Fig. 5c).  
261 Towards the top these sandstone packages become thinner and fine-grained, and occasional  
262 carbonaceous intercalations increase in thickness. The marine part of the succession is merely  
263 64 m thick and consists of 14 m predominantly siliciclastic sediments

264 (Degibadam/Tangiduval Formation) followed by 50 m of fine-grained, mixed carbonate-  
265 siliciclastic sediments of the Baysun Formation. Unfortunately, no ammonites were  
266 recovered. Quite possibly, the boundaries of the formations are diachronous when compared  
267 with the sections in the Kugitang Mountains.

268

269 (8) *Sangardak section (328 m; Fig. 12)*. – The section has a similar thickness as the close-by  
270 Shargun section, but coarse-grained sandstones are mainly restricted to the lower 60 m of the  
271 section, the remaining non-marine part of the succession being dominated by argillaceous silt.  
272 The marine part is twice as thick (131 m) as at Shargun (64 m), and the Baysun Formation is  
273 missing. The sandstones in the mixed carbonate-siliciclastic Tangiduval Formation are  
274 coarser than in the other sections. The base of the overlying Kugitang Formation contains, in  
275 contrast to most other sections, planar cross-bedded oo-grainstones.

276

277 (9)-(10) *Vuariz sections (84 m; Figs. 13, 14)*. – Four short sections, 1.5 to 2.5 km apart, were  
278 measured north and northeast of the Vuariz village. The distance to the Dalut Mine section is  
279 61 km. The first two sections, which strongly overlap, comprise the Gurud Formation (82 m)  
280 up to the base of the Degibadam Formation (Fig. 13a, b). The Palaeozoic basement is overlain  
281 by a thin conglomerate and a few metres of poorly exposed carbonaceous argillaceous silt  
282 followed by a 48-m-thick stack of coarse-grained, partly conglomeratic sandstones, with  
283 erosional bases. Towards the top fine-grained siliciclastics with plant debris and root  
284 horizons, which are subordinate in the lower half, dominate. Remarkable is the strongly  
285 reduced thickness of the Gurud Formation.

286 The transgression is indicated by trace fossils and shell concentrations. The  
287 Degibadam and Tangiduval formations cannot be differentiated and comprise only around 25  
288 m of sandstones, bioclastic sandy siltstones and soft silt (Fig. 13c). The Baysun Formation  
289 starts with nearly 40 m of bioturbated limestones, mainly onco-floatstones, -rudstones, and  
290 fine-grained intra-packstones topped by nearly 5 m of oo-grainstones. The following  
291 approximately 50 m to the base of the Kugitang Formation have been removed by faulting. A  
292 26-m-thick lateral equivalent of the carbonates, largely developed as peritidal packstones with  
293 birdseyes and fenestral fabrics, has been measured beyond the northeastern end of the pass at  
294 N 38°49'29.6'', E 67°11'26.3'' (Fig. 14). The following approximately 50 m up to the base of  
295 the Kugitang Formation are largely covered by scree, but are clearly composed predominantly  
296 of soft, fine-grained sediments (?marl/silty marl). The base of the Kugitang Formation

297 consists of 6 m of coarse-grained, partly gravelly, large-scale trough cross-bedded sandstones  
298 alternating with sandy lime mudstone beds.

299

300

### 301 **Facies associations and palaeoenvironments**

302

303 The investigated succession consists of continental facies in the lower part and of fully marine  
304 environments in the upper part. The transgressive surface is difficult to pinpoint  
305 sedimentologically but can be identified with the help of trace fossils. The following chapter  
306 is a brief description and discussion of the main environments. A summary can be found in  
307 Table 2.

308

309

310 *Braided river deposits (e.g., basal parts of Vuariz, Shalkan, and Vandob sections; lower part*  
311 *of the Shalkan section; Fig. 15a)*

312

313 Coarse-grained to gravelly or conglomeratic sandstone bodies that fine up to medium or fine  
314 grain size are composed of stacked units with convex erosional bases and lateral variations in  
315 thickness. They form packages up to 35 m in thickness and occur mainly at the base of the  
316 Jurassic succession. The degree of maturity strongly varies: In some areas (e.g., at Vandob)  
317 sand grains and pebbles consist mainly of quartz and mica flakes are common, in others the  
318 sandstones are arkosic or lithic and the pebbles consist of black chert, metamorphic rock  
319 fragments and subangular to subrounded quartz (e.g., at Shalkan, and Vuariz; Fig. 16a). Wood  
320 fragments are abundant and locally tree trunks may be found at the base of the individual  
321 units. Large-scale trough cross-stratification is pervasive. It may grade into ripple lamination  
322 in the finer-grained top parts.

323

324 The sandstones can be interpreted as the fills of amalgamated shallow braided river

325

326

327

328

329 *Meandering river deposits (e.g., base of Shargun section, Dalut Mine section at 154 m; Fig.*  
330 *15b)*

331

332 In the Gurud Formation, fine- to coarse-grained, commonly arkosic sandstones with erosional  
333 base, several metres to decametres in thickness, exhibit large-scale trough cross-stratification.  
334 They fine up into ripple-laminated silty sandstone or siltstone, and in some cases the top is  
335 rooted. Plant debris and wood fragments are common, and wood logs occur occasionally near  
336 the base of the sandstone bodies. Distinct epsilon cross-bedding is developed in some cases  
337 (e.g., in the Dalut Mine section; Fig. 9b). Stacking of several-metres-thick sandstone bodies is  
338 commonly seen. In the valley immediately W of the Shargun section intercalated dark-grey  
339 silty clay with some indistinct siltstone beds may laterally grade into intercalations of thick  
340 siltstone-sandstone beds with epsilon cross-bedding.

341 The sandstone bodies clearly are the fill of fluvial channels (Miall 1996). Epsilon  
342 cross-bedded units can be interpreted as point-bar deposits produced by lateral migration of  
343 the channel. The fine-grained, thinner-bedded top parts of individual units with occasional  
344 rootlets correspond to levee deposits. These fluvial channels are clearly of the meandering  
345 type. The lenticular fine-grained deposits that laterally grade into point-bar deposits are  
346 interpreted as the fills of abandoned channels (oxbow lakes).

347

348

349 *Flood plain deposits (e.g., Dalut Mine section at 70-82 and 86-97 m; Fig. 15c)*

350

351 Dark-grey argillaceous silt and silty clay with intercalations of cm- to dm-thick siltstones and  
352 fine-grained sandstones with sharp, commonly erosional base, rich in plant debris, are  
353 widespread in the Gurud Formation. The sandstones exhibit large-scale trough cross-bedding  
354 or current ripple-lamination and occasionally are topped by a rootlet horizon. The fine-grained  
355 sediments in-between are, in some cases, highly carbonaceous and may contain thin layers of  
356 coal. Rarely, strongly ferruginous, mottled, fine-sandy silt layers with rootlets form  
357 conspicuous horizons. At the base of the Shalkan section (Fig. 3) brown clay with scattered  
358 quartz granules fills pockets of the underlying deeply weathered metamorphic Palaeozoic  
359 basement.

360 The argillaceous silt is an alluvial deposit. The sandstone/siltstone interbeds  
361 correspond to overbank deposits (crevasse splays) that formed on a swampy flood plain with  
362 vegetation (rootlets) that was occasionally so dense that highly carbonaceous to coaly rocks  
363 resulted. Mottled ferruginous siltstones are interpreted as soil horizons on a wet flood plain. A  
364 different kind of paleosol occurs at the base of the Shalkan section. The very poorly sorted

365 brown gravely clay is a brown soil, rich in iron, that today forms in temperate climates (e.g.,  
366 Schaetzl & Anderson 2005). Together with the strongly altered basement it points to a  
367 prolonged phase of weathering on the incipient flood plain.

368

369 *Swamps (e.g., Dalut Mine section at 40-47 m, 267 m, 418 m, 500 m; Shargun section at 17-19*  
370 *m; Fig. 15d)*

371

372 Coal layers and dark-grey to blackish, highly carbonaceous clay or silty clay, rich in plant  
373 fragments and underlain by rootlet horizons, are interpreted as swamp deposits. Commonly,  
374 such swamps formed at the margins of lakes as can be seen from their stratigraphic context  
375 (e.g., in the Dalut Mine section at 267 m), but also developed on wet flood plains (e.g., Dalut  
376 Mine section at 500 m). The thickest coal layer recorded in any of the sections was 120 cm  
377 thick.

378 In many of the coal layers and highly carbonaceous fine-grained siliciclastics of the  
379 Gurud Formation the plant material is, however, allochthonous. This assumption is  
380 corroborated by their occurrence within lake successions (e.g., Dalut Mine section at 318-322  
381 m) and by a lack of rootlet horizons. Apparently, the plant material has been transported into  
382 the lakes from swampy coastal areas or has been introduced by rivers that reworked swamp  
383 deposits on the flood plain.

384

385 *Lake deposits (e.g., Dalut Mine section at 24-40 m, 234-267 m, 396-429 m, Shalkan section*  
386 *395-453 m, Fig. 15e, f)*

387

388 Monotonous dark-grey argillaceous silt and silty clay, in some horizons strongly  
389 carbonaceous or with dm-thick coal layers, are the dominant facies types in the Gurud  
390 Formation of the Shalkan and Dalut Mine sections. The fine-grained siliciclastics are  
391 occasionally interrupted by cm- to dm-thick fine-grained sandstones that exhibit ripple  
392 lamination and may contain wood fragments. Large orange carbonate and claystone  
393 concretions occur at some levels; small ferruginous concretions are rare. A second very  
394 common facies association in these two sections are m-scale coarsening-upward cycles. They  
395 start with dark-grey argillaceous silt or silty clay and grade upward into silt, fine-sandy silt  
396 and fine-grained sandstone. Plant fragments, carbonaceous beds and thin coal layers are  
397 common. Rarely, finely interlayered bedding is developed at the base of such cycles. The  
398 silty-sandy beds commonly are ripple-laminated and the top sandstones often exhibit large-

399 scale trough cross-stratification and occasionally rootlets. In some cases (e.g. Shalkan section  
400 at 356 m) bedded fine-grained sandstones are parallel-laminated with sharp erosional base or  
401 display hummocky cross-stratification. Some of the large-scale cross-bedded sandstones on  
402 top of the cycles display a sharp erosional base.

403 The facies associations described above are best interpreted as deposits of various lake  
404 subenvironments. The monotonous fine-grained siliciclastic sediments clearly correspond to  
405 basinal parts of lakes. Thin coal layers, common plant debris, and the carbonaceous nature of  
406 some beds indicate that much plant material was introduced into the lakes which must have  
407 been surrounded by dense vegetation. The coarsening-upward sequences are progradational  
408 cycles that record shallowing of the lake from basinal to marginal environments. They also  
409 document an increase in water energy as is shown by the primary sedimentary structures.  
410 Rootlet horizons at the top of the some of the cycles indicate a transition to swampy areas.  
411 Rare HCS and parallel-laminated beds are evidence that parts of the lakes were influenced by  
412 storm-waves and storm-induced flows. These coarsening-upward successions document the  
413 development from offshore to shoreface and foreshore environments and are probably related  
414 to lacustrine delta progradation. A distinction between the two developments is difficult, if no  
415 fluvial channel is found on top of the shallowing sequence.

416 The size, depth, and duration of these lakes differed considerably, judging from the  
417 variable thicknesses of the lacustrine sediments. Small shallow lakes and large lakes,  
418 persisting for thousands of years, apparently existed side by side. Moreover, the common  
419 development of progradational cycles (see below) points to repeated phases of contraction and  
420 expansion of these lakes.

421

422 Following the transgression in the Late Bajocian, several marine facies associations are  
423 documented in the Degibadam, Tangiduval, and Baysun formations.

424

425 *Distributary channel deposits (e.g., Iron Gate section at 97-115 m, Vandob section at 378-*  
426 *388 m, Shalkan section at 617-634 m; Fig. 15g)*

427

428 Ten- to twenty-metres-thick packages of immature sandstone with a sharp erosional base,  
429 fining up-section from medium or coarse to a fine grain size are found in the marine  
430 Degibadam Formation of the Iron Gate (Fig. 9d top), Vandob, and Shalkan sections.  
431 Sedimentary structures change up-section from large-scale trough cross-bedding to ripple-  
432 lamination. Wood pieces are common, particularly near the base.

433            Their erosional base and fining-upward nature identify the sandstones as channel  
434 deposits. At Vandob and Iron Gate they are underlain by coarsening-upward successions  
435 interpreted as delta front deposits (see below). Consequently the channel deposits represent  
436 distributary channels of the delta plain.

437

438 *Prodelta and delta front deposits (e.g., Iron Gate section 55-97 m, Vandob section at 370-388*  
439 *m; Fig. 15h, i)*

440

441 In the case of the Iron Gate section, the coarse-grained sandstones interpreted as fill of a  
442 distributary channel are underlain by six metre-scale coarsening-upward sequences grading  
443 from fine-grained ripple-laminated sandstone to medium-grained large-scale trough cross-  
444 bedded sandstone (Fig. 16g). In one sequence, HCS was encountered in the basal part, in  
445 another sharp-based parallel-laminated sandstone beds occur in the same position. Wood  
446 pieces are present in two of the cycles. Trace fossils include *Thalassinoides* and *Gyrochorte*.

447            Below these units bioturbated silty clay prevails. It contains cm- to dm-thick  
448 intercalations of ripple- or parallel-laminated sandstone, spaced 1 to 2 m, with *Gyrochorte*,  
449 some wood fragments, and rare ammonites.

450            The strongly bioturbated fine-grained units are interpreted as prodelta deposits which  
451 are occasionally punctuated by coarser hyperpycnal flow deposits which may reflect flooding  
452 events in the hinterland and a corresponding greater discharge of sediment-laden waters (e.g.,  
453 Mutti *et al.* 2003). They grade upwards into stacked lower to upper delta-front cycles. The  
454 increase in grain size and the change from ripple lamination to large-scale cross-bedding  
455 indicates an increase in the energy level due to shallowing. In the Vandob section, the delta  
456 front deposits are composed of amalgamated HCS sandstones which develop from  
457 bioturbated silty fine-grained sandstone. At Shalkan, in contrast, the distributary sandstones  
458 are underlain with sharp boundary by argillaceous silt, which documents a sudden lowering of  
459 the base level.

460

461 *Deposits of the tide-influenced inner siliciclastic ramp (e.g., Panjab section at 24-39 m;*  
462 *Vandob section at 483-494 m; Fig. 15j)*

463

464 In the Panjab section interlayered bedding is prevalent for about 15 m near the base of the  
465 exposed succession. It is developed either as coarsely interlayered bedding consisting of 2- to  
466 5-cm-thick ripple-laminated fine-grained sandstone beds and thin argillaceous interbeds or as

467 a finer variety where sandstones are 0.5-1 cm and argillaceous silt interbeds 1-2 cm in  
468 thickness. Near the top of this facies type a 50-cm-thick ripple-laminated, medium-grained  
469 sandstone occurs. It has a sharp base, contains mud clasts, and displays some lenticular  
470 bedding in the middle. Lenticular bedding and flaser bedding usually occur associated with  
471 the interlayered bedding in the Panjab and Vandob sections.

472 The interlayered, flaser, and lenticular bedding points to regular changes in water  
473 energy suggestive of some tidal influence (but not necessarily of intertidal conditions). The  
474 medium-grained sandstone with clay pebbles may be the submarine continuation of a tidal  
475 channel.

476

477 *Protected low-energy inner ramp deposits (e.g., Shalkan section at 571-574 and 577-596 m,*  
478 *Vandob section at 406-452 m; Panjab section at 34-36 m; Fig. 15k)*

479

480 In the upper part of the Degibadam Formation of the Kugitang Mountains dark-grey, partly  
481 bioturbated, argillaceous silt and fine-sandy silty clay predominate. At Vandob they are rich  
482 in plant fragments. Highly carbonaceous levels are also present. Intercalated between these  
483 fine-grained sediments are cm-thick fine-grained sandstone beds. In the Shalkan section they  
484 are parallel laminated and form the top of metre-scale coarsening-upward sequences that start  
485 with argillaceous silt, which grades into ripple-laminated siltstones as an intermediate facies.

486 The scarcity of large-scale sedimentary structures, the predominantly fine-grained  
487 sediment, and the pervasive bioturbation point to prevalent low-energy conditions. The high  
488 organic carbon content, including highly carbonaceous beds, suggests that the sediments were  
489 deposited nearshore, most likely in a protected embayment. The coarsening-upward cycles  
490 record shallowing and the intermittent influence of storm-induced flows.

491

492 *Submarine dune deposits of the inner to middle siliciclastic ramp (e.g., Panjab section at 95-*  
493 *98.0 m, and 102.5-104 m, Vandob section at 542-545.5 m, Shalkan section at 646-648.5 m;*  
494 *Fig. 15l)*

495

496 Dm- to m-thick, commonly bioclastic, fine- to medium-grained sandstones with large-scale  
497 cross-stratification and sharp base occur repeatedly in the Tangiduval Formation of the  
498 Panjab, Shalkan, and Vandob sections. They are commonly associated with shell debris, more  
499 rarely with pavements and lenticles of disarticulated bivalve shells, and form the upper part of  
500 coarsening-upward sequences. The top of the sandstones exhibits, in some cases, oscillation

501 ripples. Beds lower down in the succession may also be thoroughly bioturbated (e.g., Fig.  
502 16c).

503 The sedimentary structures indicate deposition during high-energy conditions and, at  
504 the top, occasional wave influence. Abundant bioclasts and mollusc remains point to fully  
505 marine conditions. Found at the top of coarsening- and shallowing-upward cycles they are  
506 interpreted as small submarine dunes that developed on the middle to partly inner siliciclastic  
507 ramp. Alternatively, they may represent upper shoreface deposits.

508

509 *Storm-wave dominated middle siliciclastic ramp deposits (e.g., Vandob section at 503-514 m,*  
510 *Shalkan section at 454-513 m, 524-540 m; Fig. 15m)*

511

512 In the Kugitang Mountains the lower part of the marine succession is characterised by  
513 bioturbated argillaceous silt or silt with numerous intercalations of fine-grained cm- to dm-  
514 thick sandstones. The latter have a sharp base and exhibit HCS (e.g. Fig. 16b), in some cases  
515 ripple lamination. The thicker HCS beds are commonly amalgamated. Bedding planes  
516 occasionally are developed as shell pavements, whereas in the bioturbated parts scattered  
517 bivalves (e.g., *Myopholas*, *Pseudolimea*, *Pleuromya*), rare ammonites, some wood fragments,  
518 and the trace fossils *Chondrites* and *Taenidium* occur. Generally, the HCS sandstones are  
519 arranged as thickening-upward cycles.

520 The fossils indicate a fully marine environment. The finer-grained, high bioturbated  
521 sediment document low-energy conditions, whereas the sandstones with HCS can be  
522 interpreted as products of storm waves (e.g., Aigner 1979; Aigner & Reineck 1982). The  
523 depositional environment can therefore be classified as the middle ramp below the fair-  
524 weather wave-base.

525

526 *Storm-flow influenced outer siliciclastic ramp deposits (e.g., Iron Gate section at 14-39 m,*  
527 *Panjab section at 4-16 m, Dalut Mine section at 552-562 m, Vandob section at 461-483 m;*  
528 *Fig. 15n)*

529

530 A facies association composed of highly bioturbated argillaceous silt alternating with cm-  
531 thick fine-grained sandstones that exhibit ripple lamination or parallel lamination topped by  
532 ripple lamination is common in the Bajocian marine succession of southern Uzbekistan. The  
533 sandstones have a sharp base and are commonly associated with flute casts and/or tool marks.  
534 Sand-filled structures, semicircular in cross-section and often with a shell lag at the base,

535 occur isolated or at the base of the sandstone beds. Trace fossils include *Gyrochorte*,  
536 *Chondrites*, *Thalassinoides*, and *Rhizocorallium irregulare*. Bivalves such as *Meleagrinnella*  
537 commonly form shell pavements, ammonites are rare.

538 As in the case of sandstones produced by storm-waves (see above), the parallel- and/or  
539 ripple-laminated sandstones indicate brief high-energy events that episodically disturbed a  
540 generally low-energy environment. The sharp base with flute casts and the semi-circular  
541 sandstones are indicative of erosional events produced by a high flow regime, whereas normal  
542 grading and the change from parallel to ripple lamination within single beds is evidence of  
543 flow deceleration. The semi-circular sandstones are interpreted as gutter casts, i.e. narrow,  
544 elongated erosional structures (Aigner 1982). All these features are characteristic of the outer  
545 ramp under the episodic influence of storm-induced offshore-directed currents that originate  
546 after the waning of storms (e.g., Aigner & Reineck 1982). The fine-grained bioturbated  
547 background sediment, in contrast, indicates low energy conditions.

548

549 *Low-energy mixed carbonate-siliciclastic outer ramp deposits (e.g., Shalkan section at 732-*  
550 *830 m, Vandob section at 580-696 m, Panjab section at 142-207 m; Fig. 15o)*

551

552 The lower part of the Baysun Formation in all sections is characterized by monotonous fine-  
553 grained, partly shaley, partly bioturbated silty marl. Poorly preserved small bivalves such as  
554 *Corbulomima* and *Nicaniella* occur scattered or concentrated in thin bands.

555 The sediments clearly belong to the low-energy outer ramp. The silt has been most  
556 likely introduced by suspension clouds, possibly in connection with storms, or by bed-load  
557 transport in form of thin laminae and streaks which subsequently were destroyed by  
558 bioturbation. The thin shell concentrations testify that occasionally winnowing took place,  
559 probably produced by distal storm-induced flows.

560

561 *Condensed mixed carbonate-siliciclastic outer ramp deposits (e.g., Vandob section at 573-*  
562 *579 m, Shalkan section at 729-733 m, Panjab section at 141-144 m; Fig. 15p)*

563

564 At the base of the Baysun Formation, several metres of strongly bioturbated, rubbly, partly  
565 nodular, fine-sandy bio-wacke- to biofloatstone with interbeds of marly silt are developed in  
566 the Kugitang Mountains and at Panjab. The beds are highly fossiliferous with common  
567 bivalves (e.g., *Entolium*, *Pleuromya*, *Ctenostreon*, large *Liostrea*, and *Bucardiomya*),  
568 ammonites (mainly large *Procerites*), brachiopods, and some gastropods (e.g., *Obornella*).

569 Many of the bivalves are articulated and some of the burrowing bivalves are preserved in  
570 growth position.

571         Considering that ammonites are generally rare in the succession, the abundant  
572 ammonites and in situ preserved benthic faunal elements point to low rates of sedimentation  
573 persisting for quite some time. This increased the proportion of biogenic hardparts in the  
574 sediment. The facies is clearly condensed compared to the sediments below and above, but  
575 stratigraphic condensation i.e., mixing of taxa belonging to different zones or subzones, has  
576 not been observed. Both sediment and taphonomic features indicate a low-energy outer ramp  
577 environment.

578

579 *Low-energy marl and mud- to wacke-/floatstones of the outer carbonate ramp (e.g., Vandob*  
580 *section at 696-799 m, Iron Gate section at 280-409 m, Panjab section at 207-330 m; Fig.*  
581 *15q)*

582

583 This facies association is similar to the last one except that the silt fraction is negligible.  
584 Bioturbation is pervasive and primary sedimentary structures are absent. The wacke- to  
585 floatstones are bioclastic and commonly contain oncoids (Fig. 16e, f). Occasional packstone  
586 beds consist mainly of bioclasts. The carbonates commonly have a nodular texture. Trace  
587 fossils include *Thalassinoides*, and body fossils occasional bivalves (e.g., *Pleuromya*,  
588 *Protocardia*, *Corbulomima*, oysters), rare gastropods (*Pseudomelania*), corals, and  
589 ammonites (*Macrocephalites*).

590         Occasionally, bio-onco-rudstones are intercalated within the succession (e.g., Fig.  
591 16d). As their matrix is, in most cases, micritic and as they exhibit a nodular texture it is  
592 likely that they formed in-situ on the outer ramp. In contrast, rare, thin beds of rudstone with  
593 sparitic matrix and small coated grains or oyster fragments most likely were introduced from  
594 shallower areas of the ramp by storms.

595

596 *Low-energy, peritidal lagoonal carbonates (Vuariz section IV; Fig. 14)*

597

598 Sediments of peritidal origin are rare in the investigated succession. They have been  
599 encountered only in the Baysun Formation of Vuariz. The sediments consist of very fine-  
600 grained packstones, rarely of carbonate mudstones, with scattered birdseyes and laminoid  
601 fenestral fabrics (Fig. 14). Repeatedly, cm-thick, irregularly laminated bands are intercalated

602 as are rare beds of oncoid rudstones. Scattered gastropods are the only faunal element. The  
603 birdseye limestones develop from onco-floatstones embedded in a fine packstone matrix.

604 Birdseyes, laminoid fenestral fabrics, and fine, irregular lamination are typical of algal  
605 origin and generally interpreted as having formed in the intertidal to very shallow subtidal  
606 zone (e.g., Shinn 1983; Flügel 2010). At Vuariz they are the lateral equivalent of ooid  
607 grainstones (Vuariz section III; Fig. 13c). This suggests that they formed in a low-energy  
608 lagoonal environment protected by ooid bars. Their occurrence in the Baysun Formation,  
609 which at most other sections represents offshore environments, supports the interpretation of  
610 the Vuariz area as being close to the basin margin.

611

### 612 **Macroflora and benthic macrofauna**

613

614 Several land plant associations have been recognised in the non-marine part of the succession,  
615 but no identifiable macroflora has been encountered during the field work. Thus, Gomolitzky  
616 (in Shayakubov & Dalimov 1998) recognised the Kamyshbash Flora (with e.g., *Osmundopsis*  
617 *Phlebopteris*, *Dictyophyllum*, *Thaumatopteris*, and *Nilssonia*) and the Shurab Flora (documented  
618 by *Neocalamites*, *Marattiopsis*, *Coniopteris*, *Phlebopteris*, *Clathropteris*, *Dictyophyllum*,  
619 *Hausmannia*, *Cladophlebis*, and *Anomozamites gracilis*) in the Lower Jurassic Sandzhar  
620 Formation and another association with *Equisetum*, *Mazattina*, *Coniopteris*, *Cladophlebis*,  
621 *Ptilophyllum*, and *Nilssonia* in the Gurud Formation. According to Vakhrameev *et al.* (1988)  
622 floral associations allow to differentiate between the Hettangian-Sinemurian, Toarcian, Aalenian,  
623 Bajocian, and Bathonian stages. These associations have been used extensively to date the non-  
624 marine rocks.

625 No benthic macrofauna has been found in the non-marine part, in which Martinson and  
626 Mikulina (in Shayakubov & Dalimov 1998) recorded molluscan assemblages characterized by the  
627 bivalves *Unio*, *Ferganoconcha*, and *Sibireconcha* (Kim *et al.* 2007). In the marine part of the  
628 succession bivalves are common at some levels. In the Upper Bajocian they commonly form  
629 pavements of disarticulated valves, common elements being the infaunal *Myopholas* and the  
630 epibyssate *Camptonectes*. Bivalves increase in abundance in the Tangiduval Formation and  
631 particularly in the condensed basal beds of the Baysun Formation. Common taxa include  
632 *Pholadomya* (*Bucardiomya*), *Pleuromya*, *Homomya*, *Inoperna*, *Integricardium*, *Protocardia*,  
633 *Actinostreon*, *Liostrea*, and *Nanogyra*. These genera are typical elements of the benthic  
634 macrofauna occurring in shallow-marine environments of the Jurassic epicontinental seas from  
635 western and eastern Europe to Iran. Gastropods (e.g., *Obornella*) are comparatively rare as are

636 brachiopods, the latter occurring mainly in the condensed base of the Baysun Formation where  
637 they are represented by at least five genera.

638         At a first glance, the marls and silty marls of the Baysun Formation appear to be devoid of  
639 fossils, but in fresh material small infaunal bivalves such as *Corbulomima* and *Nicaniella* are  
640 common at numerous levels as poorly preserved composite or external moulds. They constitute  
641 typical softground assemblages, well known from numerous fine-grained Jurassic successions  
642 elsewhere (e.g., Fürsich 1977; Fürsich & Werner 1986; Fürsich *et al.* 2004). As the percentage of  
643 endemic faunal elements appears to be low, the Amu Darya and Afghan-Tajik basins appear to  
644 have been well connected with other shelf seas situated on the southern margin of the Turan  
645 Platform.

646

647

## 648 **Cycles**

649

650 As has been mentioned in the facies descriptions, the various facies are commonly organised  
651 into cycles. These cycles are highly asymmetric and represent either thickening-/coarsening-  
652 upward cycles or fining-/thinning-upwards sequences.

653

### 654 *Fluvial cycles (Fig. 17a, b)*

655

656 Fining-upward cycles are nearly exclusively developed in the non-marine part of the  
657 succession. They start with fine-to coarse-grained, large-scale trough cross-stratified  
658 sandstones, which may be gravelly or pebbly, and exhibit an erosional base. Up-section they  
659 fine to ripple-laminated sandstone or siltstone and, finally, to argillaceous silt.

660         These cycles can be interpreted as classical fluvial cycles, the basal sandstone  
661 representing channel deposits which fine upwards into levee deposits, which may be rooted,  
662 and into fine-grained sediments of the flood plain. Commonly these cycles are stacked on top  
663 of each other and the fine-grained parts often have been cannibalized by the next channel  
664 generation (e.g., in the Shargun section at 0-32 m and the Vandob section at 0-12 m). This  
665 applies particularly to braided river channels as at Vandob, but is also seen in the point-bar  
666 deposits composing the lower 32 m of the Shargun section. In the latter case, the flood plain  
667 must have been relatively narrow so that laterally migrating channels repeatedly cut into older  
668 channel deposits.

669

### 670 *Progradational lacustrine cycles (Fig. 17 c, d)*

671

672 Coarsening- and thickening-upward cycles are widespread in the lacustrine successions of the  
673 Gurud Formation. Starting with argillaceous silt to silty clay, these sediments are followed by  
674 intercalations of thin ripple-laminated siltstone to fine-grained sandstone beds which thicken  
675 upwards into m-thick fine-grained sandstone, the top of which may be rooted and followed by  
676 coal. In some cases, the latter is overlain by large-scale trough cross-bedded fine- to medium-  
677 grained sandstones with erosional base.

678         These cycles indicate a shallowing of the lake, commonly caused by progradation of  
679 small deltas. This is confirmed where the top sandstone is a lenticular deposit, which can be  
680 interpreted as a distributary channel. In other cases, the shallowing was a result of lacustrine  
681 coastline progradation and led to the development of swamps as is demonstrated by root  
682 horizons and/or coal layers. The fact that these lacustrine progradational cycles are often only  
683 a few metres thick and alternate with fluvial channel and flood plain deposits indicates that  
684 most of the lakes were shallow and of limited extent and duration.

685

686 *Marine deltaic cycles (Fig. 17e)*

687

688 Large-scale, decametre-thick thickening- and coarsening-upward cycles are comparatively  
689 rare and restricted to the Degibadam Formation (e.g., in the Iron Gate and Vandob sections).  
690 They start with bioturbated silty clay to fine-sandy silt, followed by ripple-laminated, parallel-  
691 laminated or hummocky to large-scale trough cross-stratified sandstones. The latter are cut by  
692 distinctly incised large-scale trough cross-bedded medium- to coarse-grained sandstones,  
693 which in the case of the Vandob example contain large wood fragments. In the case of the  
694 Iron Gate section, this nearly 20-m-thick sandstone body fines upwards into ripple-laminated  
695 fine-grained sandstones (Fig. 20).

696         The described successions are classical delta cycles (e.g., Reading & Collinson 1996),  
697 starting with bioturbated prodelta deposits which are replaced up-section by delta-front  
698 sandstones, partly under storm-wave influence and end with large distributary channels. In the  
699 Iron Gate section (Fig. 10 at 70-96 m) several delta-front sandstone cycles are stacked on top  
700 of each other recording either autocyclic switching of the position of the nearby distributary  
701 channel or small-scale sea-level fluctuations.

702

703 *Progradational cycles of the storm-wave influenced ramp (Fig. 17f)*

704

705 Much of the Degibadam Formation is composed of cycles which are usually a few metres in  
706 thickness and start with strongly bioturbated silty clay to silt with sporadic intercalations of  
707 cm-thick HCS sandstones. These sandstones thicken up-section and become more common.  
708 The top bed often is a dm- to m-thick fine-grained sandstone composed of amalgamated HCS  
709 beds. Modifications of this cycle type consist of bioturbated silt coarsening-upward into fine-  
710 grained sandstone with only the top bed exhibiting HCS (e.g., Vandob section at 296-302 m  
711 and 337-370 m).

712 The widespread hummocky cross-stratification indicates that these cycles developed  
713 on the storm-wave influenced middle ramp. The increase in grain size, bed thickness, and  
714 abundance of HCS beds up-section either record shallowing and a shift of the depositional  
715 environment towards the inner part of the middle ramp or else increasing storm intensity, in  
716 this case being a climatic signal and not necessarily involving changes in relative sea level  
717 (resulting from local vertical movements due to tectonics and from eustasy). However, even  
718 changes in relative sea level may be ultimately climatically controlled in shallow-water areas  
719 by greater erosion and run-off during more humid phases.

720 Cycles where only the top part exhibits HCS, the rest being thoroughly bioturbated,  
721 probably represent the outer middle ramp close to the storm wave-base, where much evidence  
722 of storm-wave sedimentation was subsequently destroyed by bioturbation.

723

724 *Cycles of the outer to middle siliciclastic ramp (Fig. 17g)*

725

726 Metre-scale cycles composed of bioturbated argillaceous silt which grades into bioturbated to  
727 ripple-laminated fine-grained sandstone and end with large-scale trough cross-bedded  
728 sandstone occur commonly in the Tangiduval Formation. Bivalves and brachiopods may  
729 occur in the bioturbated parts, while in the cross-bedded top part shell debris prevails.

730 The cycles reflect an increase in the energy level, most likely in connection with  
731 shallowing. The cross-bedded top unit is interpreted as megaripples or small dunes, which  
732 may have migrated across the ramp during times of elevated water energy such as storms.

733

734 *Cycles of the storm-flow dominated outer siliciclastic ramp (Fig. 17h)*

735

736 Cycles of the siliciclastic outer ramp consist mainly of bioturbated argillaceous silt with  
737 occasional intercalations of 2-5 cm thick sharp-based ripple-laminated fine-grained  
738 sandstones. Towards the top, the density of the sandstone intercalations increases and the top

739 sandstone bed may reach 10 cm or more in thickness. Occasionally the sandstones represent  
740 couplets whereby a parallel-laminated lower part is overlain by a ripple-laminated upper part.  
741 The lower surface of the sandstones exhibits flute casts and tool marks. In some cases, gutter  
742 casts are associated with the sandstones.

743           The sedimentary structures and lower surface features are indicative of short-lived  
744 high velocity currents produced by storm processes, which transport sand in an offshore  
745 direction (e.g., Walker & Plint 1992). The increase in thickness and density of the sandstone  
746 beds reflects increasing storm intensity which most likely is related to shallowing but as  
747 discussed above might also be due to climatic changes. As HCS is not encountered, an outer  
748 ramp position of the cycles is envisaged.

749

750 *Cycles of the outer carbonate ramp (Fig. 17i, j)*

751

752 Cycles are also developed in the fine-grained mixed carbonate-siliciclastic part of the  
753 succession (Baysun Formation). They are several decimetres to metres in thickness and start  
754 with marl or silty marl, commonly shaley but also containing some winnowed pavements of  
755 small infaunal bivalves. Towards the top of the cycles the carbonate content increases, which  
756 is documented by bioturbated carbonate mudstones to bio-wackestones and onco-floatstones,  
757 commonly of a nodular texture.

758           These cycles are characterized by directed changes in the carbonate-clay ratio. They  
759 are interpreted as reflecting a decrease in the input of fine-grained siliciclastic material. This  
760 may have been brought about by an increasing distance of the sediment source and thus  
761 would correspond to a deepening, assuming that carbonate production remained more or less  
762 constant. The cycles can, however, be also explained to reflect shallowing, assuming that this  
763 led to increased carbonate production. The latter view is favoured due to the widespread  
764 occurrence of microbial oncoids, which are never present in the marls and which are evidence  
765 that the depositional environment was at least in the lower part of the photic zone. As in the  
766 case of some other cycles discussed above, an alternative explanation involving a reduced  
767 terrigenous input due to climatic changes is also feasible. The latter alternative would not  
768 require changes in water depth.

769

770

771 **Discussion**

772

773 *Lateral and temporal facies pattern (Fig. 18)*

774

775 The study area comprises only the northwestern part of the Afghan–Tadjik Basin. In this area,  
776 the greatest thickness of the Lower Jurassic – Lower Callovian succession is found in the  
777 Kugitang Mountains with 924 m (Shalkan section), the smallest at Sangardak (328 m),  
778 although at Vuariz, where only part of the marine succession could be measured (the rest  
779 could just be estimated), it is even considerably less (probably around 200-210 m).

780 Palaeogeographic facies maps have been produced by Egamberdiev and Ishniyazov (1990).

781 Their facies interpretations are, however, not always supported by our data.

782

783 *Gurud Formation.* The non-marine part of the succession reaches 453 m at Shalkan as  
784 opposed to 290 m at Vandob, situated only 18 km further SSE. At the Dalut Mine near  
785 Baysun (Fig. 1) the thickness of the formation is 534 m, although this figure may not be quite  
786 correct as the section is disturbed by folding and faulting at two levels. Towards the border  
787 with Tajikistan at Shargun Mine the thickness of the formation is 290 m and at Vuariz a mere  
788 88 m. These figures suggest that the Palaeozoic basement exhibited a considerable relief and  
789 that the age of the lowest Jurassic sediments may differ considerably between the various  
790 areas. The facies pattern in the Kugitang Mountains and at the Dalut Mine is very similar:  
791 Alternations of fluvial sandstones, fine-grained flood plain deposits, thin coal seams  
792 indicative of swamps, and argillaceous-silty, often organic-rich, to sandy lacustrine deposits.  
793 Many of these lakes appear to have been small and to have become infilled rapidly, but the  
794 thick, uniform silty clay succession at Shalkan and probably also at Vandob must represent a  
795 large and deep lake persisting for a considerable period of time. At Shargun and Vuariz, in  
796 contrast, the Gurud Formation is strongly dominated by coarse-grained to gravelly fluvial  
797 channel deposits with fine-grained floodplain deposits being of only minor importance.  
798 Where the latter occur, they also contain coal beds, but lake deposits are rare.

799 The thickness and facies variations indicate that the area of the northern part of the  
800 SW Gissar Mountains was a high area during the Early and early Middle Jurassic where  
801 erosion took place at the time when further south, in the Kugitang Mountains, the Palaeozoic  
802 relief became already filled with sediment. At Vuariz and Shargun a short distance to the  
803 source area is also indicated by the coarse, highly immature sediment. The presence of  
804 meandering river deposits at Shargun as opposed to braided stream deposits at Vuariz and the  
805 very small thickness of the formation at the latter locality suggest that the Vuariz area was  
806 very close to the sediment source.

807

808 *Degibadam and Tangiduval formations.* At the top of the Gurud Formation the morphological  
809 relief appears to have largely been levelled as the change to marine conditions was more or  
810 less synchronous across the study area, from the Kugitang Mountains to the Dalut Mine and  
811 the Iron Gate where Late Bajocian ammonites were found very close to the transgressive  
812 surface. At the remaining sections either no ammonites have been recorded (e.g., Vuariz,  
813 Shargun) or the transgressive surface is not exposed (e.g., at Panjab).

814         The thickness of the two formations is fairly uniform (276-284 m) except at Sangardak  
815 (143 m) and Shargun (14 m) where it is greatly reduced. In most of the study area the  
816 sedimentation pattern was mosaic, oscillating between partly tidal-influenced, partly high-  
817 energy inner ramp deposits, storm-wave influenced middle ramp deposits, and storm-flow  
818 dominated outer ramp deposits. The common arrangement of the sediments in coarsening-  
819 upward parasequences indicates that this sedimentation pattern was governed by changes in  
820 relative sea level and probably also by cyclic changes in climate. From the Kugitang  
821 Mountains to the Iron Gate the carbonate content of the sediment increases towards the top as  
822 does the amount of molluscs, mainly bivalves.

823

824 *Baysun Formation.* The thickness of the Baysun Formation from Vandob to Panjab is similar  
825 (195-226 m), but at Iron Gate it is reduced to 130 m and at Shargun to 51 m,. The fairly  
826 uniform sediment (marl or silty marl with intercalations of carbonate mud- and wackestones,  
827 the latter increasing towards the top) continues the trend of strong reduction of even fine-  
828 grained terrigenous input towards the top. In parts of the formation cycles recording an  
829 increase in carbonate are developed which most likely reflect shallowing. At present it is not  
830 clear how the strongly reduced Baysun Formation at Shargun should be explained. Due to the  
831 lack of age-diagnostic fossils no statement can be made whether the boundaries of the  
832 formation are isochronous or diachronous when compared with the remaining sections.  
833 Moreover at close-by Sangardak, a fine-grained mixed carbonate-siliciclastic succession  
834 resembling the Baysun Formation below the massive walls of the Kugitang Formation is  
835 repeatedly interrupted by intercalations of medium- to coarse-grained ripple-laminated to  
836 large-scale trough cross-bedded quartz sandstones. The latter feature points to a close-by  
837 source area and a steep bathymetric gradient, underpinning that we are adjacent to a land area.  
838 This view is corroborated by the fact that also in the basal part of the overlying Kugitang  
839 Formation sandy intercalations are common and the carbonate microfacies (including oo-  
840 grainstones) and sedimentary structures are indicative of a high energy setting (pers. comm.

841 R. Bourillot, Dec. 2013). Similar features can be seen at Vuariz. Oo-grainstone intercalations  
842 between marl and wackestones in the Baysun Formation at Vuariz and Shargun point to partly  
843 shallow-water environments. At Vuariz, oo-grainstones and packstones, interpreted as high-  
844 energy bars, are laterally replaced by algal limestones with birdseyes and fenestral fabrics  
845 (Fig. 14), which are interpreted as representing lagoonal deposits of peritidal origin. Despite  
846 these local differences in facies all localities show a gradual transition to the overlying thick-  
847 bedded limestones of the Kugitang Formation. In the Kugitang Mountains this transition is  
848 characterised by the complete lack of terrigenous input into the basin.

849

850

851 *Palaeoenvironmental evolution of the northwestern Afghan-Tajik Basin: Interplay of*  
852 *tectonics, eustatic sea-level changes, and climate (Fig. 19)*

853

854 The evolution of the northwestern Afghan-Tajik Basin during the Jurassic has been shaped  
855 mainly by tectonics, subsidence, eustatic sea-level changes, and climate. Extensional tectonics  
856 (?back-arc rifting; Brookfield & Hashmat 2001) starting in the Late Permian–Triassic was  
857 responsible for the formation of the basin (Ulmishek 2004; Klett *et al.* 2006), which was  
858 apparently subdivided into a number of grabens and horsts. No Triassic sedimentary rocks  
859 have been encountered in the study area (see also Dzhililov *et al.* 1982) and sedimentation  
860 appears to have started only in the Toarcian on the northern margin of the basin. The  
861 basement consists mainly of Palaeozoic metamorphic rocks. Judging from the distinct  
862 differences in thickness of the non-marine succession between some of the sections a  
863 considerable relief must have existed during the Early Jurassic; consequently, the base of the  
864 succession most likely is highly diachronous, although this cannot be proven by index fossils.

865

866 *Non-marine stage.* During the Late Early Jurassic erosion of elevated areas produced plenty  
867 of sediment, and low-lying areas were filled with deposits of braided or meandering river. The  
868 coarse-grained, highly immature sediment points to short transport distances. The stacking of  
869 fluvial channels, a common feature in the lower part of the non-marine succession, can be  
870 explained by relatively narrow river plains. In the Kugitang and Baysun areas levelling of the  
871 relief must have occurred comparatively soon, as the mean grain size decreased distinctly  
872 after a few tens of metres as did the sandstone-shale ratio. Up to the Early Bajocian extensive  
873 flood plains existed which were dotted with lakes. Some of these lakes were apparently of  
874 considerable size and duration, others only short-lived. The flood plains were also crossed by

875 numerous streams, which commonly emptied into lakes where they built small deltas.  
876 Swampy areas developed on the flood plain and especially at the margins of the lakes. The  
877 dark-grained, organic-rich lake sediments, common root horizons, carbonaceous silt and coal  
878 layers, and the ubiquitous plant and wood remains point to the presence of a dense vegetation  
879 and consequently to a fairly humid climate. Subsidence and rate of sediment accumulation  
880 appear to have been close to equilibrium. The cyclic nature of many lake deposits is the result  
881 of lacustrine delta or shoreline progradation.

882         The comparatively thin non-marine successions at Shargun, Sangardak and especially  
883 at Vuariz with their high sandstone-shale ratio suggest that sedimentation in these areas  
884 started much later and that the sediment source was very close. Most likely, the central parts  
885 of the Gissar Mountains were the main source area for the sediments delivered to the Baysun  
886 and Kugitang mountains.

887

888 *Marine stage.* The sea invaded the area in the Late Bajocian. Evidence are the presence of  
889 marine shells and trace fossils and finds of the ammonite *Parkinsonia* close to the lowermost  
890 marine beds. As nowhere a transgressive conglomerate is developed and the transgressive  
891 surface is very inconspicuous, a flat coastal plain must have existed at the time of  
892 transgression. Wherever ammonite evidence is available, it suggests that flooding of the basin  
893 took place at roughly the same time. A distinct transgression at this point in time is also  
894 recorded from neighbouring basins such as the Kashafrud Basin in the Kopet Dagh area and  
895 the southern margin of the South Caspian Basin (i.e., the Alborz Mountains) (Fürsich *et al.*  
896 2009a). As the global sea-level started to rise in the late Early Bajocian (Hallam 2001), it is  
897 tempting to relate the transgression to this eustatic signal. However, the two events are not  
898 strictly synchronous. Moreover, the transgression in the Alborz area and in the Kopet Dagh  
899 has been explained by Fürsich *et al.* (2009b) by a distinct subsidence pulse caused by the  
900 onset of seafloor spreading in the South Caspian Basin. Similarly, in the Afghan-Tajik Basin  
901 increased subsidence is thought to be the main factor causing the change to marine conditions  
902 in the basin as well as in the Amu Darya Basin (Brunet *et al.* 201X).

903         The marine sediments were initially purely siliciclastic and range from argillaceous  
904 silt to fine-grained sandstone. Abundant HCS and parallel-/ripple-laminated sandstones and  
905 gutter casts indicate that for long time depositional environments corresponded to the storm-  
906 wave and storm-flow influenced ramp. Commonly the sediments are organised in thickening-  
907 and coarsening-upward parasequences which indicate to shallowing and thus correspond to  
908 small-scale relative sea-level fluctuations. These parasequences may either reflect a eustatic

909 signal or else climatic conditions which oscillated between dryer and wetter periods. During  
910 the latter, sediment influx into the basin was higher and the storm intensity greater. The  
911 greater storm intensity might have contributed to disperse coarser-grained coastal sediments  
912 across the ramp.

913         Within the Upper Bajocian Degibadam Formation a thick deltaic complex is  
914 developed in several sections (Vandob, Shalkan, Iron Gate, to a lesser extent also at Panjab).  
915 These deltaic sandstones are most likely not coeval but are part of a succession with an inner  
916 ramp character (shown e.g., by tidal influence and allochthonous coal layers). Apparently, at  
917 this time the sedimentation rate exceeded subsidence on the margins of the basin resulting in  
918 progradation of the shoreline.

919         The increasing carbonate content in the Tangiduval Formation does not go hand in  
920 hand with a decreasing grain size of the siliciclastic material. It therefore appears that the  
921 mixed carbonate-siliciclastic sediment is above all the result of increased carbonate  
922 production and only secondarily due to a reduction in terrigenous input. Both features point to  
923 a gradual change in climate from humid to increasingly drier and warmer conditions. The  
924 input of siliciclastic material, however, decreased distinctly from the Middle Bathonian  
925 onwards. This led to the formation of a several-metres-thick condensed unit at the base of the  
926 Baysun Formation. This is the only level within the investigated time slice where ammonites  
927 are common, associated with abundant benthic elements such as bivalves, gastropods and  
928 brachiopods. During the Late Bathonian the percentage of silt gradually decreased so that by  
929 the Early Callovian only clay-sized terrigenous material reached the southern part of the study  
930 area which occupied an outer ramp to basinal position. The occurrence of concentrations of  
931 small infaunal bivalves suggests that the sea floor was intermittently winnowed by currents.  
932 The presence of bio-floatstones and, more rarely, bio-rudstones in a cyclical manner points to  
933 phases during which the input of terrigenous fines ceased completely. The shell debris that  
934 abounds in some of these carbonates is clearly of shallow-water origin and is commonly  
935 associated with oncoids. Thus the depositional environment was within the photic zone. As  
936 has been argued above, climatic changes are the most plausible cause for these carbonate  
937 cycles.

938         The Baysun Formation at Sangardak and Shargun differed not only in a reduced  
939 thickness from the remaining localities but also by intercalations of medium- to coarse-  
940 grained quartz sandstones in the silty marl. The sharp base, sedimentary structures such as  
941 ripple lamination and large-scale cross-bedding, and associated trace fossils (*Ophiomorpha*)  
942 at Sangardak indicate episodic influx from a very nearby source area and a considerable relief.

943 As this influx is very sudden, the most likely explanation is a tectonic origin that led to uplift  
944 of a close-by land area. At Vuariz, in turn, the basin was considerably shallower leading to the  
945 establishment of high-energy ooid bars and peritidal carbonate flats. Intercalations of coarse-  
946 grained sandstones at the base of Kugitang Formation are interpreted in a similar way as at  
947 Sangardak.

948 By Middle Callovian times, the terrigenous influx had ceased completely. As result a  
949 carbonate regime became established across the study area. In most areas, the thick-bedded  
950 limestones of the Kugitang Formation record low to moderate energy conditions below the  
951 fair-weather wave-base which persisted until the Kimmeridgian, as subsidence and rate of  
952 sedimentation continued to be close to equilibrium.

953

954 *Sequence stratigraphic aspects (Fig. 20)*

955

956 Both the marine and non-marine part of the succession exhibit a pronounced cyclicity. In the  
957 non-marine part, this cyclicity is documented mainly by progradational lacustrine cycles  
958 which might be partly autocyclic, partly reflecting changes in base level. As there is, however,  
959 at present only a very coarse biostratigraphic control of the succession and the fine-grained  
960 lacustrine succession in the Kugitang Mountains is only partly exposed no attempt at a  
961 sequence stratigraphic interpretation is made.

962 In the marine succession two 3rd-order sequences spanning the Late Bajocian to Early  
963 Callovian time interval can be recognised. They are very well seen in the Iron Gate section  
964 (Fig. 20), although the transgressive systems tract (TST) of the lower sequence is missing. It  
965 is represented in the Shalkan and Vandob sections by storm-influenced ramp sediments. The  
966 maximum flooding zone (MFZ) is represented by bioturbated argillaceous silt. The highstand  
967 systems tract (HST) starts again with storm-influenced ramp deposits, which grade into  
968 prodelta, delta-front, and delta-top sediments (Iron Gate), the latter characterised by being  
969 fine-grained and often carbonaceous with minor coal beds or exhibiting tidal influence. The  
970 TST of the second sequence more or less coincides with the base of the Tangidival Formation  
971 and typically consists of sandy sediments with a calcareous matrix and common shell debris  
972 and oyster shells. The MFZ is a several-metres-thick condensed unit, rich in ammonites and  
973 benthic macrofauna and forms the base of the Baysun Formation. The HST comprises the  
974 sediments of the Kugitang Formation. In contrast to what would be expected the terrigenous  
975 input decreases towards the top. This, however, does not reflect increasing distance from the  
976 shoreline but is the result of the distinct change to a more arid climate (see below). The base

977 of the next sequence corresponds to the onset of a large carbonate ramp system (Kugitang  
978 Formation), which is studied in detail in a companion project (Bourillot pers. comm.;  
979 Carmeille *et al.* 2014).

980 As has been shown above, the 3-rd order sequences are composed of numerous  
981 parasequences. Most likely, higher-order sequences may also be discernable in some cases,  
982 but a more detailed analysis is beyond the scope of this paper.

983

984 *Tectonics, sea-level fluctuations, and climate as driving mechanisms of the sedimentation*  
985 *pattern*

986

987 The main factors for the formation of the Afghan-Tajik Basin were extensional tectonics and  
988 resulting subsidence (Brookfield & Hashmat 2001; Ulmishek 2004). Differential uplift due to  
989 block faulting influenced the sedimentation pattern as it created basins and uplifted areas, the  
990 former receiving the sediment eroded from the latter. This setting must have created a mosaic  
991 sediment pattern with areas close to horsts receiving coarser sediment than areas further away.  
992 Apart from Vuariz and Shargun-Sangardak the study area must have occupied a relatively  
993 basinal position as basement rocks are nowhere overlain by alluvial fan deposits but either by  
994 paleosol or braided river deposits. Moreover, soon after deposition of the initial sandstones  
995 fine-grained lake and flood plain deposits became conspicuous elements indicating little  
996 relief. Tectonic activity appears to have been restricted to the major fault systems and  
997 affecting sedimentation within the basin mainly by changes in the supply of coarser  
998 siliciclastic material. A tectonic influence, documented by an angular unconformity,  
999 apparently affected the area of Sangardak-Shargun somewhere in the Callovian (Fig. 9h). This  
1000 unconformity is developed between the Baysun and the Kugitang Formation and can be  
1001 explained by slight tilting of a fault block. How much sediment has been eroded prior to  
1002 deposition of the carbonates of the Kugitang Formation cannot be reconstructed due to the  
1003 insufficient stratigraphic control. Differential tectonic uplift is also documented by the  
1004 thickness differences of the marine part of the succession which changed from >400 m at the  
1005 Iron Gate to 130 m at Sangardak and to 65 m at Shargun along a distance of 90 km.

1006 Several factors appear to have shaped the overall basin development. According to  
1007 Hardenbol *et al.* (1998) the peak of a transgressive-regressive megacycle occurred in the Late  
1008 Bajocian. This major sea-level rise probably contributed to the flooding of the basin to some  
1009 extent. In addition, the change to marine conditions could also have been caused by active  
1010 subsidence or else by a general reduction of sediment input into the basin caused by an

1011 increasingly lower relief of the hinterland and less humid conditions. A major change in  
1012 climate towards drier and possibly warmer conditions is indicated by the change from  
1013 siliciclastic to carbonate sedimentation from the Early to the late Middle Jurassic. This trend  
1014 to increasing aridity continues into the Kimmeridgian and Tithonian when widespread  
1015 evaporites and red beds dominated the sedimentation pattern.

1016         Controversial is the origin of the numerous parasequences that compose much of the  
1017 rock succession. In the marine environments they correspond to relative changes in sea level  
1018 which could be eustatic-, tectonic- or else climatic-controlled. As no clear pattern is visible  
1019 that allows grouping these parasequences into higher hierarchy cycles a climatic control is  
1020 thought to be more likely. In the non-marine part of the succession, in contrast, the fining-  
1021 upward cycles developed on the flood plains and the progradational lacustrine cycles are  
1022 thought to be largely the result of autocyclic processes but probably steered by an underlying  
1023 climatic pattern that regulated the sediment supply.

1024         In conclusion, the Jurassic fill of the North Afghan-Tajik Basin reflects the interplay  
1025 of extensional tectonics creating a syn-rift subsidence, a subsequent more regular thermal  
1026 subsidence, eustatic sea-level changes, and climate, whereby the importance of the various  
1027 factors varied through time.

1028

#### 1029 *Comparison with sedimentary basins in northern Iran*

1030

1031 In order to put the Jurassic history of the investigated northwestern part of the Afghan-Tajik  
1032 Basin into a broader perspective, it is compared with the Jurassic history of neighbouring  
1033 basins. For this reason, the geological development of two sedimentary basins in northern  
1034 Iran, the Kashafrud Basin (Kopet Dagh) and the southern passive margin of the South  
1035 Caspian Basin (Alborz Mountains), is briefly commented upon (Fig. 21).

1036         In the southern Alborz Mountains, marine conditions became established in some  
1037 areas as early as the Hettangian (Fürsich *et al.* 2009a). In the Early Jurassic Alasht Formation  
1038 and in the Early Bajocian Dansirit Formation terrestrial environments with lakes, fluvial  
1039 systems and widespread coal swamps similar to those in the Afghan-Tajik Basin prevailed.

1040         In both basins a pronounced transgression took place in the Late Bajocian following  
1041 the Mid Cimmerian tectonic event in the Early Bajocian (Fürsich *et al.* 2009a, b; Taheri *et al.*  
1042 2009). In the case of the Alborz Mountains the origin of this transgression has been explained  
1043 by these authors as related to the onset of sea-floor spreading in the South Caspian Basin. At  
1044 the same time rifting, most likely related to Neotethys back-arc rifting, started in the Kopet

1045 Dagh area and initiated the Kashafrud Basin, which has been interpreted as the eastward  
1046 extension of the South Caspian Basin (Brunet *et al.* 2003, 2007; Taheri *et al.* 2009). In both  
1047 basins siliciclastic sediments prevailed until they were gradually replaced by carbonates. This  
1048 replacement started in the Kashafrud Basin in the Callovian with fine-grained mixed  
1049 carbonate-siliciclastics of the Chaman Bid Formation and continued into the Late Jurassic  
1050 with the establishment of a large carbonate platform system, the Mozduran Formation.

1051 On the southern passive margin of the South Caspian Basin, marine siliciclastic  
1052 sediments overlying the Mid-Cimmerian unconformity are usually only a few metres thick,  
1053 except in the eastern Alborz where the so-called Bashkalateh Formation (Afshar-Harb 1994),  
1054 a lateral equivalent of the Kashafrud Formation of the Kopet Dagh (Seyed-Emami *et al.*  
1055 2001), represents a largely fine-grained deep-marine environment with turbiditic  
1056 intercalations. The change to a carbonate regime started already in Late Bajocian times, as is  
1057 indicated by the silty marls and marls of the Dalichai Formation. Initially representing basinal  
1058 sediments these marls change up-section to allodapic carbonates of the slope and finally to the  
1059 shallow-water platform of the Callovian–Tithonian Lar Formation. A similar change from  
1060 fine-grained mixed carbonate-siliciclastic sediments to shallow-water carbonates occurs also  
1061 in the Binalud Mountains of north-eastern Iran (*pers. obs.*). Moreover, the widespread  
1062 replacement of siliciclastic sediments by carbonates towards the end of the Middle Jurassic  
1063 can also be observed on the Tabas and Lut blocks of the Central-East Iranian microcontinent  
1064 where the silty to marly Bathonian to Lower Callovian Baghamshah Formation grades up-  
1065 section into the Upper Callovian to Oxfordian Esfandiar Limestone Formation (Wilmsen *et*  
1066 *al.* 2009). As in the Afghan-Tajik Basin, the carbonates in the Iranian basins are generally  
1067 followed by red beds and evaporites towards the end of the Jurassic.

1068 The replacement of siliciclastic sediments by carbonates is therefore a widespread  
1069 feature and occurred not only in the Afghan-Tajik Basin as well as the Amu Darya Basin but  
1070 also in various basins of Iran. This strongly suggests that the change in sedimentation pattern  
1071 is due to a regional change towards more arid conditions.

1072 In the sedimentary basins east of the Afghan-Tajik Basin, e.g. in southern Kyrgyzstan,  
1073 the situation is different: There, non-marine siliciclastic rocks similar to those of the Gurud  
1074 Formation characterize the complete Jurassic succession (*pers. obs.*). A direct comparison is,  
1075 however, hampered by still missing chronostratigraphic information. Thus, it is not clear  
1076 whether the several-thousand-metres-thick siliciclastic succession cropping out in the Jerzy  
1077 River area near the border to China represents the whole or only part of the Jurassic Period. A  
1078 palynological analysis to clarify this problem is in progress.

1079

1080 *Geodynamic framework*

1081

1082 The Afghan-Tajik and Amu Darya basins are situated on the southern part of the Turan  
1083 Platform. Their early extensional history during Late Permian – Early Triassic is not well  
1084 known as these deposits, possibly filling grabens, are deeply buried. Permian and Triassic  
1085 sediments occur on the southern margins of the Amu-Darya and Afghan-Tajik basins in south  
1086 Turkmenistan and North Afghanistan where they unconformably overlie Palaeozoic beds  
1087 (Brookfield & Hashmat 2001; Ulmishek 2004; Klett *et al.* 2006; Abdullah *et al.* 2008). The  
1088 narrow grabens were linked to intra-arc and back-arc extension behind subduction of the  
1089 Palaeotethys towards the North, below the Turan Platform.

1090         Several Cimmerian blocks became detached from Gondwana during the Permian and  
1091 collided with Eurasia leading to the formation of the Eo-Cimmerian unconformity and the Eo-  
1092 Cimmerian belt (Zanchi *et al.* 2009; Zanchetta *et al.* 2013 and references herein). First the  
1093 Iranian blocks collided in Late Triassic, followed by the Central Afghanistan and Central  
1094 Pamir blocks at the end of the Triassic, accounting for a slightly younger unconformity,  
1095 deformation and post-collisional magmatism towards the East (Klett *et al.* 2006; Zanchi *et al.*  
1096 2009, 2012; Zanchetta *et al.* 2013; Siehl 201X). From the eastern part of Iran and the Amu  
1097 Darya Basin towards the East, Palaeozoic and Triassic sediments are unconformably covered  
1098 by Jurassic sediments (Brookfield & Hashmat 2001; Ulmishek 2004; Klett *et al.* 2006;  
1099 Abdullah *et al.* 2008; Zanchi *et al.* 2009, 2012; Zanchetta *et al.* 2013; Siehl 201X). Eo-  
1100 Cimmerian reliefs were uplifted and eroded, providing Jurassic siliciclastic sediments that  
1101 filled the new basins (Amu Darya and Afghan-Tajik basins) created by extensional tectonics  
1102 (Brookfield & Hashmat 2001; Ulmishek 2004; Klett *et al.* 2006; Brunet *et al.* 201X).

1103         The northwestern Afghan-Tajik Basin of the study area in southern Uzbekistan was  
1104 shaped by this framework of horst and grabens created in the Early Jurassic as result of the  
1105 dismembering of a part of the Eo-Cimmerian orogenic belt. Here no Triassic sedimentary  
1106 rocks have been encountered; sedimentation started in the Toarcian and was probably  
1107 diachronous. Extensional tectonics induced active tectonic subsidence. This explains the  
1108 observed variations in thickness, the progressive deepening, and the onset of marine  
1109 conditions in the Late Bajocian. The area of the Kugitang Mountains occupied a deep part of  
1110 the extensional margin which shallowed towards the North-East. The extension ceased during  
1111 the Middle Jurassic to give way to a more continuous thermal subsidence.

1112           During Mesozoic and Early Palaeogene times, the Afghan-Tajik and Amu Darya  
1113 basins formed a single basin (Ulmishek 2004). The Late Palaeogene-Neogene collision of the  
1114 Indian Plate with the Eurasian Plate uplifted the southern margins of the basins, mainly  
1115 shaped the southwestern Gissar range, which divided the northern portion into the two basins,  
1116 and strongly deformed the Afghan-Tajik Basin, situated nearest to the Pamirs (Klett *et al.*  
1117 2006).

1118

1119

## 1120 **Conclusions**

1121

1122 The Lower Jurassic to Lower Callovian sedimentary succession of the Afghan-Tajik Basin in  
1123 southern Uzbekistan records the history of an extensional basin with pronounced topography.  
1124 The non-marine siliciclastic rocks overlying the Palaeozoic basement rocks represent  
1125 environments ranging from braided and meandering streams to floodplains, swamps, and  
1126 lakes. The latter are either short-lived or long-ranging and wide-spread. Their sediments are  
1127 commonly arranged in progradational cycles. Plant growth was ubiquitous as is documented  
1128 by rootlets, coal layers, wood pieces and plant debris and indicates a humid climate.

1129           In the Late Bajocian the sea flooded the basin. Initially, the sedimentation regime  
1130 remained siliciclastic, representing storm-influenced ramp environments that shallowed into a  
1131 deltaic setting, locally with paralic coal. With the return to a storm-influenced ramp setting  
1132 the siliciclastic sediment influx decreased and mixed carbonate siliciclastic sediments were  
1133 deposited.

1134           Part of the Middle Bathonian time interval is marked by sediment starvation. The Late  
1135 Bathonian to Early Callovian interval represents an outer ramp to basinal setting,  
1136 characterized by an increasing carbonate content of the sediment. It is followed by a thick  
1137 carbonate unit, which is beyond the scope of this study. The marine unit is composed of  
1138 metre-scale parasequences and corresponds to two third-order depositional sequences.

1139           Marked lateral thickness changes of the investigated succession point to a pronounced  
1140 relief of the basement. Maximum subsidence occurred from the Kugitang Mountains in the  
1141 South to the Baysun area in the North, whereas further north in the Gissar Mountains and  
1142 north of Denau strongly reduced thicknesses with a dominance of coarse-grained fluvial  
1143 channel deposits indicate the margin of the basin.

1144 The replacement of siliciclastic sediments by carbonates in the course of the Bathonian  
1145 to Early Callovian time interval is interpreted to partly reflect a reduced topography of the  
1146 hinterland, partly a change in climate from humid to arid.

1147 A similar shift in sediment composition occurs also in central-east Iran, the Alborz  
1148 Mountains, Kopet Dagh, and Binalud Mountains of Iran and demonstrates that this climate  
1149 shift was of at least regional significance. Furthermore, flooding of these Iranian basins and  
1150 the Afghan-Tajik Basin around the Early-Late Bajocian boundary suggests a more or less  
1151 synchronous active subsidence and some shared geodynamic history.

1152

1153

1154 We would like to thank I. Sidorova, B. Nurtaev, D.P. Ishniyazov, Dmitriy Mordvintsev,  
1155 Matthias Alberti, Martin Regelsberger, Johann Schnyder, and Raphael Bourillot for assistance  
1156 in the field, Eric Barrier for discussions, and Martin Regelsberger, Golda Schugmann,  
1157 Matthias Alberti, and Manja Hethke for drafting the diagrams. Vitali Mitta kindly helped with  
1158 obtaining some of the Russian literature. Kazem Seyed-Emami kindly identified the  
1159 ammonites. The comments of two anonymous reviewers helped to improve the manuscript.

1160

1161

## 1162 References

1163 ABDULLAEV, G. S. & MIRKAMALOV, H. H. 1998. Unification stratigraphic nomenclature of  
1164 commercial horizons of carbonate formations of the Jurassic, southern and southwestern  
1165 Uzbekistan. *Journal of Uzbek Oil and Gas*, **1998**(4), 13–16.

1166 ABDULLAH, S. H., CHMYRIOV, V. M. & DRONOV V. I. (eds) 2008. Geology and Mineral  
1167 Resources of Afghanistan. 2 Volumes. *British Geological Survey Occasional Publication*,  
1168 **15**. <http://www.bgs.ac.uk/downloads/browse.cfm?sec=7&cat=83>

1169 AFSHAR-HARB, A. 1994. Geology of the Koppet Dagh. *Geological Survey of Iran, Report*, **11**,  
1170 1–275 (in Farsi).

1171 AIGNER, T. 1979. Schill-Tempestite im Oberen Muschelkalk (Trias, SW-Deutschland). *Neues*  
1172 *Jahrbuch für Geologie und Paläontologie, Abhandlungen*, **157**, 326–343.

1173 AIGNER, T. 1982. Calcareous tempestites: storm-dominated stratification in Upper  
1174 Muschelkalk limestones (Middle Trias, SW-Germany. *In*: EINSELE, G. & SEILACHER A.  
1175 (eds) *Cyclic and event stratification*. Springer, Berlin, Heidelberg, 180–198.

- 1176 AIGNER, T. & REINECK, H.-E. 1982. Proximity trends in modern storm sands from the  
1177 Helgoland Bight (North Sea) and their implications for basin analysis. *Senckenbergiana*  
1178 *Maritima*, **14**, 183–215.
- 1179 BARRIER, E. & VRIELYNCK, B., 2008. *Palaeotectonic Maps of the Middle East. Tectono-*  
1180 *Sedimentary-Palinspastic Maps from Late Norian to Piacenzian*. Commission for the  
1181 Geological Map of the World (CGMW)/UNESCO. Atlas of 14 maps, scale 1/18 500 000.
- 1182 BROOKFIELD, M. E. & HASHMAT, A. 2001. The geology and petroleum potential of the North  
1183 Afghan platform and adjacent areas (northern Afghanistan, with parts of southern  
1184 Turkmenistan, Uzbekistan and Tajikistan. *Earth-Science Reviews*, **55**, 41–71.
- 1185 BRUNET, M.-F., KOROTAEV, M. V., ERSHOV, A. V. & NIKISHIN, A. M. 2003. The South  
1186 Caspian Basin: a review of its evolution from subsidence modelling. *Sedimentary*  
1187 *Geology*, **156**, 119–148.
- 1188 BRUNET, M.-F., SHAHIDI, A., BARRIER, E., MÜLLER, C. & SAÏDI, A. 2007. Geodynamics of the  
1189 South Caspian Basin southern margin now inverted in Alborz and Kopet-Dagh (Northern  
1190 Iran). *Geophysical Research Abstracts*, European Geosciences Union, Vienna, 9, 08080.  
1191 <http://www.cosis.net/abstracts/EGU2007/08080/EGU2007-J-08080.pdf>
- 1192 BRUNET, M.-F., ERSHOV, A. V., KOROTAEV, M. V., MORDVINTSEV, D. O., SIDOROVA, I. P. &  
1193 BARRIER, E. 201X. Late Palaeozoic and Mesozoic evolution of the Amu Darya Basin  
1194 (Turkmenistan, Uzbekistan). *This volume*.
- 1195 CARMEILLE, M., BOURILLOT, R., BARRIER, E., FÜRSICH, F., THIERRY, J., PELLENARD, P.,  
1196 SCHNYDER, J., AUXIÈTRE, J.L., MUNSCH, H., MORTVINTSEV, D. & SIDOROVA I. 2014.  
1197 Facies, architecture and diagenesis of middle to upper Jurassic carbonates in the Ghissar  
1198 Range (Uzbekistan). Abstract EGU meeting Vienna.
- 1199 DZHALILOV, M. R., ALEKSEEV, M. N., ANDREEV, YU. N. & SALIBAEV, G. KH. 1982. Mesozoic  
1200 and Cenozoic deposits of the northern part of the Afghano – Tajik basin. ESCAP Atlas of  
1201 Stratigraphy. III. *United Nations Mineral Resources Development Series No. 48*,  
1202 131–137.
- 1203 EGAMBERDIEV M. E. & ISHNIYAZOV D. P. 1990. *Comparative lithologic and facial-*  
1204 *palaeogeographic characteristics of lower and middle Jurassic deposits of South*  
1205 *Uzbekistan and North Afghanistan with hypothetical resources evaluation of coalfield*,  
1206 Final Report (1986-1990) by the Institute of Geology & Geophysics of Academy of  
1207 Sciences of Uzbekistan, Tashkent, 2 volumes (in Russian).
- 1208 FLÜGEL, E. 2010. *Microfacies of carbonate rocks. Analysis, interpretation and application*.  
1209 Springer, Berlin, Heidelberg, 984 p.

- 1210 FÜRSICH, F. T. 1977. Corallian (Upper Jurassic) marine benthic associations from England  
1211 and Normandy. *Palaeontology*, **20**, 337–385.
- 1212 FÜRSICH, F. T. & WERNER, W. 1986. Benthic associations and their environmental  
1213 significance in the Lusitanian Basin (Upper Jurassic, Portugal). *Neues Jahrbuch für*  
1214 *Geologie und Paläontologie, Abhandlungen*, **172**, 271–329.
- 1215 FÜRSICH, F. T., WILMSEN, M., SEYED-EMAMI, K. & MAJIDIFARD, M. R. 2009a.  
1216 Lithostratigraphy of the Upper Triassic – Middle Jurassic Shemshak Group of Northern  
1217 Iran. In: BRUNET, M.-F., WILMSEN, M. & GRANATH, J. W. (eds) *South Caspian to Central*  
1218 *Iran Basins. Geological Society, London, Special Publications*, **312**, 129–160.
- 1219 FÜRSICH, F. T., WILMSEN, M., SEYED-EMAMI, K. & MAJIDIFARD, M. R. 2009b. The Mid-  
1220 Cimmerian tectonic event (Bajocian) in the Alborz Mountains, Northern Iran: evidence of  
1221 the break-up unconformity of the South Caspian Basin. In: BRUNET, M.-F., WILMSEN, M.  
1222 & GRANATH, J. W. (eds) *South Caspian to Central Iran Basins. Geological Society,*  
1223 *London, Special Publications*, **312**, 189–203.
- 1224 FÜRSICH, F.T., OSCHMANN, W., PANDEY, D.K., JAITLEY, A.K., SINGH, I.B. & LIU, C.  
1225 2004. Palaeoecology of Middle to lower Upper Jurassic macrofaunas of the  
1226 Kachchh Basin, western India: an overview. *Journal of the Palaeontological Society*  
1227 *of India*, **49**, 1–26.
- 1228 GOMOLITZKY, N. P. & LOBANOVA, A. V. 1969. K stratigrafii yurskikh otlozheniy Angrena.  
1229 *Sovetskaya geologiya*, **9**, 110–115 (On the stratigraphy of the Jurassic sediments of  
1230 Angren, in Russian).
- 1231 HARDENBOL, J., THIERRY, J., FARLEY, M.B., JAQUIN, TH., DE GRACIANSKY, P.-C. & VAIL, P.R.  
1232 1998. Mesozoic and Cenozoic sequence chronostratigraphic framework of European  
1233 basins. In: DE GRACIANSKY, P.-C., HARDENBOL, J., JAQUIN, TH. & VAIL, P.R. (eds)  
1234 *Mesozoic-Cenozoic sequence stratigraphy of European basins. Society of Economic*  
1235 *Paleontologists and Mineralogists, Special Publication*, **60**, 763–781, and chart  
1236 supplements.
- 1237 KIM, A. I., SALIMOVA, F. A., ABDUASIMOVA, I. M. & MESHCHANKINA, N. A. (eds) 2007.  
1238 *Palaeontological Atlas of Phanerozoic faunas and floras of Uzbekistan. Volume II.*  
1239 *Mesozoic and Cenozoic (Jurassic, Cretaceous, Palaeogene).* Republic of Uzbekistan State  
1240 Committee on Geology and Mineral Resources, Tashkent.
- 1241 KLETT, T. R., ULMISHEK, G. F., WANDREY, C. J., AGENA, W. F. & U.S. GEOLOGICAL SURVEY-  
1242 AFGHANISTAN MINISTRY OF MINES AND INDUSTRY JOINT OIL AND GAS RESOURCE  
1243 ASSESSMENT TEAM. 2006. Assessment of undiscovered technically recoverable

- 1244 conventional petroleum resources of northern Afghanistan. *U.S. Geological Survey Open-*  
1245 *File Report*, 2006-1253, 1□237.
- 1246 KLETT, T. R., SCHENK, C. J., WANDREY, C. J., CHARPENTIER, R. R., BROWNFIELD, M. E.,  
1247 PITMAN, J. K., POLLASTRO, R. M., COOK, T. A. & TENNYSON, M.E. 2012. *Assessment of*  
1248 *undiscovered Oil and gas resources of the Amu Darya Basin and Afghan–Tajik Basin*  
1249 *provinces, Afghanistan, Iran, Tajikistan, Turkmenistan, and Uzbekistan, 2011*. U.S.  
1250 Department of the Interior, U.S. Geological Survey, Fact Sheet 2011–3154.
- 1251 KRYMHOLTS, G. YA. & ZAKHAROV, E. V. 1971. Bathonian ammonites of Kugitang. *In*:  
1252 SHAYKUBOV, T. SH. (ed) *Paleontological substantiation of reference sections of the*  
1253 *Jurassic system in Uzbekistan and adjacent areas*. Leningrad, Nedra, 4□40 (in Russian).
- 1254 KRYMHOLTS, G. YA., MESEZHNIKOV, M. S. & WESTERMANN, G. E. G. (eds) 1988. *The*  
1255 *Jurassic ammonite zones of the Soviet Union*. *Geological Society of America, Special*  
1256 *Paper*, **223**, 1-116.
- 1257 MIALL, A. D. 1996. *The geology of fluvial deposits*. Springer, Berlin.
- 1258 MITTA, V. V. 2001. Distribution of the Bajocian-Bathonian ammonites in the South-West  
1259 chains of Hissar Range. *Hantkeniana*, **3**, 105–129.
- 1260 MITTA, V. V. & BESNOSOV, N. V. 2007. *Jurassic system Cephalopods*. *In*: KIM, A. I.,  
1261 SALIMOVA, F. A., ABDUASIMOVA, I. M. & MESHCHANKINA, N. A. (eds) *Palaeontological*  
1262 *Atlas of Phanerozoic faunas and floras of Uzbekistan. Volume II, Mesozoic and Cenozoic*.  
1263 Republic of Uzbekistan State Committee on Geology and Mineral Resources, Tashkent,  
1264 26□41.
- 1265 MONTENAT C., 2009. The Mesozoic of Afghanistan. *GeoArabia*, **14**, **1**, 145-208.
- 1266 MUTTI, E., TINTERRI, R., BENEVELLI, G., DI BIASE, D. & CAVANNA, G. 2003. Deltaic, mixed  
1267 and turbidite sedimentation of ancient foreland basins. *Marine and Petroleum Geology*,  
1268 **20**, 733□755.
- 1269 MYROW, P. M. 1992. Pot and gutter casts from the Chapel Island Formation, Southeast  
1270 Newfoundland. *Journal of Sedimentary Research*, **62**, 992□1007.
- 1271 NIKOLAEV, V. G. 2002. Afghan–Tajik depression: Architecture of sedimentary cover and  
1272 evolution. *Russian Journal of Earth Sciences*, **4**, 399–421.
- 1273 READING, H. G. & COLLINSON, J. D. 1996. Clastic coasts. *In*: READING, H. G. (ed)  
1274 *Sedimentary environments*. Blackwell’s, London, 154□231.
- 1275 RENZHINA, E. A. & FOKINA, N. I. 1978. Terrigenous marine deposits and conditions of their  
1276 sedimentation in western Uzbekistan. *VNIGNI Transactions*, **209**, 76□90 (in Russian).

- 1277 RESOLUTIONS OF THE INTERDEPARTMENTAL STRATIGRAPHICAL MEETING ON THE MESOZOIC OF  
1278 MIDDLE ASIA. 1977. [Resheniya Mezhdedomstvennogo stratigraficheskogo  
1279 soveshchaniya po mezozoyu Srednei Asii (Samarkand, 1971)]. VSEGEI, Leningrad, 47 p.  
1280 (in Russian).
- 1281 SCHAETZL, R. & ANDERSON, S. 2005. *Soils. Genesis and geomorphology*. Cambridge  
1282 University Press, Cambridge.
- 1283 SEYED-EMAMI, FÜRSTICH, F.T. & SCHAIRER, G. 2001. Lithostratigraphy, ammonite faunas and  
1284 palaeoenvironments of Middle Jurassic strata in north and central Iran. *Newsletters on*  
1285 *Stratigraphy*, **38**, 163-184.
- 1286 SHAYAKUBOV, T. S. (Eds.) 1998. *Geological Map of Uzbekistan, scale 1:500000* (in Russian).
- 1287 SHAYAKUBOV, T. SH. & DALIMOV, T. N. (eds) 1998. Geology and minerals of the Republic of  
1288 Uzbekistan, Tashkent, National University of Uzbekistan, 723 p.
- 1289 SHINN, E. 1983. Birdseyes, fenestrae, shrinkage pores, and loferites: a re-evaluation: *Journal*  
1290 *of Sedimentary Petrology*, **53**, 619–628.
- 1291 SIEHL, A. 201X. Structural setting and evolution of the Afghan orogenic segment – a review.  
1292 *This volume*.
- 1293 STAMPFLI, G. M. & BOREL, G. D. 2002. A plate tectonic model for the Paleozoic and  
1294 Mesozoic constrained by dynamic plate boundaries and restored synthetic oceanic  
1295 isochrons. *Earth and Planetary Science Letters*, **196**, 17–33.
- 1296 TAHERI, J., FÜRSTICH, F. T. & WILMSEN, M. 2009. Stratigraphy, depositional environments and  
1297 geodynamic significance of the Upper Bajocian-Bathonian Kashafud Formation, NE Iran. *In*:  
1298 BRUNET, M.-F., WILMSEN, M. & GRANATH, J. W. (eds) *South Caspian to Central Iran*  
1299 *Basins. Geological Society, London, Special Publications*, **312**, 205–218.
- 1300 TEVELEV, A. V. & GEORGIEVSKII, B. V. 2012. Deformation history and hydrocarbon potential  
1301 of the Southwestern Gissar Range (Southern Uzbekistan). *Moscow University Geology*  
1302 *Bulletin*, **67**, 340–352.
- 1303 ULMISHEK, G. F. 2004. Petroleum geology and resources of the Amu Darya Basin,  
1304 Turkmenistan, Uzbekistan, Afghanistan, and Iran. *U.S. Geological Survey Bulletin*, **2201-**  
1305 **H**, 1–32.
- 1306 VAKHRAMEEV, V. A., ILJINA, V. I. & FOKINA, N. I. 1988. Subdivision of the continental  
1307 Jurassic based on plants. *In*: KRYMHOLTS, G. YA., MESEZHNIKOV, M. S. & WESTERMANN,  
1308 G. E. G. (eds) 1988. *The Jurassic ammonite zones of the Soviet Union. Geological Society*  
1309 *of America, Special Paper*, **223**, 63–72.

- 1310 WALKER, R. G. & PLINT, A. G. 1992. Wave-and storm-dominated shallow marine system. *In:*  
1311 WALKER, R. G. & JAMES, N. P. (eds) *Facies models: Response to sea level change*.  
1312 Geological Association of Canada, St. John's, 219–238.
- 1313 WILMSEN, M., FÜRSICH, F. T., SEYED-EMAMI, K. & MAJIDIFARD, M. R. 2009a. The  
1314 Cimmerian Orogeny in Iran – a foreland perspective. *Terra Nova*, **21**, 211–218.
- 1315 WILMSEN, M., FÜRSICH, F. T., SEYED-EMAMI, K. & MAJIDIFARD, M. R. 2009b. An overview  
1316 of the stratigraphy and facies development of the Jurassic System on the Tabas Block, east  
1317 central Iran. *In:* BRUNET, M.-F., WILMSEN, M. & GRANATH, J. W. (eds) *South Caspian to*  
1318 *Central Iran Basins. Geological Society, London, Special Publications*, **312**, 323–343.
- 1319 Zanchetta, S., Berra, F., Zanchi, A., Bergomi, M., Caridroit, M., Nicora, A., Heidarzadeh, G.  
1320 2013. The record of the Late Palaeozoic active margin of the Palaeotethys in NE Iran:  
1321 Constraints on the Cimmerian orogeny. *Gondwana Research*, **24**, 1237–1266.
- 1322 ZANCHI A., ZANCHETTA S., BERRA F., MATTEI M., GARZANTI E., MOLYNEUX S., NAWAB A.  
1323 & SABOURI J. 2009. The Eo-Cimmerian (Late? Triassic) orogeny in north Iran. *In:*  
1324 BRUNET, M.-F., WILMSEN, M. & GRANATH, J. W. (eds) *South Caspian to Central Iran*  
1325 *Basins. Geological Society, London, Special Publications*, **312**, 31–55.
- 1326 ZANCHI, A., ZANCHETTA, S., ANGIOLINI, L., VEZZOLI, G. 2012. Is SE-Pamir a Cimmerian  
1327 Block? *Rendiconti online della Società Geologica Italiana*, **22**, 239–242.
- 1328

1329

1330 Captions of figures and tables

1331

1332 **Fig. 1.** Position of the study area in the framework of the Amu Darya and Afghan-Tajik  
1333 basins **(a)** and section localities in southern Uzbekistan **(b)**; see also Table 1). **(a)** Outlines of  
1334 the Amu Darya and Afghan-Tajik basins according to Klett *et al.* (2012), topography  
1335 background from USGS SRTM-3 [http://dds.cr.usgs.gov/srtm/version2\\_1/SRTM3/](http://dds.cr.usgs.gov/srtm/version2_1/SRTM3/). **(b)**  
1336 Background topography from USGS SRTM3, geology according to geological map of  
1337 Uzbekistan 1:500 000 (Shayakubov 1998). Jurassic rocks are shown in blue colour.

1338

1339 **Fig. 2.** Lithostratigraphic subdivisions (formations) of the Jurassic succession in southern  
1340 Uzbekistan (after Krymholts *et al.* 1988, modified). H: Hettangian; PL: Pliensbachian; T:  
1341 Toarcian; A: Aalenian; BAJOC: Bajocian; CALL: Callovian; O: Oxfordian; K:  
1342 Kimmeridgian; T: Tithonian; CR: Cretaceous; L: Lower; M: Middle; U: Upper.

1343

1344 **Fig. 3.** Section of the Jurassic succession near Shalkan, Kugitang Mountains. For position see  
1345 Table 1 and Fig. 1, for key of symbols Fig. 4. Siliciclastic sediments: cl, clay; s, silt/siltstone;  
1346 f, fine-grained sandstone; m, medium-grained sandstone; c, coarse-grained sandstone; g,  
1347 gravelly sandstone; carbonate microfacies: m, mudstone; w/f, wackestone/floatstone; p,  
1348 packstone; g, grainstone; r, rudstone. K., Kugitang Formation.

1349

1350 **Fig. 4.** Key of symbols.

1351

1352 **Fig. 5. (a)** Jurassic succession near Shalkan (see Fig. 3 for litholog). The arrow points to the  
1353 top of the Palaeozoic metamorphic basement, the vertical wall is the Callovian-Oxfordian  
1354 Kugitang Formation. Below is the softer Early Jurassic to early Callovian succession which is  
1355 dominated by fine-grained, often poorly indurated siliciclastic sediments and therefore  
1356 weathers more easily. **(b)** Jurassic succession at Panjab (see Fig. 7 for litholog). The lower  
1357 part of the section corresponds to the Upper Bajocian - Lower Bathonian Degibadam  
1358 Formation, the recessive middle part to the silty marl of the Baysun Formation. The vertical  
1359 cliff is composed of limestones of the Kugitang Formation. **(c)** Succession of stacked fluvial  
1360 sandstones displaying lateral accretion; basal part of the Shargun section (see Fig. 11 for  
1361 litholog). The individual sandstone bodies are separated by thin, often lenticular,  
1362 carbonaceous mudstone units. **(d)** Palaeosol (brown soil) overlying the Palaeozoic

1363 metamorphic basement and followed by a sharp-based sandstone unit representing the fill of a  
1364 small fluvial channel; Shalkan section. (e) Thin conglomerate overlying weathered  
1365 metamorphic basement rocks west of Vuariz. (f) Upper part of the non-marine Jurassic  
1366 succession, strongly reduced in thickness, at Vuariz. The figured succession consists mainly  
1367 of fine-grained floodplain deposits, with occasional intercalations of carbonaceous lacustrine  
1368 mudstones and fluvial channel sandstones. The transgressive surface at the top of the cliff is  
1369 marked with an arrow. (g) Stacked fluvial channel sandstones separated by finer-grained  
1370 floodplain deposits, south-west of the village Vuariz. (h) Transition from the marly-  
1371 calcareous Baysun Formation to the thick-bedded limestones of the Kugitang Formation; Iron  
1372 Gate section (see Fig. 10 for litholog).

1373

1374 **Fig. 6.** Section of the Jurassic succession at Vandob, Kugitang Mountains. For position see  
1375 Table 1 and Fig. 1, for key of symbols Figs. 3, 4. TR, transgressive surface. K., Kugitang  
1376 Formation.

1377

1378 **Fig. 7.** Section of the Jurassic succession at Panjab, northern Kugitang Mountains. For  
1379 position see Table 1 and Fig. 1, for key of symbols Figs. 3, 4. K., Kugitang Formation.

1380

1381 **Fig. 8.** Section of the Jurassic succession at the Dalut Mine near the village Toda. For position  
1382 see Table 1 and Fig. 1, for key of symbols Figs. 3, 4. c., ch., river channel; s., sw., swamp.

1383

1384 **Fig. 9.** (a) Thick fluvial sandstone sharply overlain by fine-grained lake deposits; base of  
1385 Dalut Mine section (Fig. 8). (b) Point bar deposits displaying lateral accretion: Dalut Mine  
1386 section at 154 m (see Fig. 8 for litholog). (c) Rootlets in overbank sediments; Dalut Mine  
1387 section. (d) Several coarsening-upward cycles of prodelta mudstones to bedded deltafront  
1388 sandstones overlain by cross-bedded sandstones of a large distributary channel (upper two-  
1389 fifths of section); Iron Gate section (see Fig. 10 at 70-115 m). (e) Sediments of the storm-flow  
1390 dominated outer ramp. Between the argillaceous silty background sediments gutter casts  
1391 (arrowed) and graded parallel-laminated sandstones are intercalated. Degibadam Formation of  
1392 the Iron Gate section (see Fig. 10 at 18-27 m). (f) Hummocky cross-stratified sandstone;  
1393 Degibadam Formation, Dalut Mine section. (g) The trace fossil *Diplocraterion parallelum* in  
1394 the basal marine sandstone at the Shalkan section, first evidence of the marine transgression.  
1395 (h) Angular unconformity between the Baysun Formation (below) and the Kugitang

1396 Formation (above) near Khanjizza, north of Denau, indicative of synsedimentary tectonic  
1397 movements produced by the slight tilting of a fault block.

1398

1399 **Fig. 10.** Section of the Jurassic succession near Derbent at the "Iron Gate". For position see  
1400 Table 1 and Fig. 1, for key of symbols Figs. 3, 4. K., Kugitang Formation.

1401

1402 **Fig. 11.** Sections of the Jurassic succession at the Shargun Mine. For position see Table 1 and  
1403 Fig. 1, for key of symbols Figs. 3, 4. K., Kugitang Fm; tr, transgression.

1404

1405 **Fig. 12.** Section of the Jurassic succession near Sangardak. For position see Table 1 and Fig.  
1406 1, for key of symbols Figs. 3, 4.

1407

1408 **Fig. 13.** Sections of the Jurassic succession near Vuariz. For position see Table 1 and Fig. 1,  
1409 for key of symbols Figs. 3, 4. D., Degibadam Fm.

1410

1411 **Fig. 14.** Middle part of the Baysun Formation NE of Vuariz (Vuariz section IV; co-ordinates:  
1412 N 38°49'29.6'', E 67°11'26.3''). The fine-grained packstones exhibit birdseyes and laminoid  
1413 fenestral fabrics characteristic of a peritidal environment. For key of additional symbols see  
1414 Figs. 3, 4.

1415

1416 **Fig. 15.** Examples of the main facies associations and their corresponding environments in the  
1417 Jurassic of southern Uzbekistan. **(a)** Braided river deposits (Vuariz section at 0-14 m). **(b)**  
1418 Meandering river deposits (Dalut Mine section at 225-231 m). **(c)** Flood-plain deposits (Dalut  
1419 Mine section at 86-98 m). **(d)** Swamp deposits (Dalut Mine section at 263-268 m and 298-304  
1420 m). **(e)** Offshore lake deposits (Shalkan section at 190-202 m). **(f)** Lake margin deposits  
1421 (Shalkan section at 348-360 m). **(g)** Distributary channel deposits (Iron Gate section at 96-110  
1422 m). **(h)** Delta front deposits (Vandob section at 370-379 m). **(i)** Prodelta - lower delta-front  
1423 deposits (Iron Gate section at 63.5-75.5 m). **(j)** Tide-influenced inner ramp deposits (Panjab  
1424 section at 40.5-52.5 m). **(k)** Protected inner ramp deposits (Panjab section at 34-46 m). **(l)**  
1425 high-energy deposits of the inner to middle ramp (Panjab section at 94.5-99.5 m). **(m)** storm-  
1426 wave dominated middle ramp (Vandob section at 503-513 m). **(n)** storm-flow dominated  
1427 outer ramp (Dalut Mine section at 552-562 m). **(o)** Low-energy outer mixed carbonate-  
1428 siliciclastic ramp deposits (Shalkan section at 740-745 m). **(p)** Condensed outer ramp deposits

1429 (Shalkan section at 728-733 m). **(q)** Low-energy outer carbonate ramp (Vandob section at  
1430 740-753 m).

1431

1432 **Fig. 16.** **(a-f)** Microphotographs of characteristic facies. Scale: 5 mm. **(a)** Poorly sorted,  
1433 immature, conglomeratic gravelly sandstone with abundant metamorphic clasts. Basal part of  
1434 Gurud Formation, Shalkan section at 31.1 m (see Fig. 3). **(b)** Hummocky cross-stratified, very  
1435 fine-grained sandstone with *Chondrites* at the base. Degibadam Formation, Shalkan section at  
1436 485 m (see Fig. 3). **(c)** Bioclastic fine-grained sandstone. Degibadam Formation, Vandob  
1437 section at 528.5 m (see Fig. 6). **(d)** Onco-rudstone strongly affected by pressure solution.  
1438 Baysun Formation, Panjab section at 221.2 m (see Fig. 7). **(e)** Onco-bio-floatstone with  
1439 abundant coral fragments. Oncoids mainly immature. Baysun Formation, Panjab section at  
1440 288 m (see Fig. 7). **(f)** Bio-onco-floatstone with abundant shell fragments. Baysun Formation,  
1441 Iron Gate section at 321.5 m (see Fig. 9). **(g)** Coarsening- and thickening-upward prodelta-  
1442 deltafront succession. Degibadam Formation, Iron Gate section at 79-84 m (see Fig. 10).

1443

1444 **Fig. 17.** Examples of cycles developed in the non-marine **(a-d)** and marine parts **(e-j)** of the  
1445 Jurassic succession. **(a)** Fluvial cycle (braided stream) (Vandob section at 0-6 m). **(b)** Fluvial  
1446 cycle (meandering river) (Vuariz section at 17.5-23.7 m). **(c-d)** Progradational lacustrine  
1447 cycles (Dalut Mine section; c: at 160-166 m; d: at 396-398 m). **(e)** Marine deltaic cycle  
1448 (Vandob section at 370-388 m). **(f)** Progradational cycle of the storm-wave influenced ramp  
1449 (Vandob section from 296-302 m). **(g)** Progradational cycle of the outer to middle siliciclastic  
1450 ramp (Iron Gate section at 52.5-55 m). **(h)** Progradational cycle of the storm-flow influenced  
1451 ramp (Iron Gate section at 16-20 m). **(i-j)** Cycles of the outer carbonate ramp (Panjab section;  
1452 i: at 263.8-268.2 m; j: at 274-278 m). c to j represent parasequences.

1453

1454 **Fig. 18.** Correlation of the Lower and Middle Jurassic succession within the study area. From  
1455 Vandob (Kugitang Mts.) in the south to Iron Gate/Dalut Mine (Ghissar Spur) in the north the  
1456 thickness is relatively uniform (800-950 m), but decreases distinctly towards the northeast  
1457 (Shargun/Sangardak; ~350 m) and even more so towards Vuariz in the north (<100 m for the  
1458 non-marine part). The latter areas clearly represent the margin of the basin, which is  
1459 supported by the coarser grain size of the sediment.

1460

1461 **Fig. 19.** Schematic development of the sedimentary environments in the Afghan-Tajik Basin  
1462 of southern Uzbekistan during the Early to early Late Jurassic. **(a)** During the Early Jurassic,

1463 non-marine conditions prevailed. Close to the basin margin coarse-grained fluvial deposits  
1464 were deposited, whereas extensive fine-grained lake deposits with coal swamps formed  
1465 towards the centre of the basin. **(b)** Flooding of the basin in the Late Bajocian, increased  
1466 levelling of the morphology of the hinterland, and a change from humid to more arid  
1467 conditions led to gradual replacement of the siliciclastic regime by a mixed carbonate-  
1468 siliciclastic regime. **(c)** By the late Callovian, a predominantly low-energy carbonate platform  
1469 covered the study area. Sporadic influx of siliciclastic material remained confined to margins  
1470 of the basin with a steep morphological gradient, whereas in deeper parts of the basin locally  
1471 organic-rich mudstones formed.

1472

1473 **Fig. 20.** Sequence stratigraphic interpretation of the marine Middle Jurassic succession at the  
1474 Iron Gate near Derbent. The siliciclastic to mixed carbonate-siliciclastic succession records  
1475 two highstand systems tracts and one transgressive systems tract within the Late Bajocian □  
1476 Early Callovian time interval. Another transgressive systems tract, recording the initial  
1477 flooding of the basin, is not exposed here. These 3rd-order sequences are composed of  
1478 numerous parasequences (see Fig. 10). Note the large deltaic succession representing  
1479 prodelta, delta front, and distributary channel in the lower part of the section.

1480

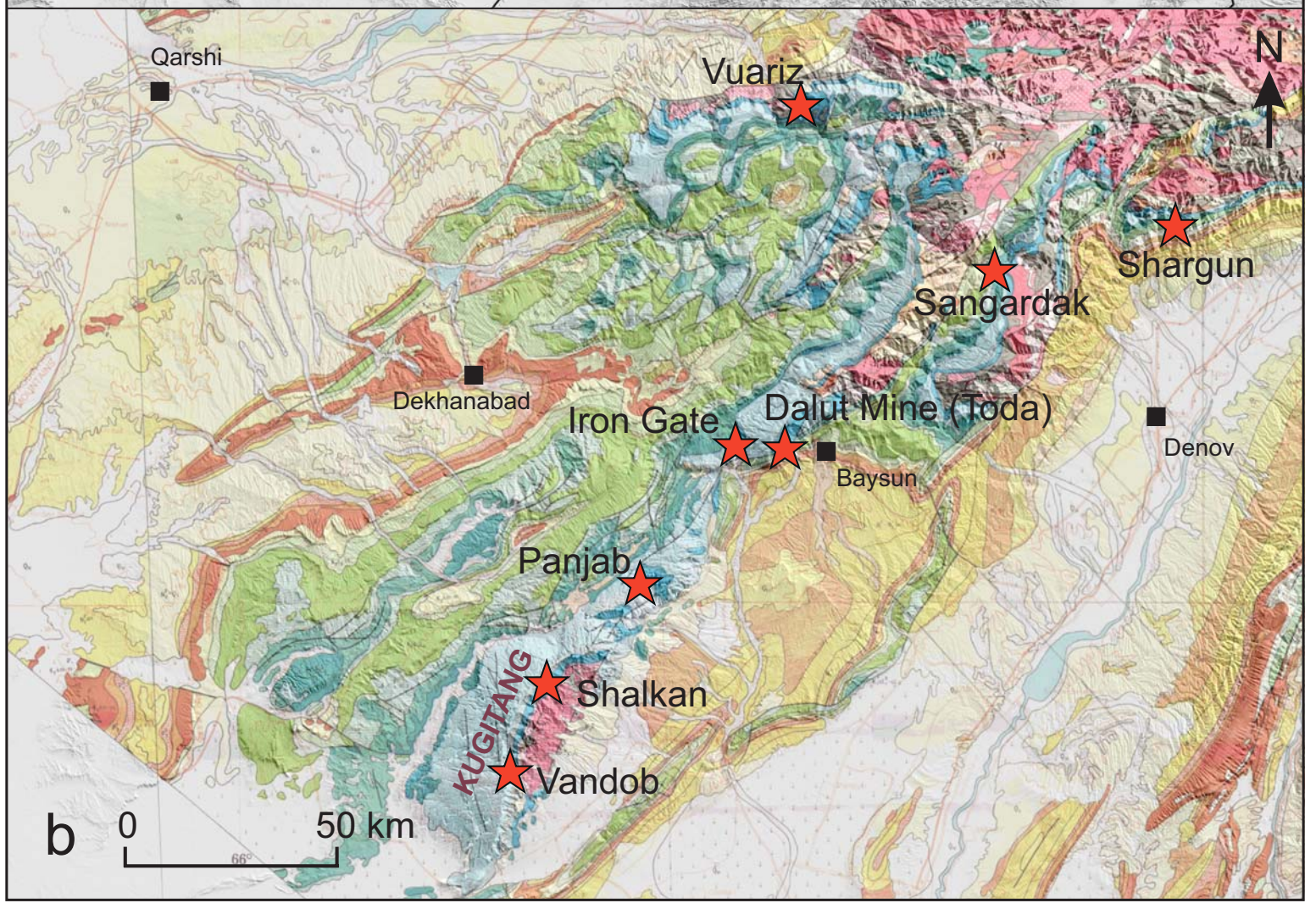
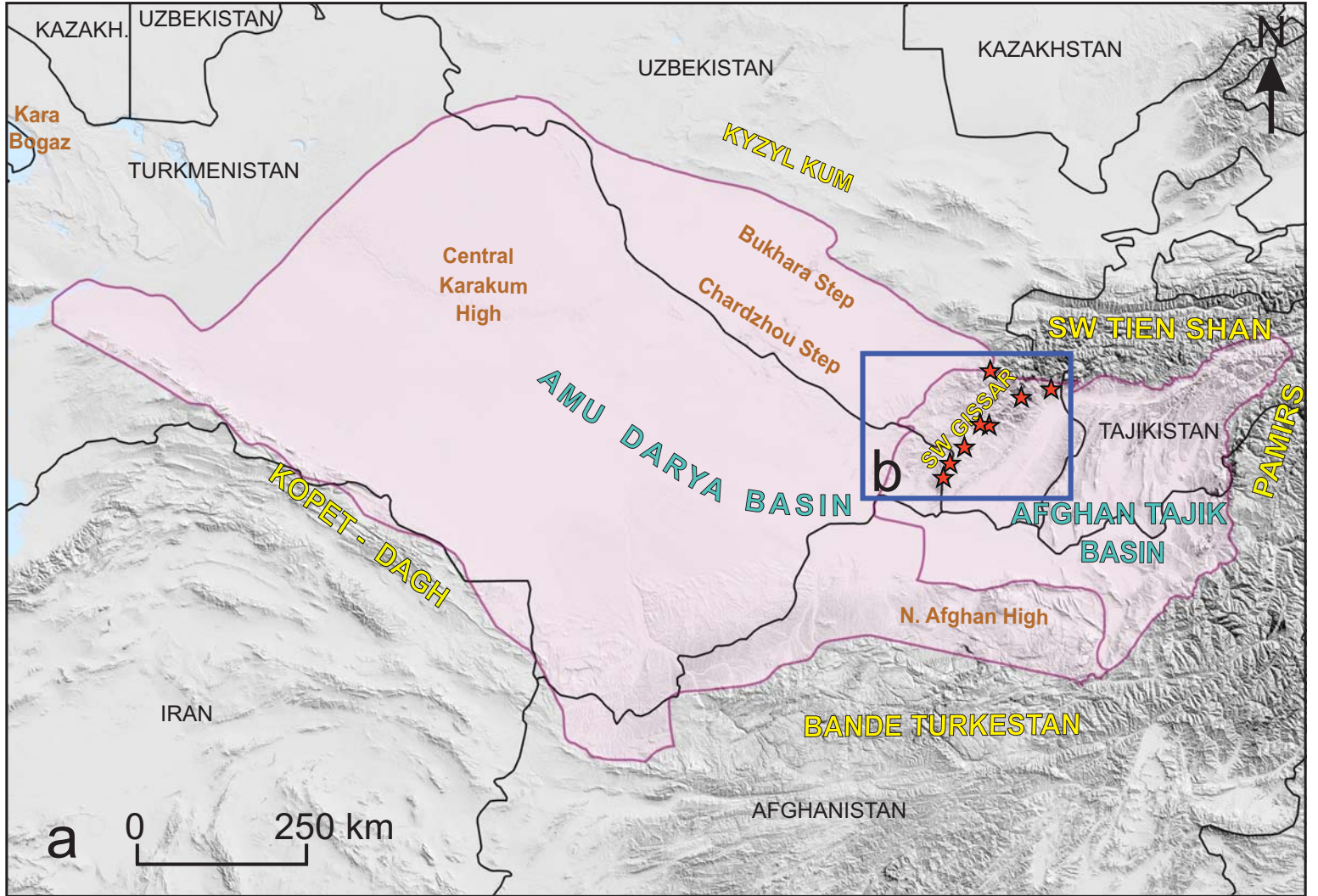
1481 **Fig. 21.** Comparison of Jurassic successions of Iran, southern Uzbekistan, and southwestern  
1482 Kyrgyzstan. CEIM, Central East Iranian Microcontinent; U.J., Upper Jurassic.

1483

1484 **Table 1.** Co-ordinates of the section localities.

1485 **Table 2.** Palaeoenvironments and their main features in the Lower to Middle Jurassic  
1486 successions. ss: sandstone.

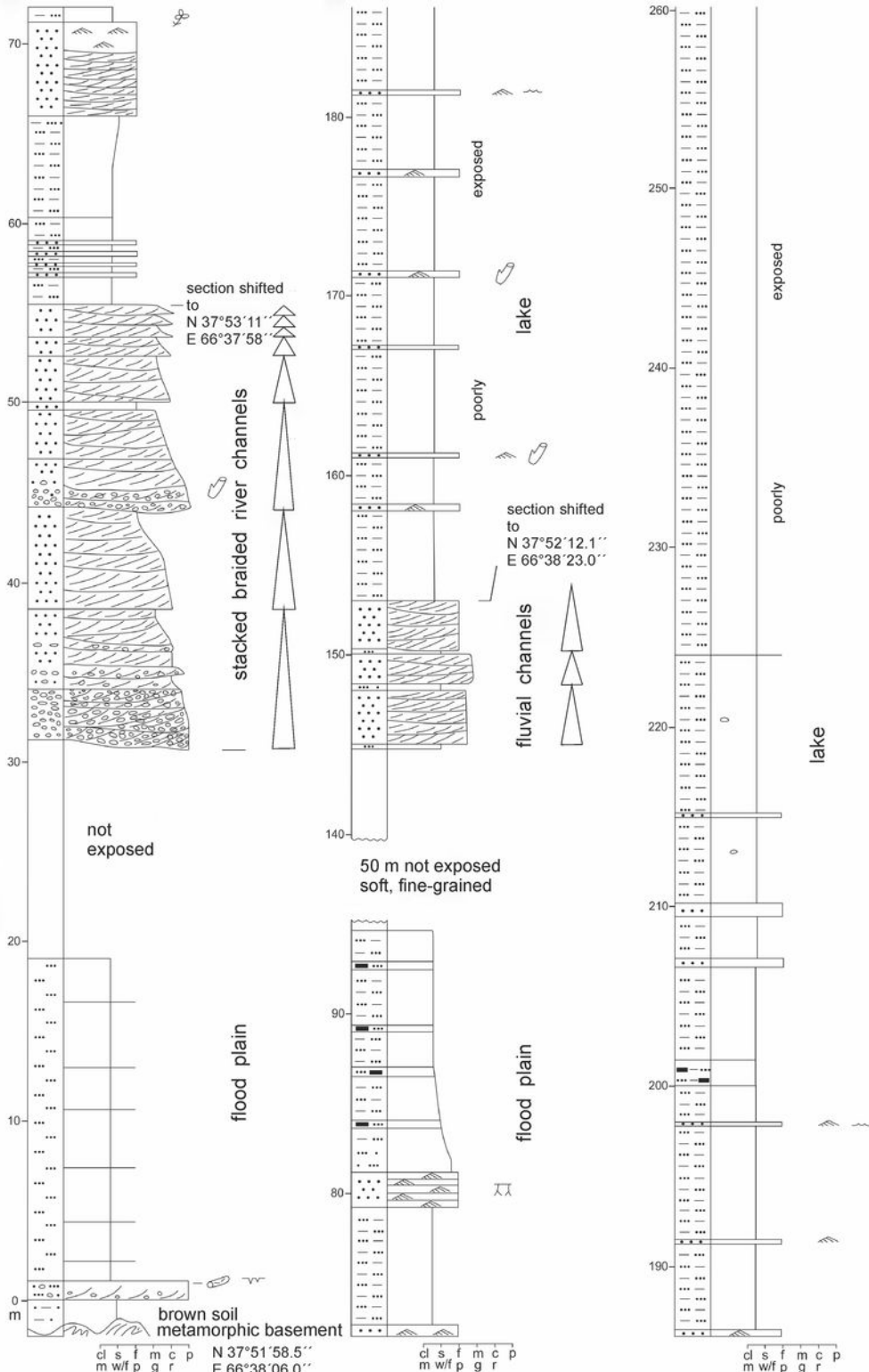
1487

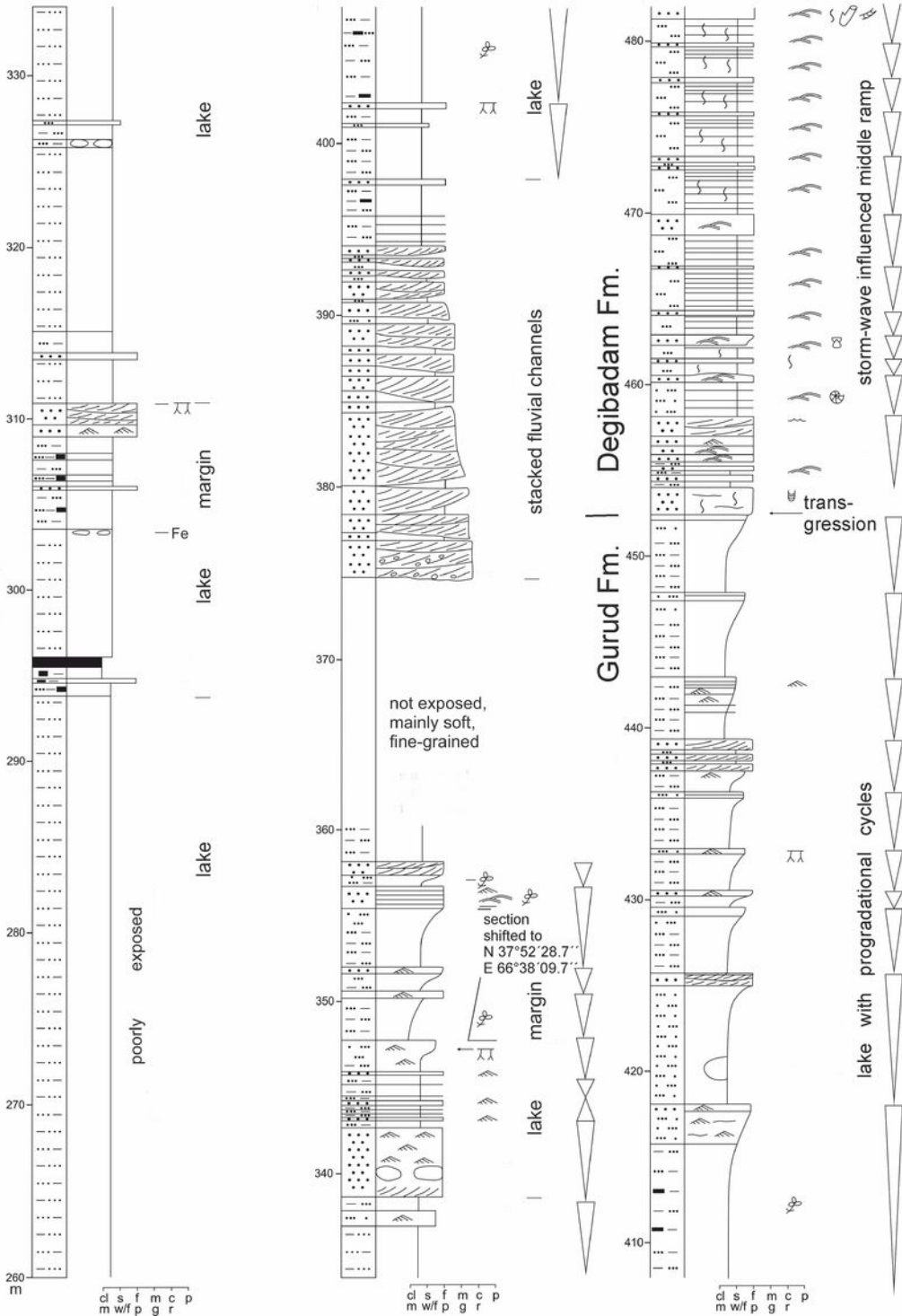


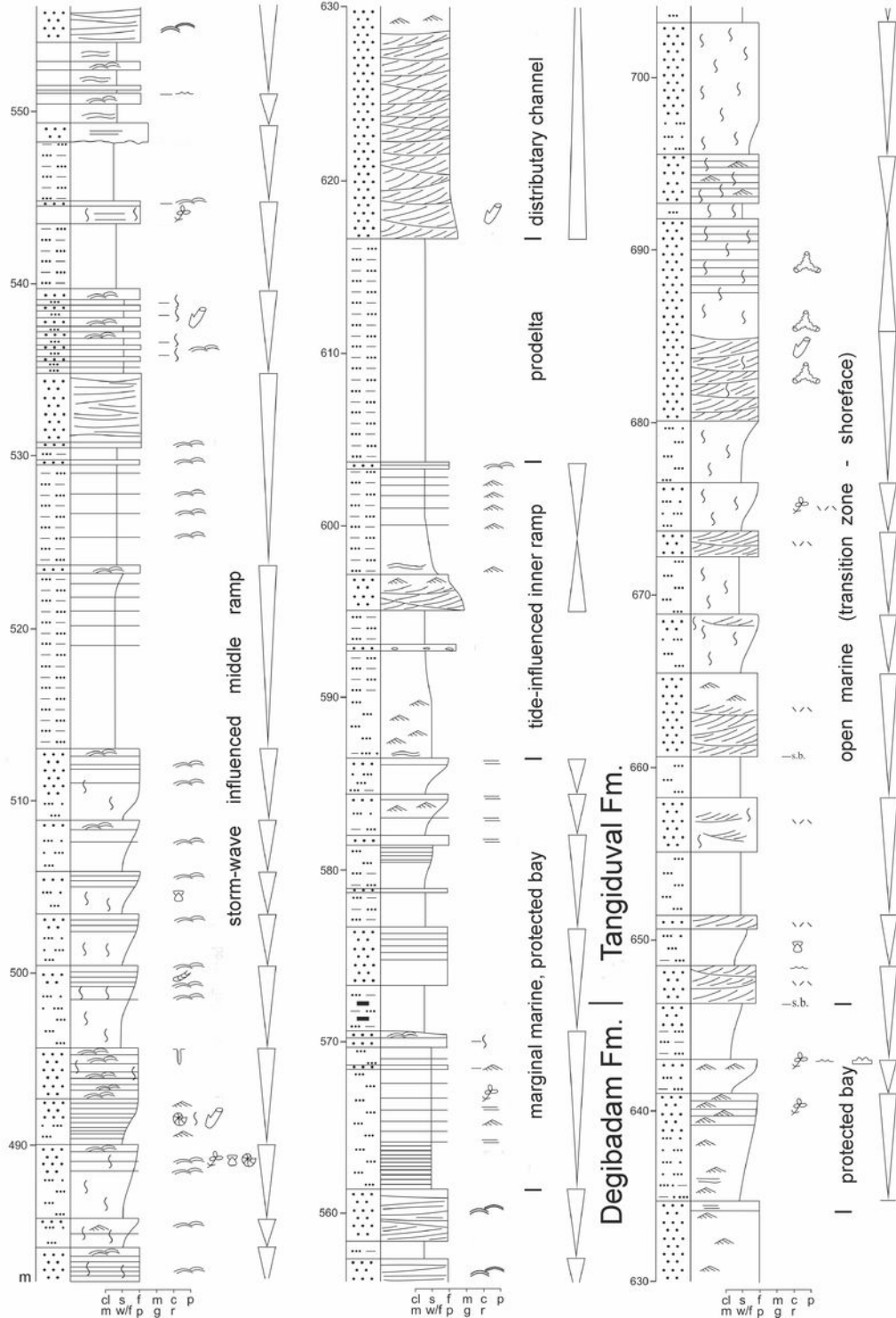
# formations

H.-PL.	T.A.	BAJOC.	BATHONIAN	CALL.	O.	K.	T.	CR.	<p><b>Karabil</b> continental red beds</p>
									<p><b>Gaurdak</b> evaporites; 1000 m</p>
									<p><b>Kugitang</b> thick-bedded carbonates; 500 m</p>
									<p><b>Baysun</b> silty marl, lime mudstones, onco-floatstones; 50-225 m</p>
									<p><b>Tangiduval</b> mudstones, calcareous silt- stones, sandstones; 30-80 m</p>
									<p><b>Degibadam</b> marine mudstones, siltstones, sandstones; 200 m</p>
									<p><b>Gurud</b> non-marine mudstones, sandstones, coal; 290-450 m</p>
									<p><b>Sandzhar</b> conglomerates, red mudstones (not present)</p>

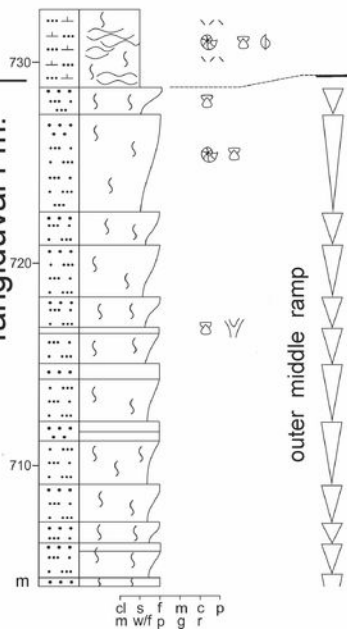
Gurud Fm.



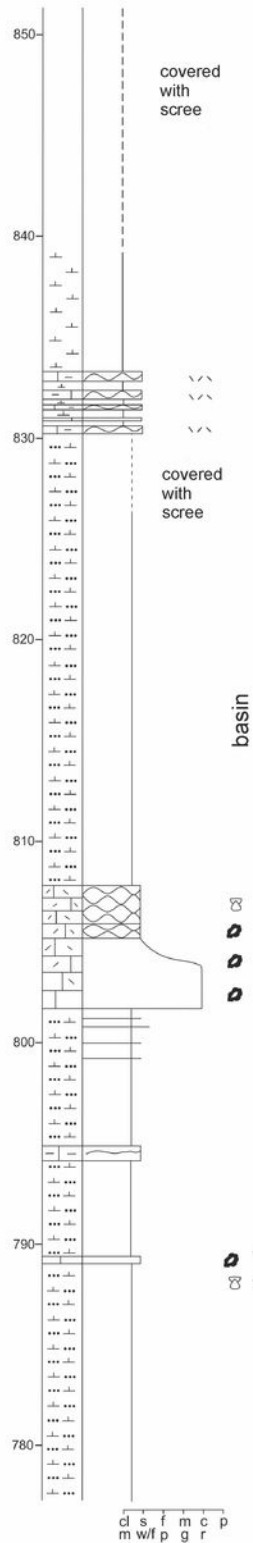
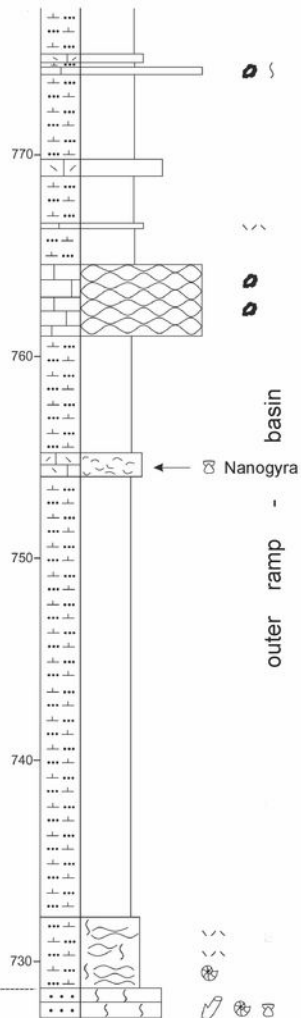




Tangiduval Fm.



Baysun Fm.



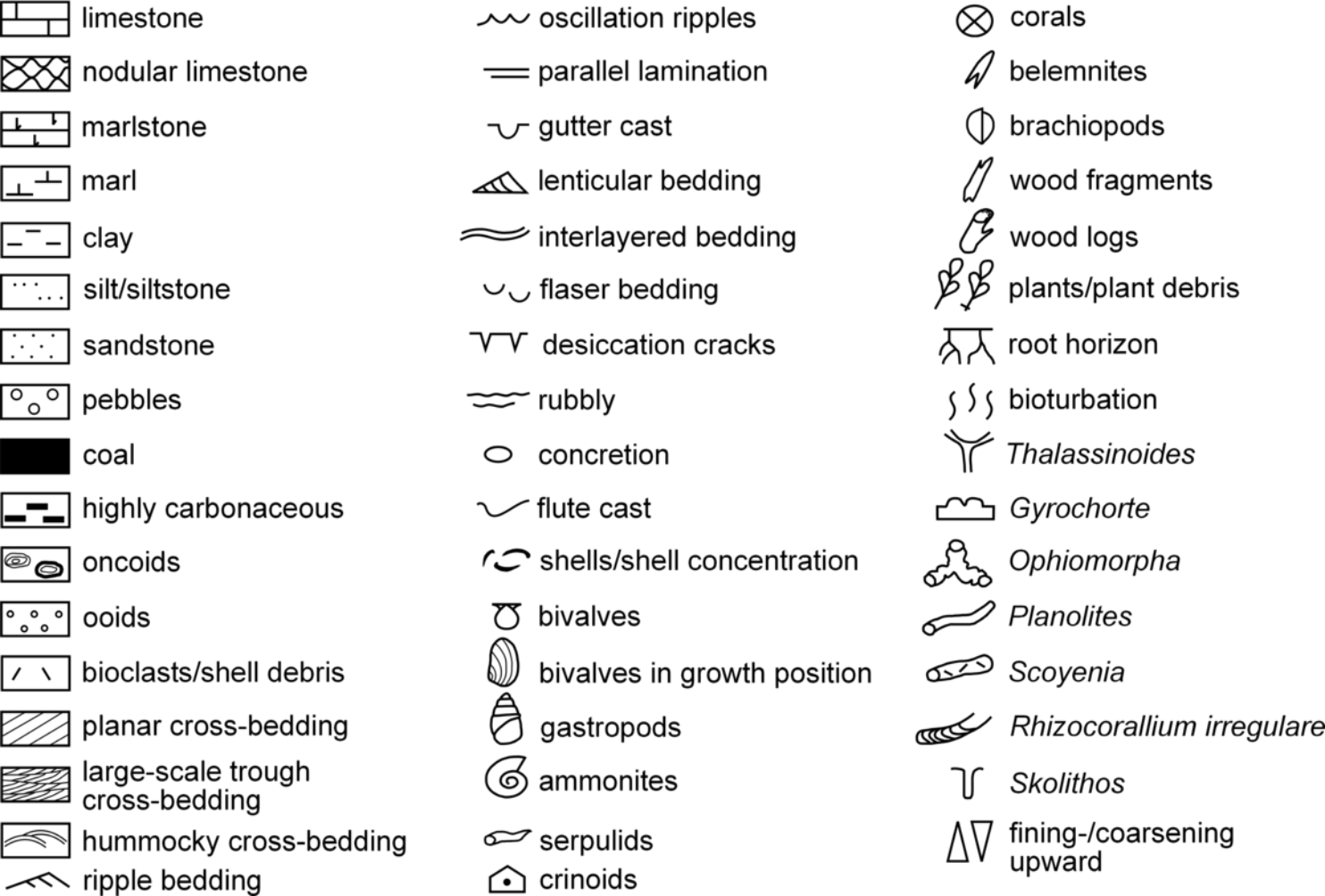
# Baysun Fm.

K.

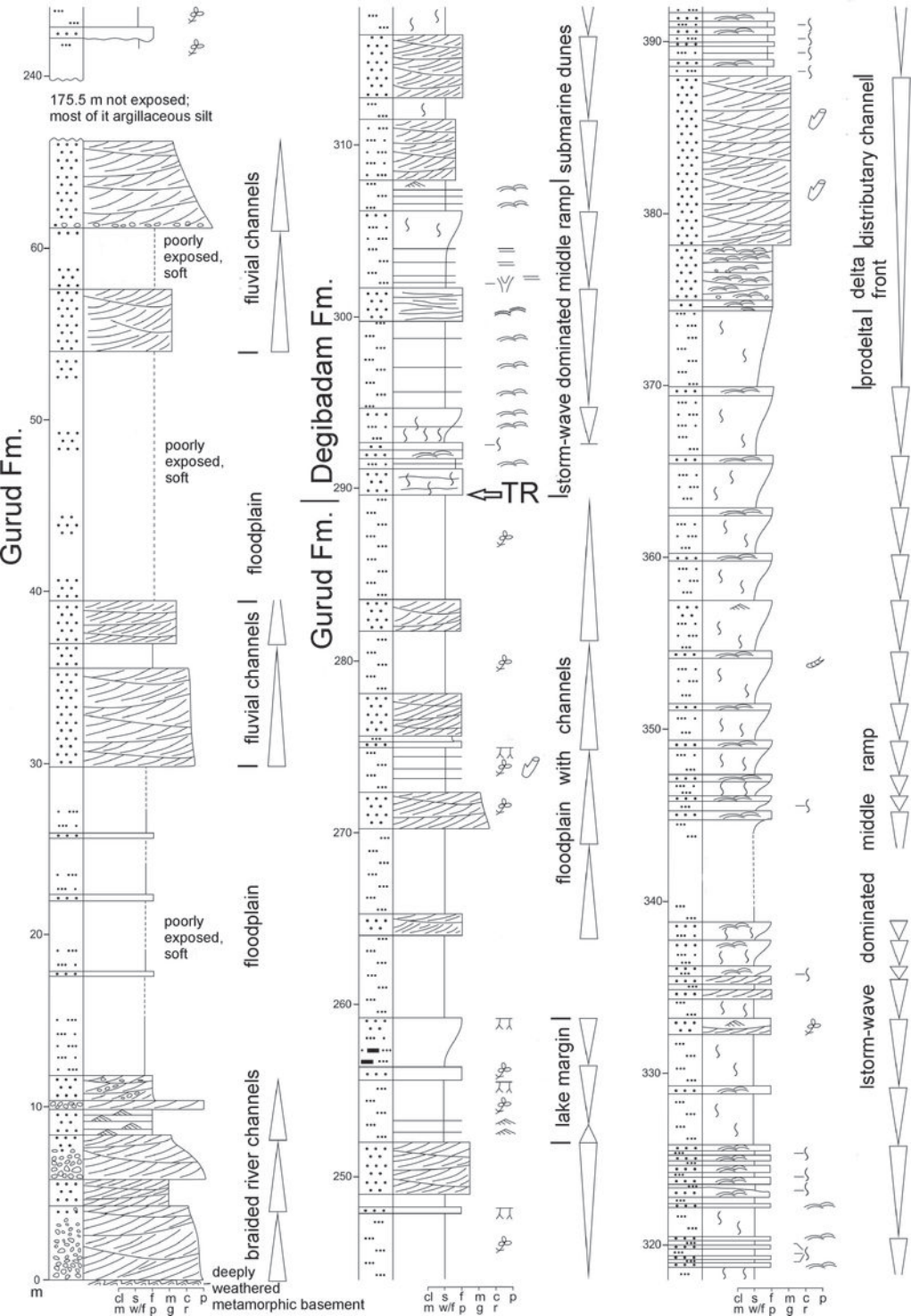


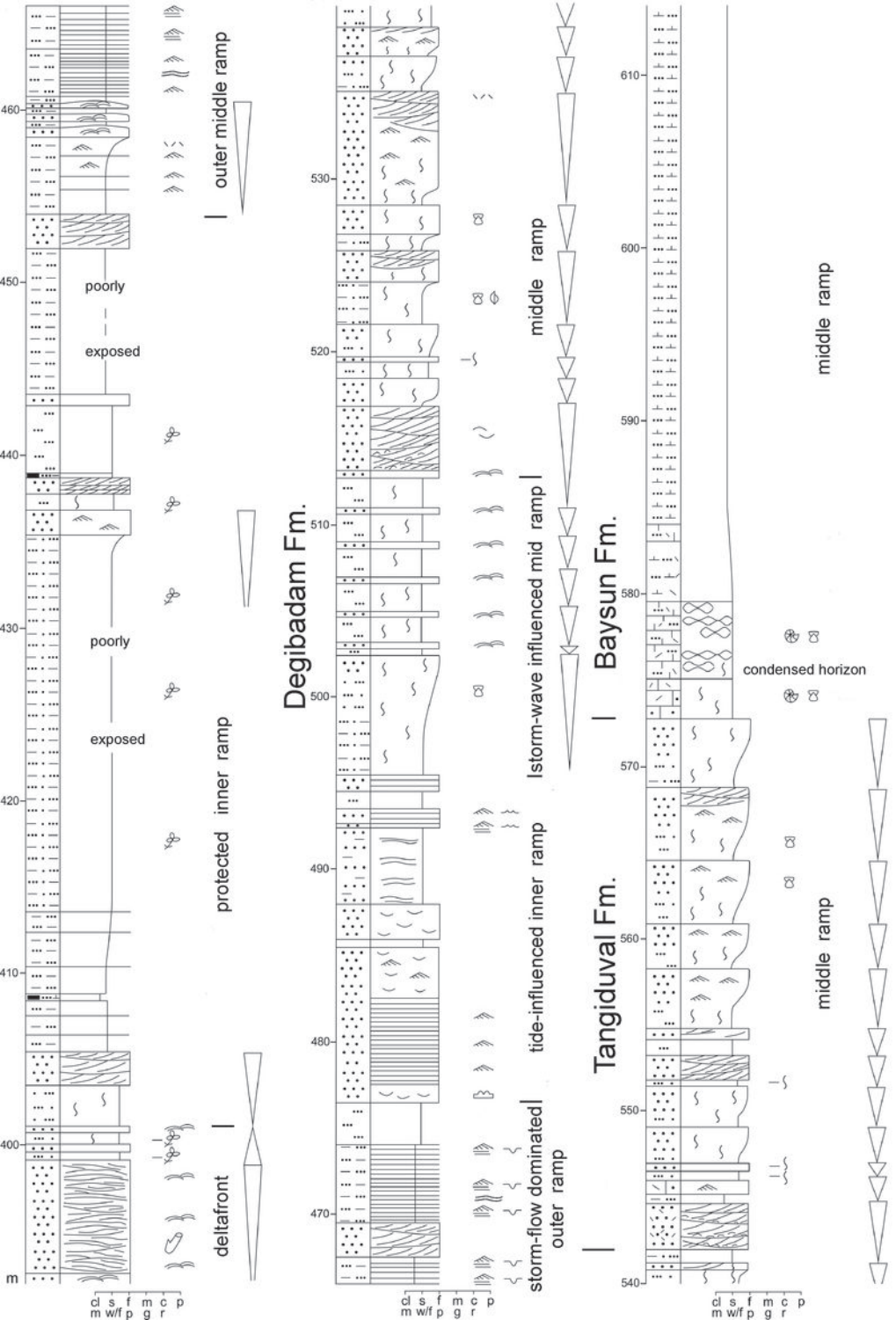
m cl s f m c p  
w/f p g r

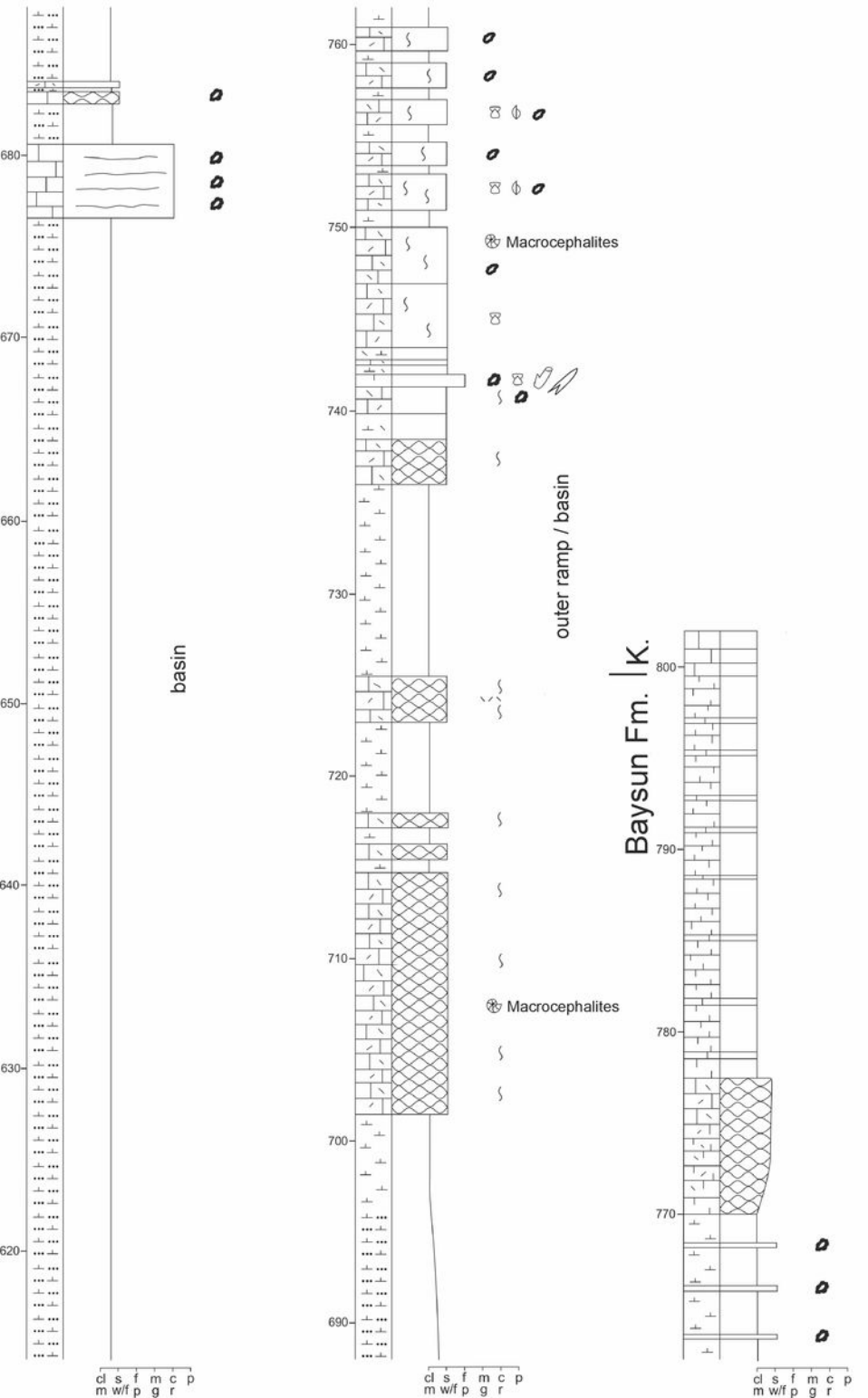
33

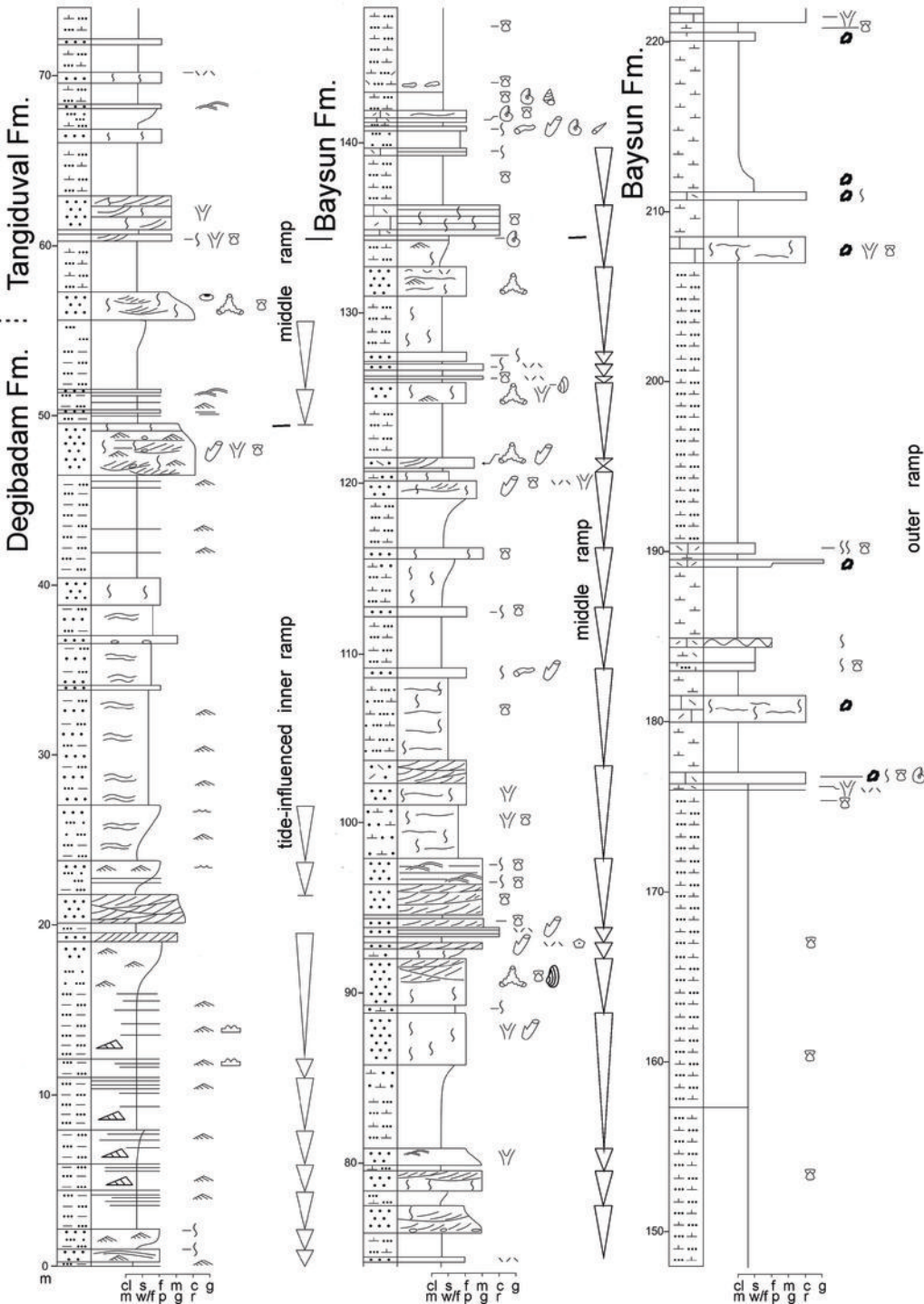






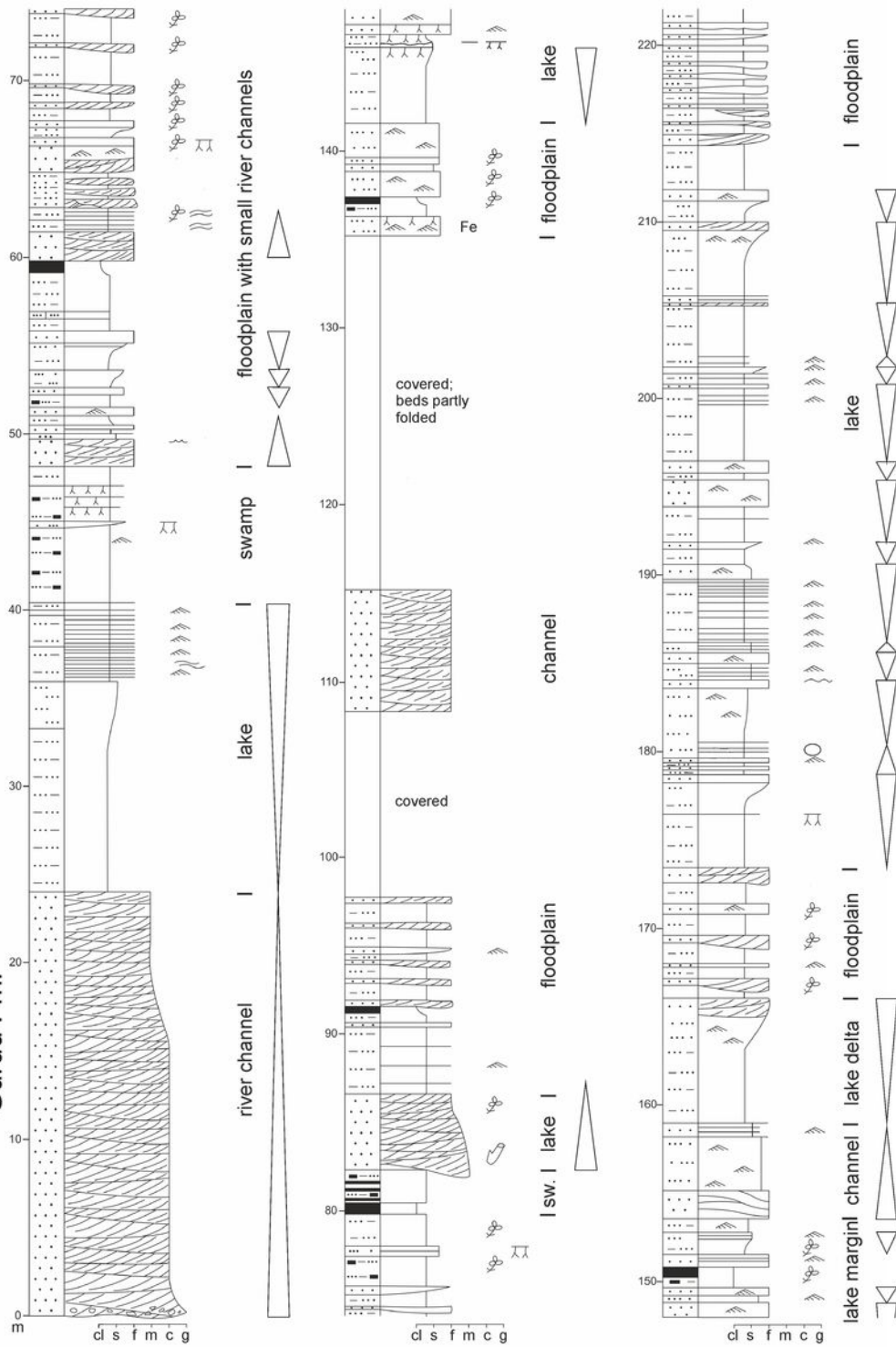




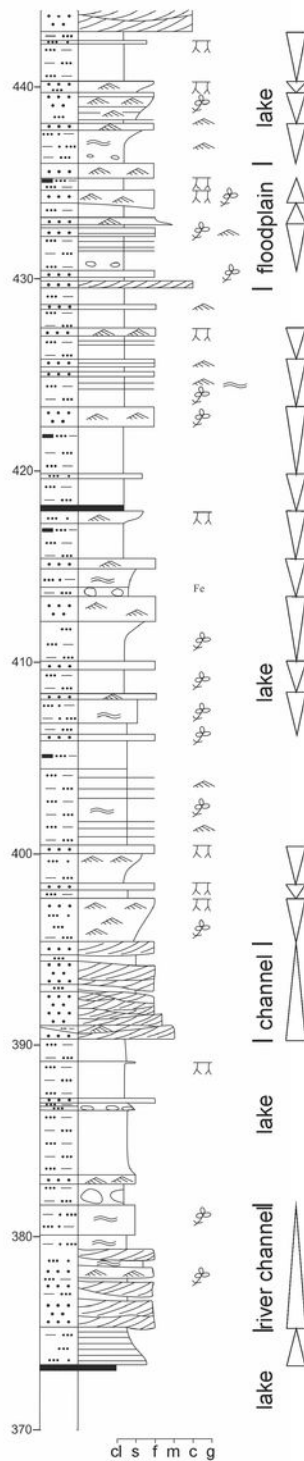
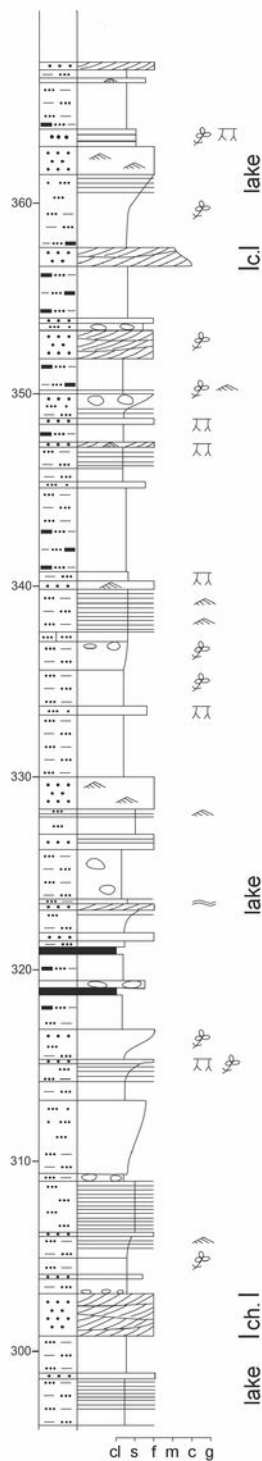
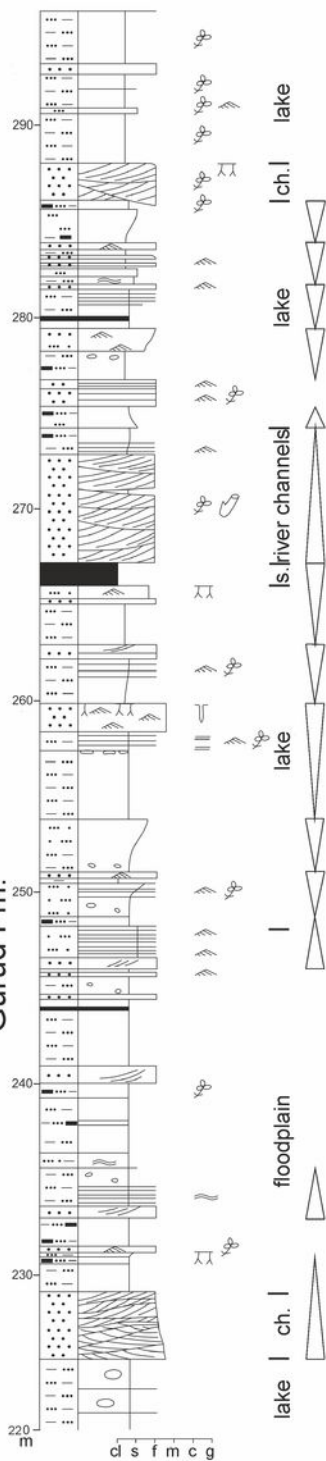




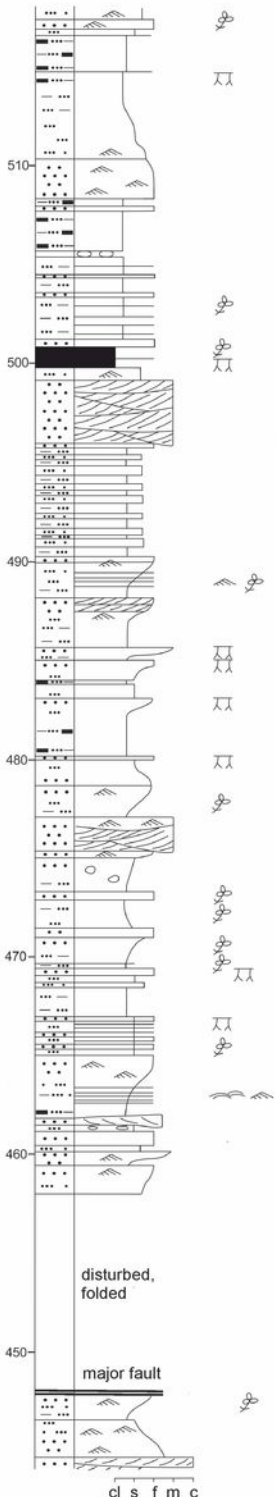
Gurud Fm.



Gurud Fm.



Gurud Fm.



floodplain

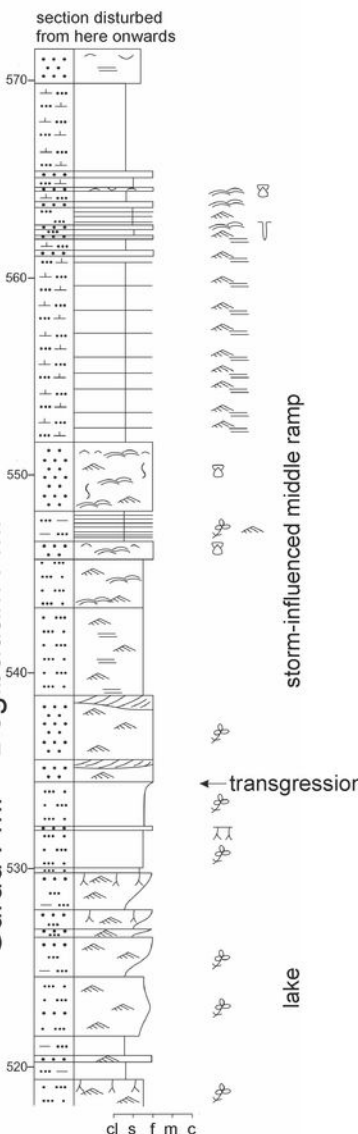
lake margin

floodplain

major fault  
disturbed, folded

cl s f m c

Gurud Fm. | Degibadam Fm.



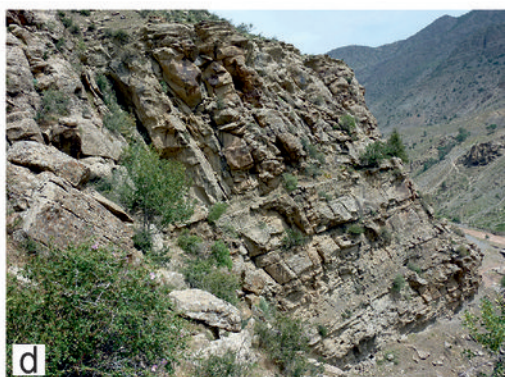
section disturbed from here onwards

storm-influenced middle ramp

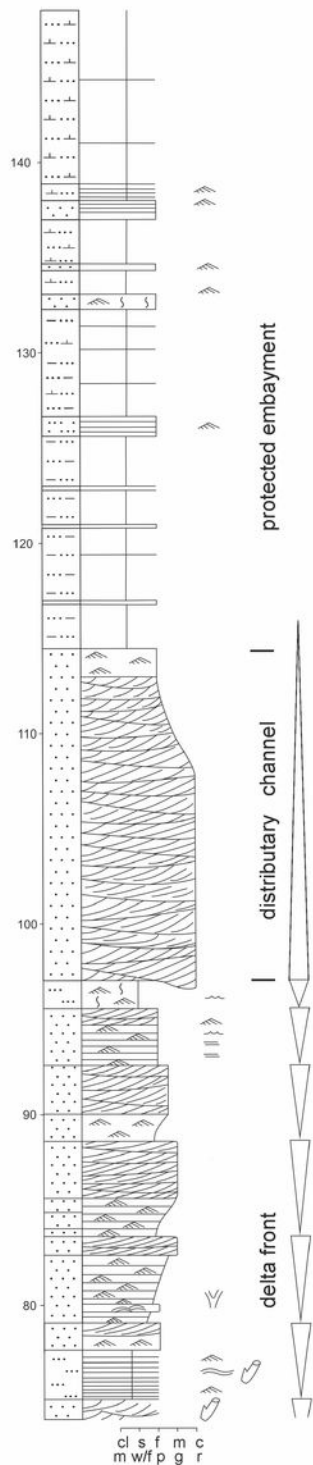
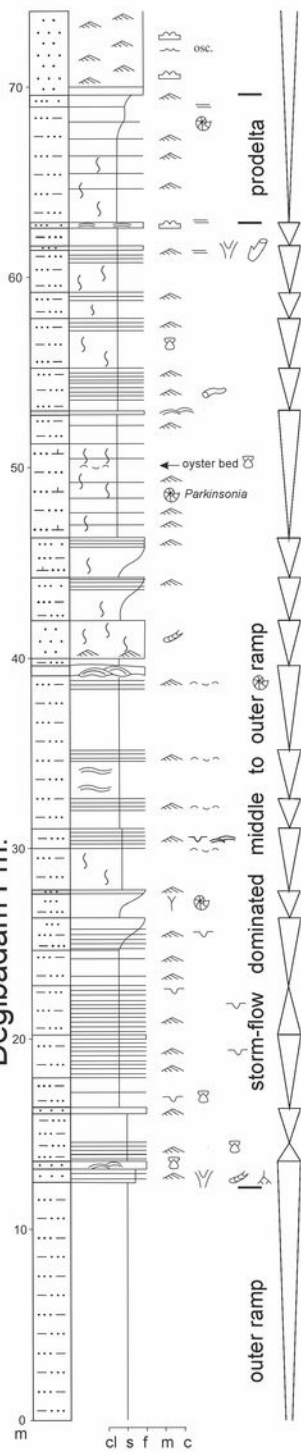
lake

← transgression

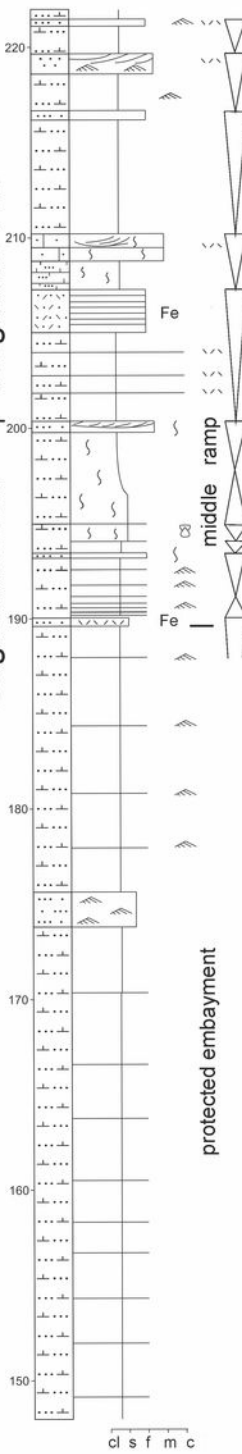
cl s f m c



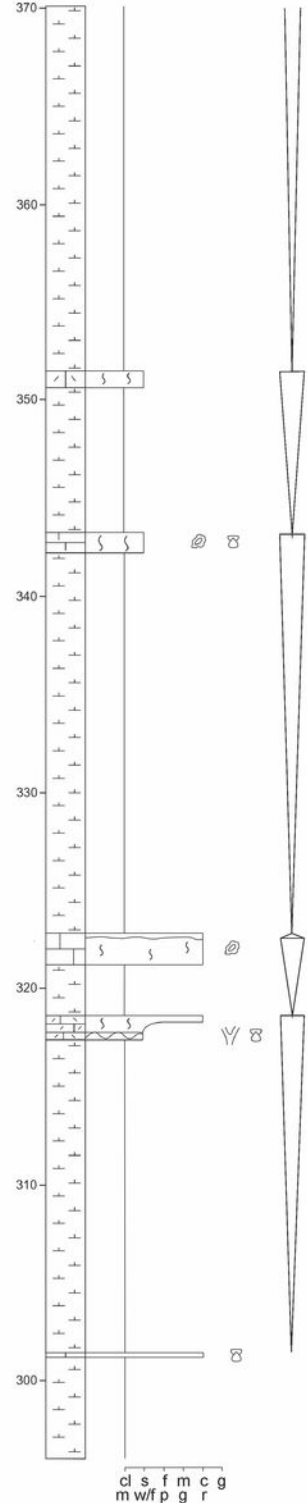
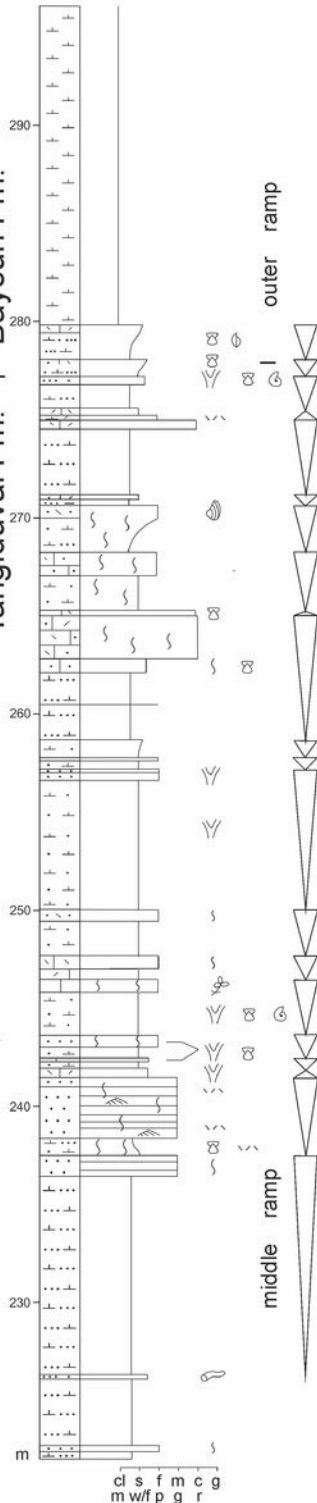
Degibadam Fm.



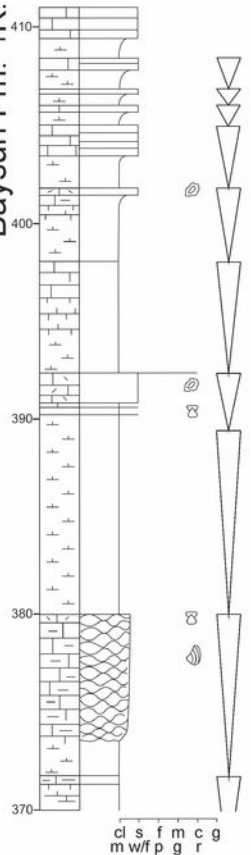
Degibadam Fm. | Tangiduval Fm.



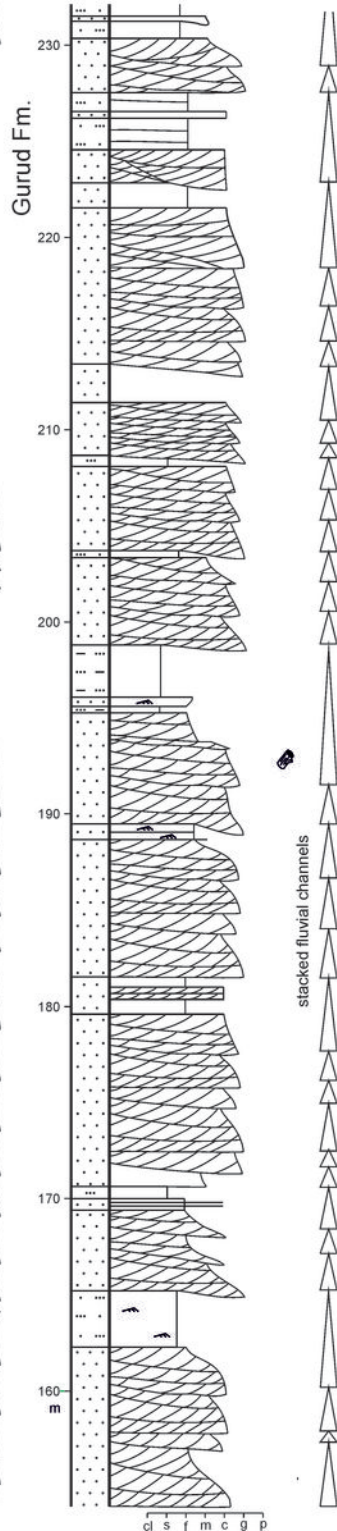
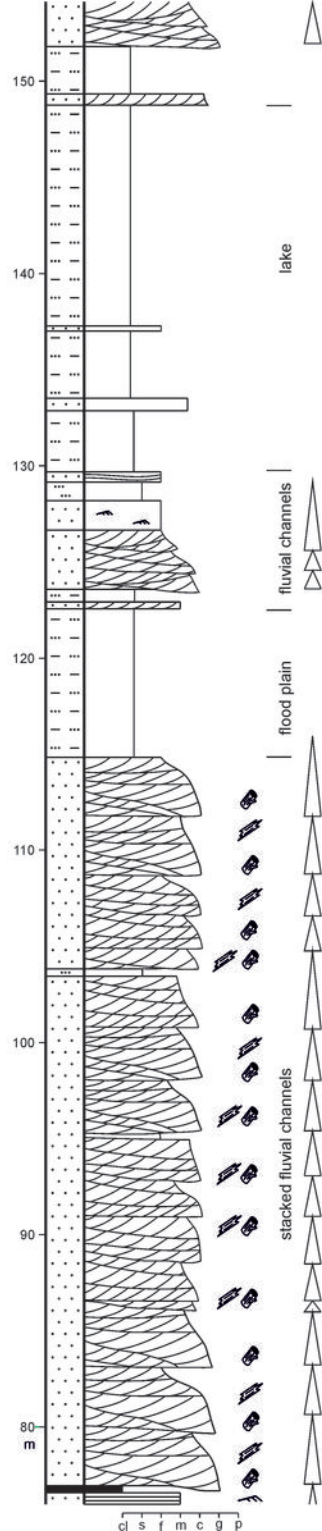
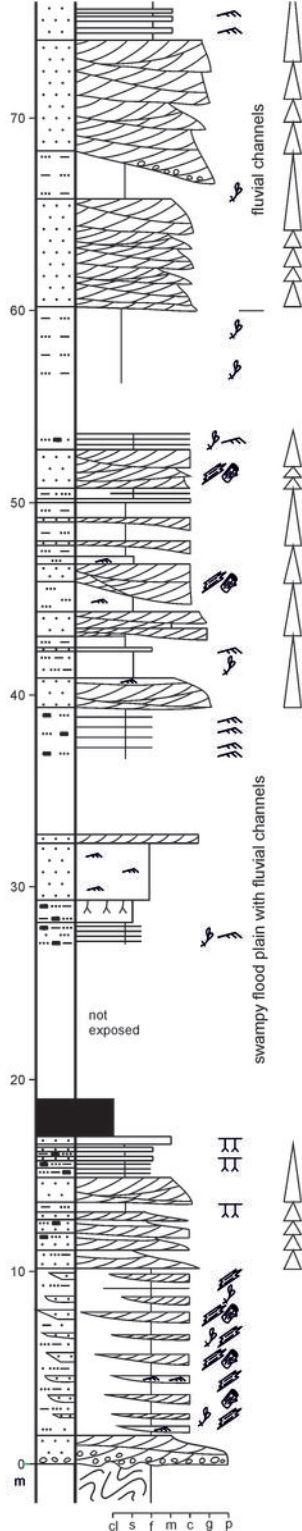
Tangiduval Fm. | Baysun Fm.



Baysun Fm. i.K.

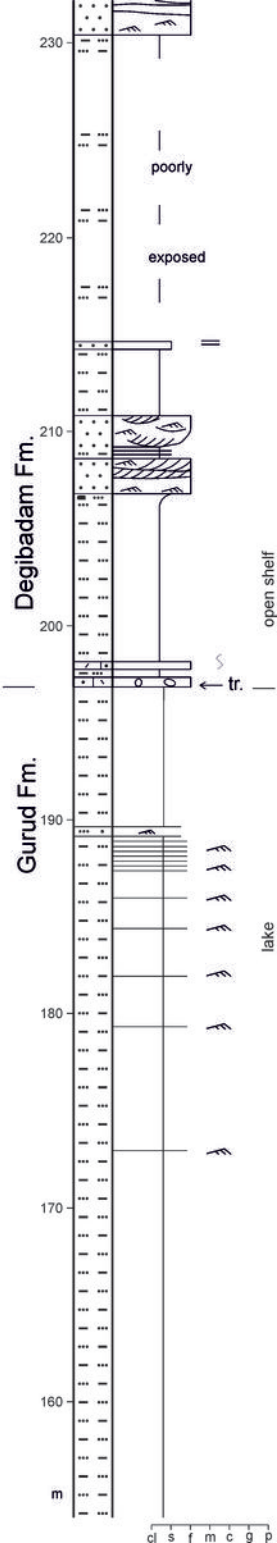
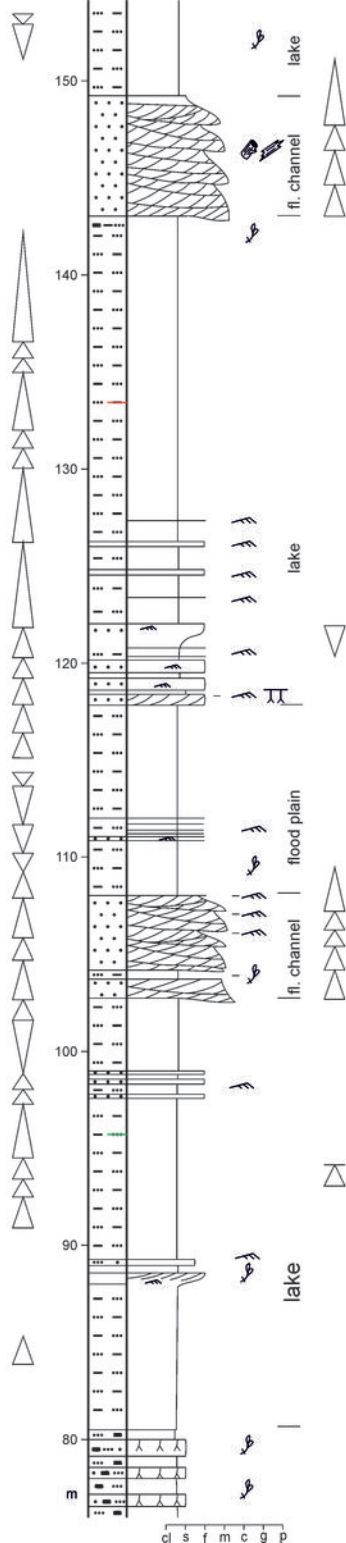
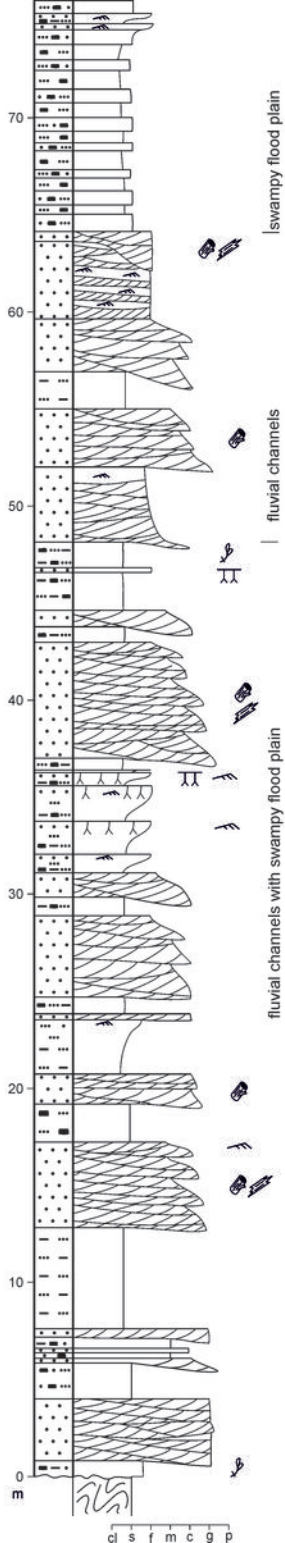


Gurud Fm.





Gurud Fm.



Degibadam Fm.

Gurud Fm.

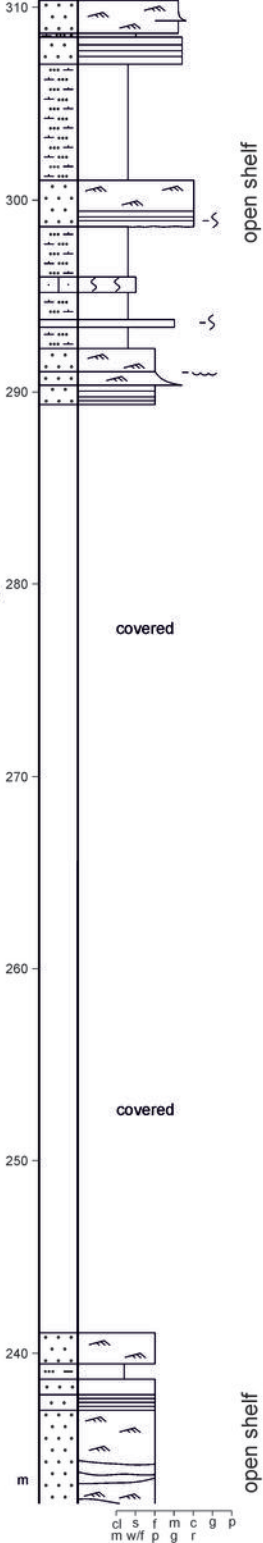
cl s f m c g p

cl s f m c g p

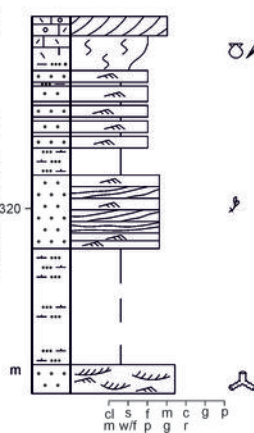
cl s f m c g p

Degibadam Fm.

Tangiduval Fm.

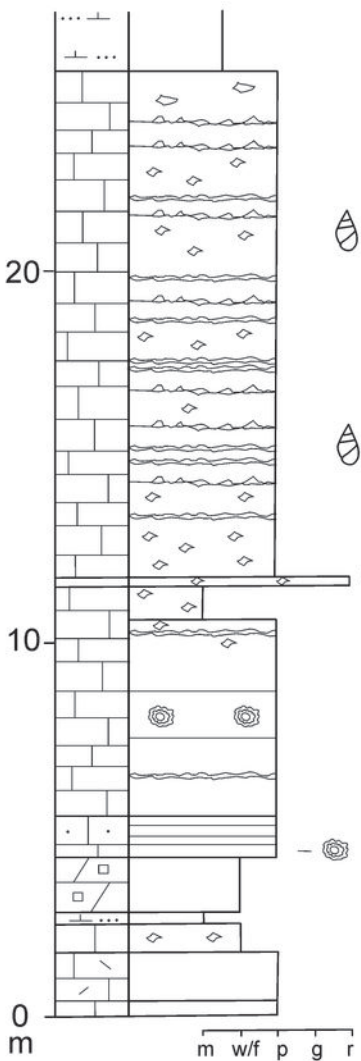


Tangiduval Fm. | k.

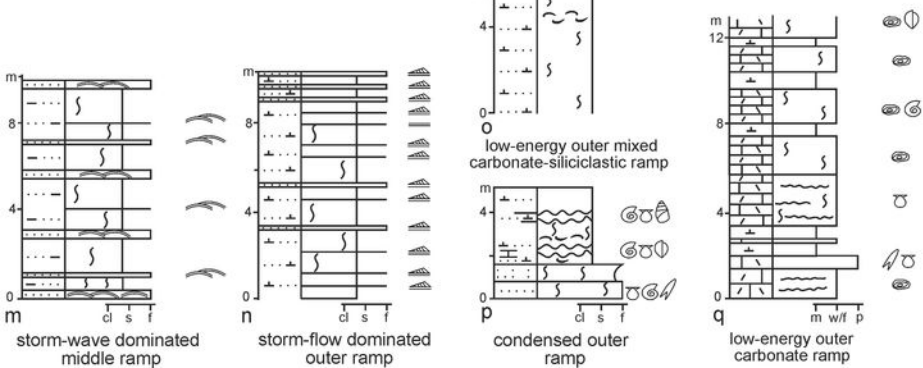
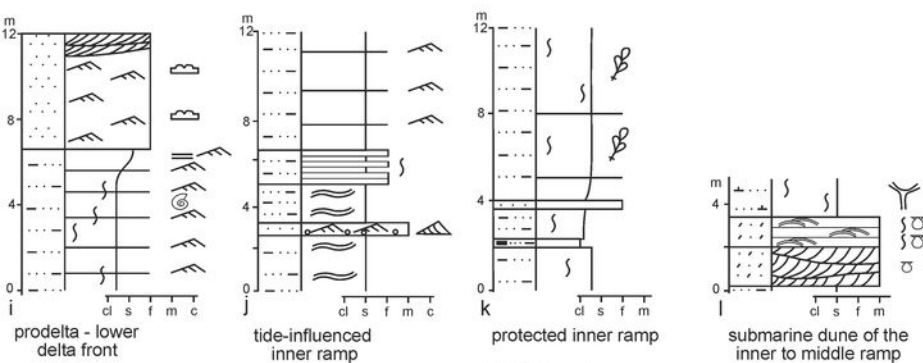
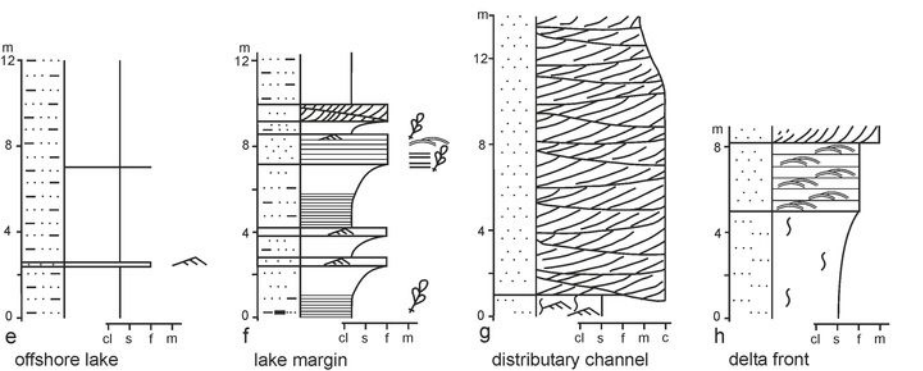
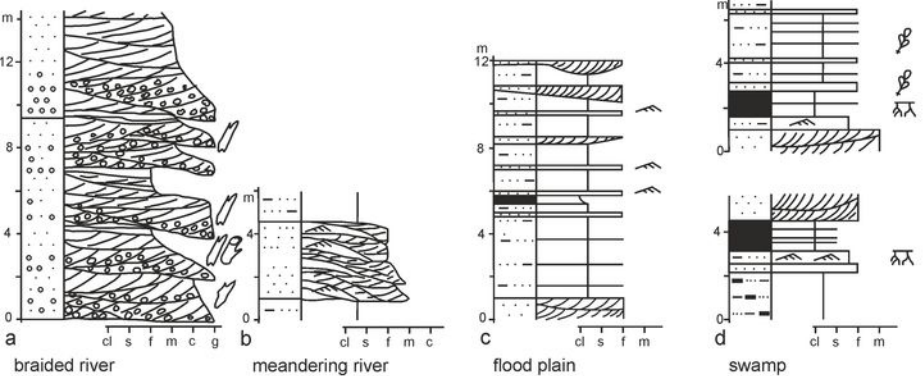


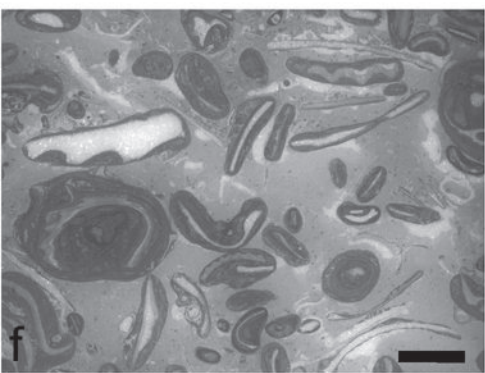
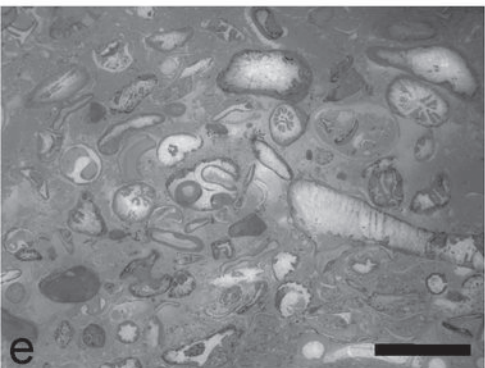
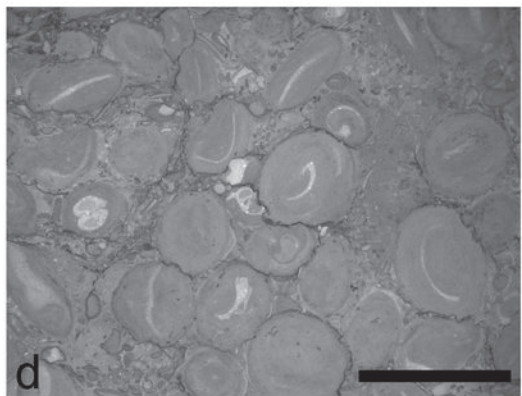
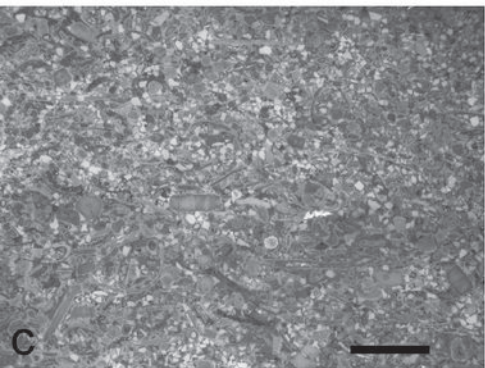
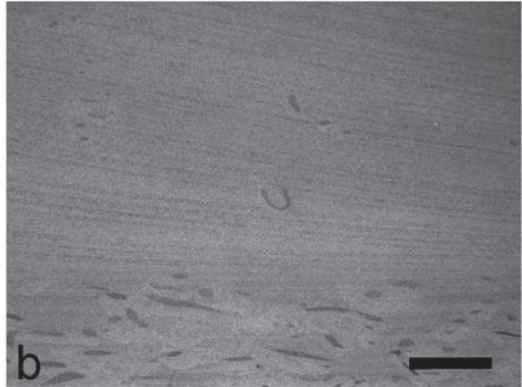
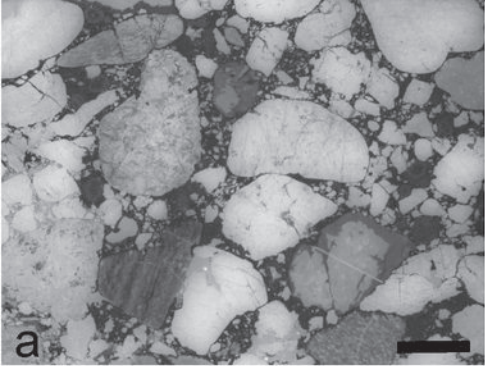


# Baysun Fm.

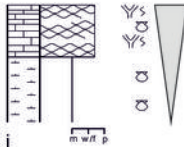
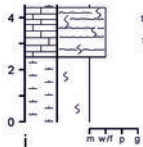
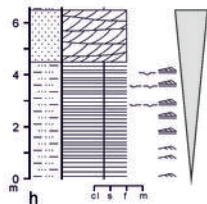
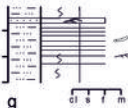
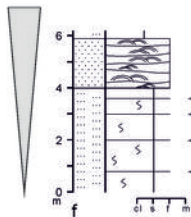
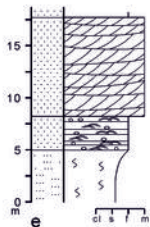
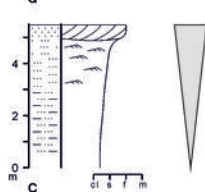
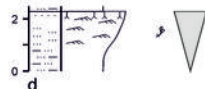
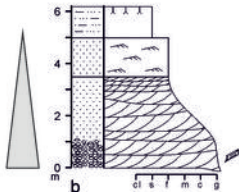
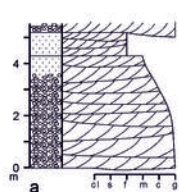


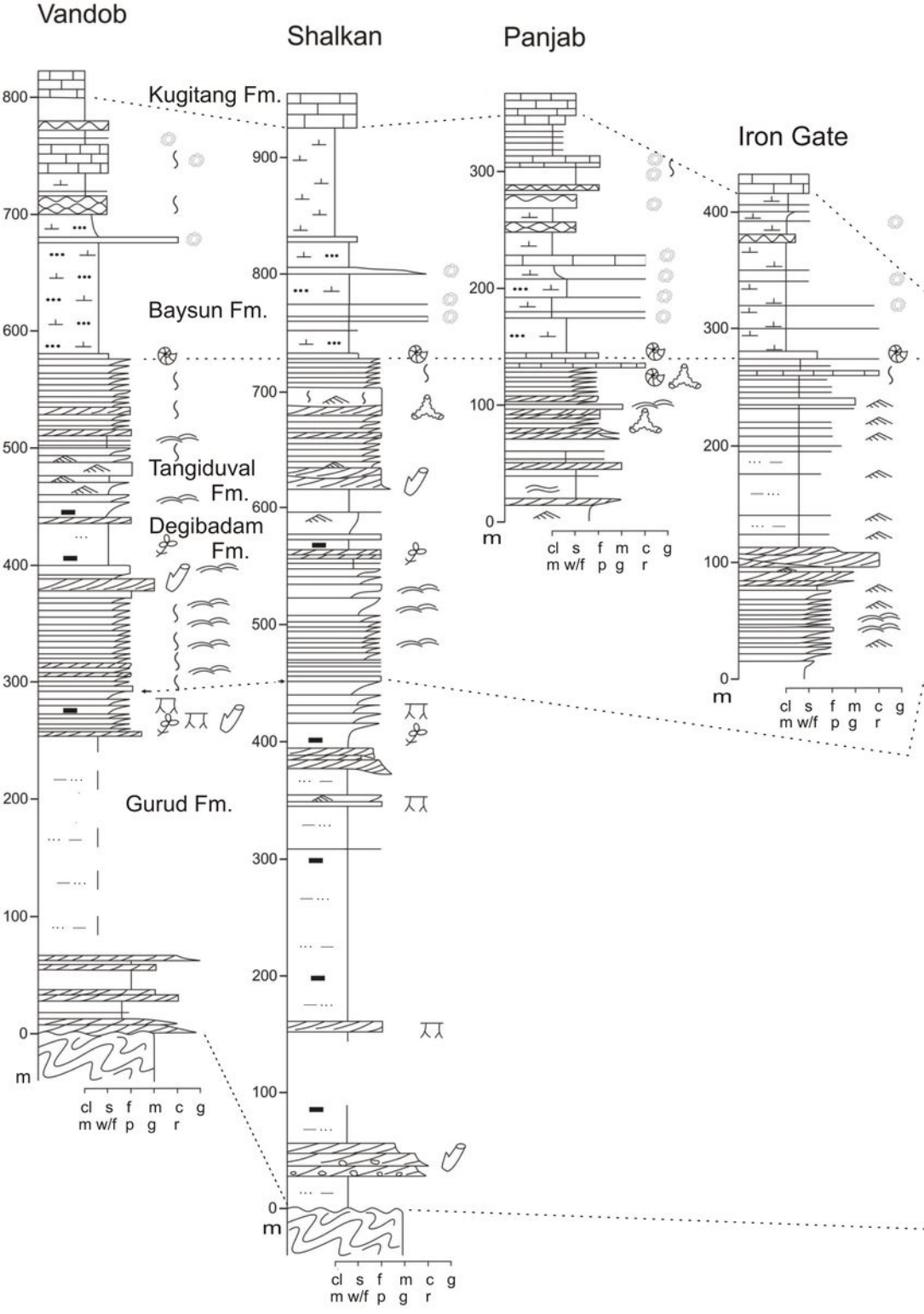
-  algal lamination
-  birdseyes
-  fenestral fabrics





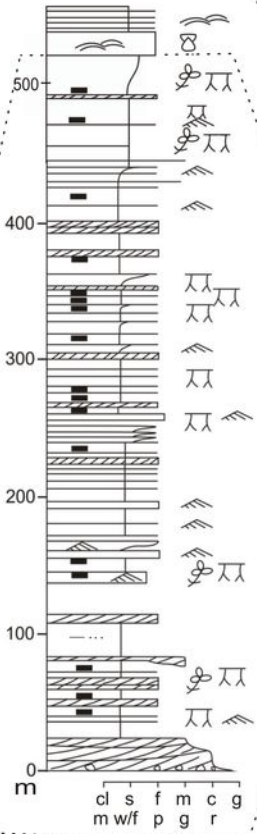
# Depositional cycles (c-j: parasequences)



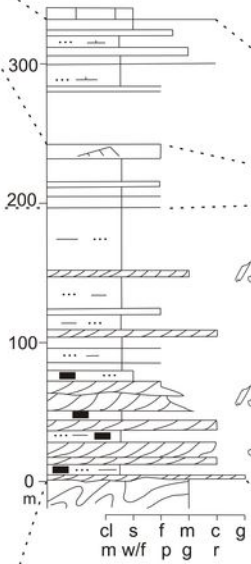




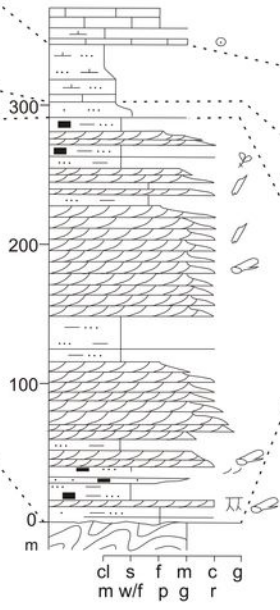
### Dalut Mine



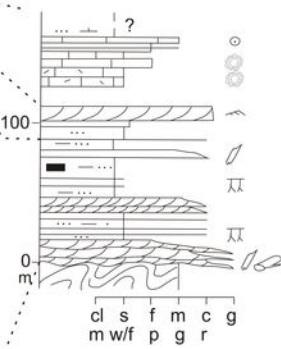
### Sangardak



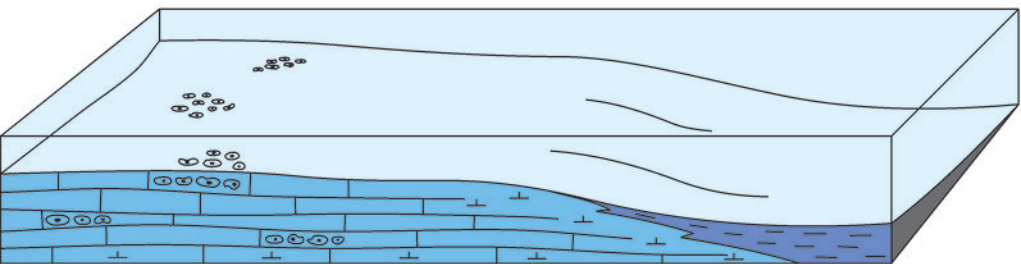
### Shargun



### Vuariz

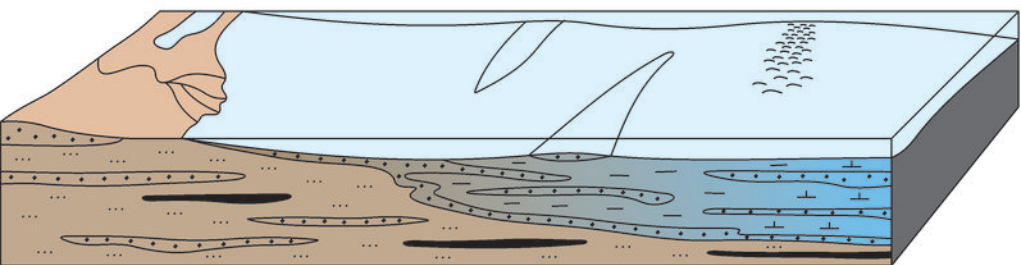


Late Jurassic



c

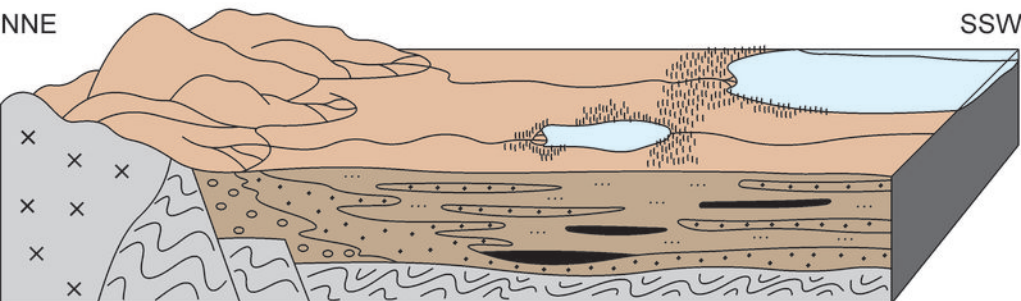
Middle Jurassic



b

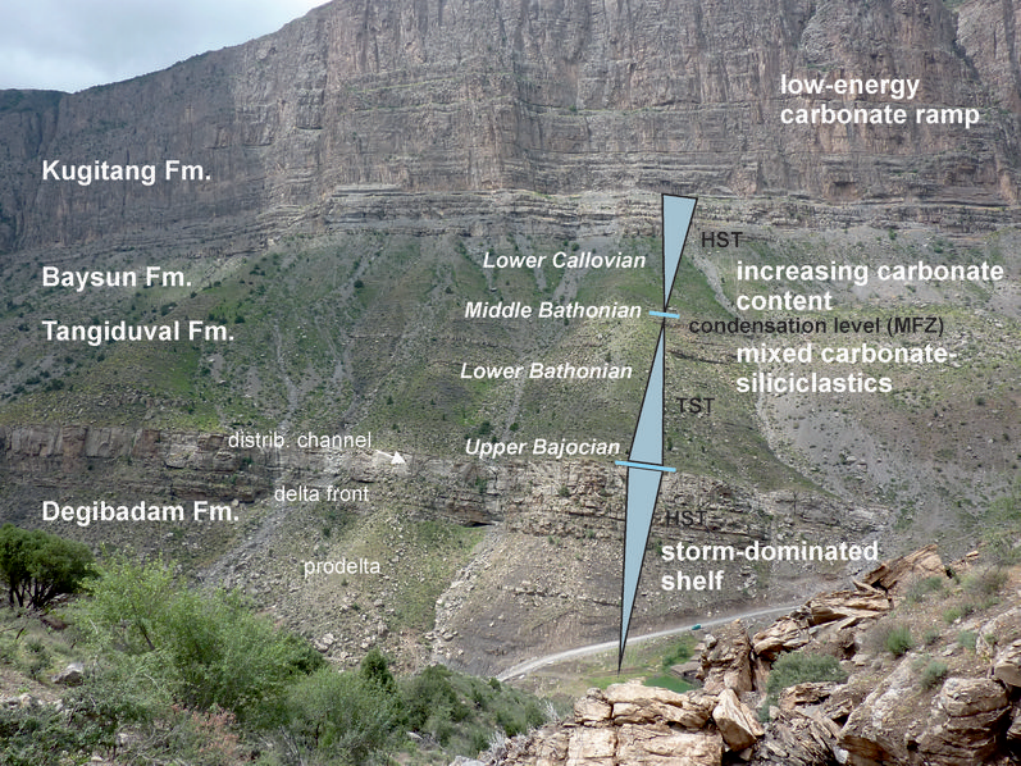
investigated segment

Early Jurassic



a

investigated segment



low-energy  
carbonate ramp

Kugitang Fm.

Baysun Fm.

Tangiduval Fm.

Degibadam Fm.

*Lower Callovian*

*Middle Bathonian*

*Lower Bathonian*

*Upper Bajocian*

HST

increasing carbonate  
content

condensation level (MFZ)

mixed carbonate-  
siliciclastics

TST

HST

storm-dominated  
shelf

distrib. channel

delta front

prodelta

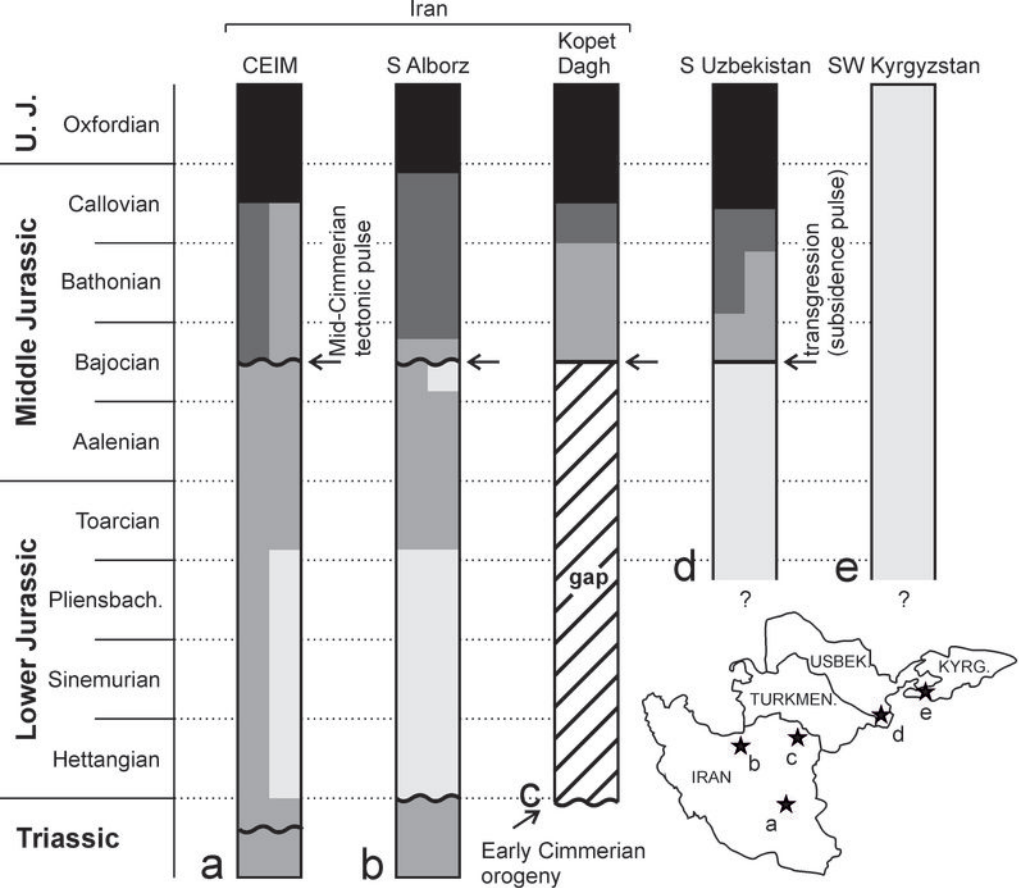


Table 2

<b>Continental palaeoenvironments</b>	<b>lithology (facies associations)</b>	<b>sedimentary structures</b>	<b>fossils/trace fossils</b>
braided river channels	fine- to coarse-grained arkosic or quartz-rich ss, partly gravely to conglomeratic, immature	large-scale trough cross-bedding, erosional base, fining-upward, vertical stacking common	wood fragments, tree trunks
meandering river channels with levee deposits	fine-grained ss, partly silty, moderately to well sorted; levee deposits: interbedded fine-grained ss and silty clay	lateral accretion, large-scale trough cross-bedding, ripple lamination, erosional base, fining-upward	plant fragments, rootlets
flood plain with crevasse splays	silty clay to argillaceous silt with cm- to dm-thick, sharp-based fine-grained ss and siltstone intercalations, partly lenticular	current ripple lamination, rootlets,	plant fragments common
flood plain with palaeosol	(a) ferruginous fine-sandy silt (b) brown clay with scattered quartz granules		(a) rootlets
floodplain swamp, swampy lake margin	coal, strongly carbonaceous clay or silty clay		rich in plant debris
lake margin	fine-grained ss, siltstone, coarsening-upward	ripple lamination, top occasionally rooted	plant debris common
lacustrine delta	coarsening-upward succession of silty clay to thin-bedded fine-sandy silt or fine-grained sandstone	coarser layers with ripple lamination, top bed in some cases with large-scale trough stratification and erosional base	plant debris common
storm-influenced lake	argillaceous silt with cm-scale fine-grained ss intercalations	ss parallel- or ripple-laminated, with sharp base; some with HCS	plant fragments common
low-energy offshore lake	argillaceous silt to silty clay, partly with claystone concretions, rarely silty micrite	partly shaly, partly bioturbated	plant debris common
<b>Marine palaeoenvironments</b>			
distributary channel	medium- to coarse-grained immature ss	base sharp, erosional, fining-upward, large-scale trough cross-stratification, top ripple-laminated	wood pieces common
protected embayment	fine-sandy silty clay, locally carbonaceous; silt,	bioturbated; silt commonly ripple-	plant debris

	fine-sandy silt, with occasional cm- to dm-thick fine-grained ss intercalations	laminated ss commonly parallel-laminated	
delta front	arkosic fine- to medium-grained ss	ripple-lamination, low-angle large-scale trough cross-stratification, coarsening-upward	wood pieces, thin bioturbated intervals ( <i>Thalassinoides</i> )
prodelta	argillaceous silt with occasional cm-thick fine-grained ss interbeds	ss ripple-laminated, argillaceous silt bioturbated	ammonites
tide-influenced inner siliciclastic ramp	interlayered bedding of fine-grained ss (0.5-5 cm) and argillaceous silt (1-2 cm); fine-grained sandstone	ss ripple-laminated; flaser-bedding, lenticular bedding, oscillation ripples	<i>Gyrochorte</i>
high-energy inner carbonate ramp	m-thick bio-oo-grainstone	large-scale planar cross-bedding, sharp base	
low-energy lagoonal intertidal carbonate flats	carbonate mudstones and fine-grained packstones	birdseyes and laminoid fenestral fabric, thin, irregular algal laminae	scattered gastropods
submarine dunes of the inner to middle siliciclastic ramp	dm- to m-thick fine- to medium-grained ss, partly bioclastic	large-scale trough cross-bedding	disarticulated bivalves, crinoid ossicles, <i>Ophiomorpha</i>
storm-wave influenced middle siliciclastic ramp	argillaceous to fine-sandy silt with intercalations of dm- to m-thick fine-grained ss	ss with hummocky cross-stratification and sharp base; beds partly amalgamated; fine-grained sediments bioturbated	<i>Thalassinoides</i> , <i>Skolithos</i>
storm-flow influenced outer siliciclastic ramp	argillaceous silt with cm-thick well sorted, fine-grained ss intercalations	ss with sharp, erosional base, either parallel-laminated, ripple-laminated or developed as couplets; partly with gutter casts, flute casts, tool marks; argillaceous silt bioturbated	<i>Thalassinoides</i> , <i>Planolites</i> , <i>Chondrites</i> , <i>Rhizocorallium irregulare</i> , wood fragments scattered bivalves; shell concentrations as fills of gutter casts
low-energy mixed carbonate-siliciclastic outer ramp	silty marl, marly silt,	bioturbated, loosely packed shell concentrations,	small softground fauna (e.g., the bivalves <i>Corbulomima</i> , <i>Nicaniella</i> ), <i>Arcomytilus</i> , <i>Integricardium</i> , <i>Ph.</i> ( <i>Bucardiomya</i> ), <i>Plagiostoma</i> , <i>Chlamys</i> )
low-energy carbonate outer ramp	marl, marlstone, biofloatstone, oncofloat-/rudstone, biowackestone	bioturbated, partly with nodular texture	ammonites (rare) occasional bivalves (e.g., <i>Plagiostoma</i> )
condensed mixed carbonate-siliciclastic outer ramp	bioclastic silty to fine-sandy micrite	highly bioturbated, in places nodular	ammonites (mainly <i>Procerites</i> ) and bivalves common (e.g., <i>Entolium</i> , <i>Bucardiomya</i> , <i>Pleuromya</i> , <i>Ctenostreon</i> , <i>Liostrea</i> ); brachiopods and gastropods

			<i>(Obornella) occur</i>
--	--	--	--------------------------

Table 1. Section localities

1	Shalkan, Kugitang Mountains	N 37° 51' 58.5'' N 37° 52' 58.4''	E 66° 38' 06.0'' (base) E 66° 38' 11.4'' (top)
2	Vandob, Kugitang Mountains	N 37° 43' 07.9'' N 37° 43' 13.3''	E 66° 33' 45.1'' (base) E 66° 32' 46.3'' (top)
3	Panjab, northern Kugitang Mts.	N 38° 02' 07.4''	E 66° 49' 44.1''
4	Dalut Mine near the village of Toda, South Gissar Mts.	N 38° 15' 09.1''	E 67° 07' 36.7''
5	Gorge N of Derbent, southern tip of Gissar Mts. (Iron Gate)	N 38° 15' 35,5''	E 67° 01' 34.8''
6	Shargun section, coal mine N of Shargun, SE Gissar Mts	N 38° 36' 54.3''	E 67° 57' 48.1''
7	Sangardak, SE Gissar Mts.	N 38° 31' 57.9''	E 67° 34' 47.4''
8	Vuariz section I, ESE of Shahrissabsz	N 38° 48' 41.5''	E 67° 10' 04.4''
9	Vuariz section II, ESE of Shahrissabsz	N 38° 48' 20.6''	E 67° 10' 49.4''
10	Vuariz section III, ESE of Shahrissabsz	N 38° 48' 50.3''	E 67° 09' 41.9''
11	Vuariz section IV, ESE of Shahrissabsz	N 38° 49' 29.6''	E 67° 11' 26.3''